Submitted to ApJS
Preprint typeset using LaTeX style emulateapj v. 6/22/04

arXiv:astro-ph/0608259 v1 11 Aug 2006

THERMONUCLEAR (TYPE-I) X-RAY BURSTS OBSERVED BY THE *ROSSI X-RAY TIMING EXPLORER*

Duncan K. Galloway[1,2], Michael P. Muno[3,4], Jacob M. Hartman[5], Pavlin Savov[6] Dimitrios Psaltis[7] and Deepto Chakrabarty[5].
Kavli Institutute for Astrophysics and Space Research, Massachusetts Institute of Technology, Cambridge, MA 02139
Submitted to ApJS

ABSTRACT

We present a sample of 1035 thermonuclear (type-I) X-ray bursts from observations of 45 accreting neutron stars by the *Rossi X-ray Timing Explorer* (*RXTE*), spanning more than nine years. This sample contains for the first time confirmed examples of burst ignition in each of the three regimes identified theoretically: H-ignition of mixed H/He fuel, He-ignition in pure He, and He-ignition in mixed H/He fuel. We combined bursts from multiple sources to investigate the variation of the burst rate, energetics, and time scale as a function of accretion rate. We found a peak burst rate of 0.2–0.3 hr^{-1} for a normalised peak flux of $\gamma \approx 0.02$–0.06, corresponding to a source luminosity of 0.3–2×10^{37} $\mathrm{ergs\,s}^{-1}$.

For 35 sources with bursts exhibiting photospheric radius-expansion, we estimated the likely distance range arising from the possible range of the Eddington limit. We found that in general the peak flux of radius-expansion bursts from individual sources is not constant, varying with a fractional standard deviation of 14% in the mean. We also examined the bursts with very short ($\lesssim 30$ min) recurrence times. We found evidence for two distinct populations of such bursts, one of faint bursts following a much stronger burst by 6–18 min, and another with comparable intensity bursts separated by 7 min or more. We describe the properties of bursts observed from 5 new bursters discovered by *RXTE*, as well as two new transient outbursts of previously known sources. Finally, we searched for burst oscillations at the known oscillation frequencies in 14 sources. We describe the distribution of the oscillation amplitudes as well as the stages of each burst in which the oscillations are detected.

Subject headings: stars: neutron — X-rays: bursts — nuclear reactions — stars: distances

1. INTRODUCTION

Thermonuclear (type-I) X-ray bursts manifest as a sudden increase in the X-ray intensity of accreting neutron stars (NSs), many times brighter than the steady persistent emission. Typical bursts exhibit rise times of between $\lesssim 1$ and 10 s, and last from tens to hundreds of seconds (Fig. 1). These events are caused by unstable burning of accreted H/He on the surface of neutron stars in low-mass X-ray binary (LMXB) systems (e.g. Strohmayer & Bildsten 2006), in contrast to type-II bursts, which are thought to be caused by sudden accretion events (e.g. Lewin et al. 1993). The H/He fuel for type-I bursts is accreted from the binary companion and accumulates on the surface of the neutron star, forming a layer about 10 m thick. The accreted material is compressed and heated hydrostatically, and if the temperature is sufficiently high any hydrogen present burns steadily into helium via the hot carbon-nitrogen-oxygen (CNO) process. After between ~ 1 and several tens of hours, the temperature and density at the base of the layer becomes high enough that the fuel ignites, burning unstably and spreading rapidly to consume all the available fuel on the star in a matter of seconds.

The primary evidence that the energy source for type-I bursts is thermonuclear comes from comparisons of the time-integrated persistent and burst flux. The ratio of the integrated persistent flux to the burst fluence is α, the standard measure of the relative efficiency of the two processes. Early in the study of type-I bursts it was realised that the energy derived from accretion was between 40 and a few hundred times greater than the energy liberated during the type-I bursts. These values are comparable to those predicted assuming that the burst energy arises from nuclear burning, firmly establishing the thermonuclear origin of type-I bursts.

The burst X-ray spectrum is generally consistent with a blackbody of color temperature $T_{\mathrm{bb}} = 2$–3 keV. Time-resolved spectral fits give evidence for an initial rise in T_{bb} followed by a more gradual decrease following the burst peak, giving an approximately exponential decay in X-ray brightness back to the persistent level. This is naturally interpreted as heating resulting from the initial fuel ignition, followed by cooling of the ashes once the available fuel is exhausted. Such bursts have been observed to date from more than 70 sources (e.g. in 't Zand et al. 2004c).

Models of unstable nuclear burning on the surface of a neutron star reproduce the observed rise times (seconds), durations (minutes), recurrence times (hours), and total energies of the bursts (10^{39}–10^{40} ergs; e.g. Fujimoto et al. 1981; Ayasli & Joss 1982; Fushiki & Lamb 1987; Fujimoto et al. 1987; Bildsten

[1] present address: The School of Physics, University of Melbourne, Victoria, 3010, Australia
[2] Centenary Fellow
[3] present address: Department of Physics and Astronomy, University of California, Los Angeles CA 90095
[4] Hubble Fellow
[5] also Department of Physics, Massachusetts Institute of Technology, Cambridge MA 02139
[6] present address: Theoretical Astrophysics 130-33, California Institute of Technology, Pasadena, CA 91125
[7] present address: Department of Physics, University of Arizona, Tucson AZ 85721
Electronic address: D.Galloway@physics.unimelb.edu.au, %duncan@space.mit.edu, mmuno@astro.ucla.edu, jhartman@space.mit.edu, pavlin@tapir.calte

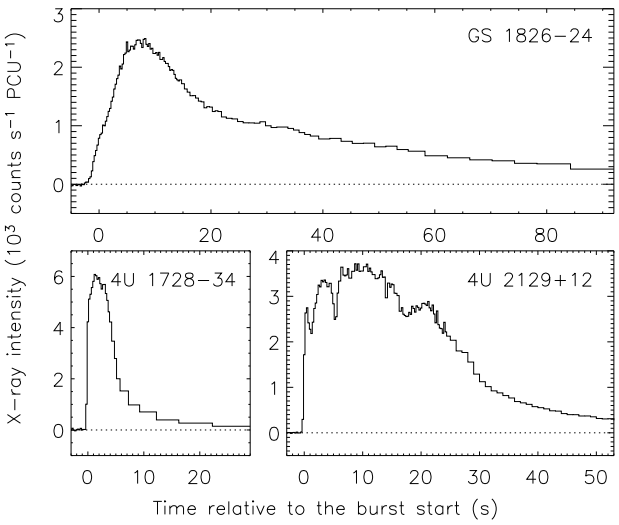

FIG. 1.— Example lightcurves of bursts observed by *RXTE*. The top panel shows a long burst from GS 1826−24 on 1998 June 8 04:11:45 UT. The lower left panel shows a burst observed from 4U 1728−34 on 1999 June 30 19:50:14 UT, while the burst at lower right was observed from 4U 2129+12 in the globular cluster M15 on 2000 September 22 13:47:41 UT. The persistent (pre-burst) level has been subtracted (dotted line). Note the diversity of burst profiles, which arises in part from variations in the fuel composition; bursts with a slow rise and decay are characteristic of mixed H/He fuel, while bursts with much faster rises likely burn primarily He. Both bursts in the lower panels exhibited photospheric radius-expansion.

1998; Cumming & Bildsten 2000; Narayan & Heyl 2003; Woosley et al. 2004). The frequency, strength, and time scales of thermonuclear bursts depend on the composition of the burning material, as well as the metallicity (here referring to the CNO mass fraction, $Z_{\rm CNO}$) of the matter accreted onto the neutron star, the amount of hydrogen burned between bursts, and the amount of fuel left-over from the previous burst. Variations from source to source are also expected because of differences in the core temperatures of the neutron stars and the average accretion rate onto the surface (Ayasli & Joss 1982; Fushiki & Lamb 1987; Narayan & Heyl 2003). Theoretical ignition models such as that described by Fujimoto et al. (1981) predict how burst properties in an individual system change as the accretion rate onto the neutron star varies. They identify three principal regimes of bursting, depending on the accretion rate ($\dot{M}$) usually expressed as a fraction of the Eddington rate $\dot{M}_{\rm Edd}$ ($\equiv 1.3 \times 10^{-8}\ M_\odot\,{\rm yr}^{-1}$ or $8.8 \times 10^4\ {\rm g\,cm^{-2}\,s^{-1}}$ locally, averaged over the surface of a 10 km NS). At the lowest accretion rates ($< 0.01\dot{M}_{\rm Edd}$, referred to as Case 3 by Fujimoto et al. 1981), the temperature in the burning layer is too low for stable hydrogen burning; the hydrogen ignites unstably, in turn triggering helium burning, which produces a type I X-ray burst in a hydrogen-rich environment. At higher accretion rates ($0.01 < \dot{M}_{\rm Edd} < 0.1$, Case 2), hydrogen instead burns stably into helium, leading to a growing pure helium layer at the base of the accreted material. The fuel layer heats steadily until ignition of the helium occurs via the triple-α process. At these temperatures and pressures, helium burning is also extremely unstable, and a rapid and intense helium burst follows. At the highest accretion rates ($0.1 < \dot{M}_{\rm Edd} < 1$, Case 1), material is accreted faster than it can be consumed by steady hydrogen burning (which is limited by the rate of β-decays in the CNO cycle), so that the helium ignites unstably in a H-rich environment (see Bildsten 1998 for dependences of these critical accretion rates on the metallicities). Above this range ($> \dot{M}_{\rm Edd}$), stable helium burning becomes viable on the surface of the neutron star, which depletes the primary fuel reserves and causes bursts to occur less frequently, or not at all.

Hanawa & Fujimoto (1982) pointed out that the luminosities of neutron star LMXBs that have been observed to burst imply accretion rates from $\sim 0.01 - 0.1$ $\dot{M}_{\rm Edd}$, so that an individual source that varies in luminosity should exhibit changes in its bursting behavior between Case 2 and Case 1. This has proved difficult to test. The accretion rate varies on time scales of weeks to months (e.g. Muno et al. 2002c), much longer than the average observation. The majority of sources either exhibit few bursts, or several bursts are seen in a single luminosity state (Lewin et al. 1993). Only a few sources have been observed to burst over a range of luminosities, and these have produced some perplexing results. As the accretion rate increases, the column of material above the burning layer builds more quickly, and thus the time required to reach the critical temperature for ignition is expected to decrease. This is best seen in the burst rate increase observed in GS 1826−24 as the persistent flux increased by a factor of ≈ 2 (Galloway et al. 2004b). On the other hand, increases in persistent flux over a wider range often result in a *decrease* in burst rate, as in 4U 1820−30 (Clark et al. 1977). This contrary result may be attributed to steady helium burning at the highest accretion rates, which reduces the amount of fuel for X-ray bursts. This causes bursts to occur less often, as also seen in EXO 0748−676 (Gottwald et al. 1986) and 4U 1705−44 (Langmeier et al. 1987), or to cease altogether, as observed in GX 3+1 (Makishima et al. 1983). However, no correlation was found between persistent flux and burst recurrence times in Ser X-1 (Sztajno et al. 1983), 4U 1735−44 (Lewin et al. 1980; van Paradijs et al. 1988b), and 4U 1636−536 (Lewin et al. 1987). This suggests either that an additional mechanism contributes to the frequency of bursts, or that the persistent flux is not a good measure of the accretion rate in these sources.

The change in the composition of the burning layer as $\dot{M}$ increases also affects the properties of the bursts. Helium burning occurs via the triple-α process, which is moderated by the strong nuclear force and proceeds very quickly at the temperatures and densities of the burning layer. Hydrogen burning proceeds more slowly, because it is limited by a β-decay that is moderated by the weak force. Therefore, faster, more intense bursts characteristic of a helium-rich burning layer should occur at relatively low accretion rates (Case 2), while hydrogen-rich bursts with slower rise and decay times should occur at higher rates (Case 1). Surprisingly, most sources behave in the opposite manner. The decay time scales of bursts from 4U 1608−52 (Murakami et al. 1980b), 4U 1636−536 (Lewin et al. 1987), and 4U 1705−44 (Langmeier et al. 1987) have all been reported to *decrease* as the apparent $\dot{M}$ increases from 0.01–0.1 $\dot{M}_{\rm Edd}$.

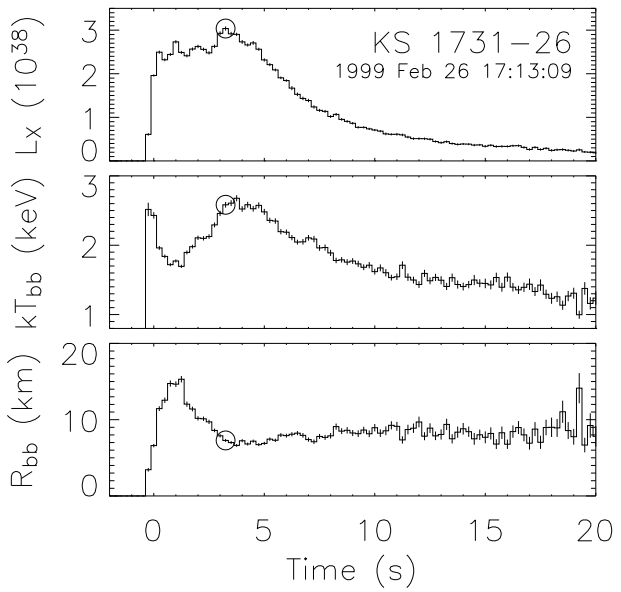

FIG. 2.— Spectral evolution in a thermonuclear burst exhibiting photospheric radius-expansion, from KS 1731−26. *Top panel* Burst luminosity L_X, in units of $\mathrm{ergs\,cm^{-2}\,s^{-1}}$; *middle panel* blackbody (color) temperature $kT_{\rm bb}$; and *bottom panel* blackbody radius $R_{\rm bb}$. L_X and $R_{\rm Bbb}$ are calculated at an assumed distance of 7.2 kpc (Table 6). Note the anticorrelation between $kT_{\rm bb}$ and $R_{\rm bb}$ in the first few seconds, indicative of the expanding photosphere, and the approximately constant flux throughout the expansion. The time at which the flux reaches a maximum is indicated by the open circle; by then the radius has declined to the asymptotic value in the burst tail, suggesting that the photosphere has settled once more on the NS surface.

The origin of this discrepancy is uncertain. It appears that we do not understand either how the composition of the burning layer varies with the accretion rate, or how the accretion rate on the surface varies with the amount of persistent X-ray flux (see Bildsten 2000 for a discussion).

The peak flux for very bright bursts can reach levels comparable to the Eddington luminosity at the surface of the NS. Such bursts frequently exhibit a characteristic spectral evolution in the first few seconds, with a local peak in blackbody radius and at the same time a dip in color temperature, while the flux remains approximately constant (Fig. 2). This pattern is thought to result from expansion of the X-ray emitting photosphere once the burst flux reaches the Eddington luminosity; the effective temperature must decrease in order to maintain the luminosity at the Eddington limit, and excess burst flux is converted into kinetic and gravitational potential energy in the expanded atmosphere. The Eddington luminosities $L_{\rm Edd}$ measured for LMXBs with independently-known distances are generally consistent to within the uncertainties, at a value estimated as $(3.0 \pm 0.6) \times 10^{38}$ $\mathrm{ergs\,s^{-1}}$ by Lewin et al. (1993), or, more recently, $(3.79 \pm 0.15) \times 10^{38}$ $\mathrm{ergs\,s^{-1}}$ (cf. with equation 5; Kuulkers et al. 2003). This result is consistent with the narrow ranges for masses and surface redshifts expected for the neutron stars in these bursters. Consequently, these photospheric radius-expansion (PRE) bursts can be used as distance indicators (Basinska et al. 1984). Time-resolved spectroscopy of radius-expansion bursts also allow in principle measurement of the surface gravitational redshift (e.g. Damen et al. 1990; Smale 2001).

The recently discovered class of extremely long-duration bursts or "super" bursts are also thought to arise from thermonuclear processes. The fuel for these bursts is probably carbon rather than H/He, giving distinctly different time scales, recurrence times and energetics (e.g. Cumming 2004). Superbursts have been detected from around 10% of the Galactic X-ray burst population, with recurrence times estimated at 1.5 yr (in 't Zand et al. 2004a). The connection with intermediate-duration events observed from GX 17+2 is not clear (in 't Zand et al. 2004b). The predicted temperatures in the fuel layer are too low to give carbon bursts with the observed fluences, suggesting that the cooling in the crust may be less efficient than previously thought (Cumming et al. 2005).

Another recently-discovered phenomenon associated with thermonuclear bursts is highly coherent burst oscillations with fractional amplitudes in the range 5–20% rms, which have been detected in bursts from 13 sources to date (Strohmayer et al. 1996; see also Strohmayer & Bildsten 2006). As the burst evolves, these "nuclear-powered pulsations" typically increase in frequency by a few Hz, most approaching an asymptotic value which is stable for a given source from burst to burst (e.g. Fig. 3; Muno et al. 2002b). That the asymptotic frequency traces the NS spin has been confirmed by the detection of burst oscillations at the spin frequency in the millisecond pulsars SAX J1808.4−3658 (Chakrabarty et al. 2003) and XTE J1814−338 (Strohmayer et al. 2003), as well as the prolonged oscillation detected during a superburst in 4U 1636−536 (Strohmayer & Markwardt 2002). The frequency drift may occur as a consequence of the expanded burning layer becoming decoupled from the star (Strohmayer et al. 1997a; Cumming & Bildsten 2000). In MXB 1659−298 the increase is ≈ 5 Hz, the greatest increase seen so far (Wijnands et al. 2001c), while 4U 1916−053 exhibits the largest fractional increase (Galloway et al. 2001). The most recent detection was in summed Fourier power spectra taken throughout the tails of 38 bursts from EXO 0748−676, in which Villarreal & Strohmayer (2004) found evidence for 45 Hz oscillations which were not detected in the persistent emission. This is the lowest spin frequency of all the bursters, and is consistent with the lack of rotational broadening in the X-ray absorption lines attributed to material on the surface of the NS by Cottam et al. (2002).

Substantial questions regarding the mechanism of burst oscillations remain, as well as what conditions determines whether or not the oscillations will be detectable in a given burst, or a given source. The oscillations have been suggested to result from initially localized nuclear burning, which spreads over the surface of the neutron star during the early stages of the burst (Strohmayer et al. 1996). However, this explanation does not account for the oscillations which persist as long as 5–10 s after the burst rise. The frequency evolution is assumed to result from changes in the velocity of a pattern in the surface brightness (Strohmayer et al. 1997a;

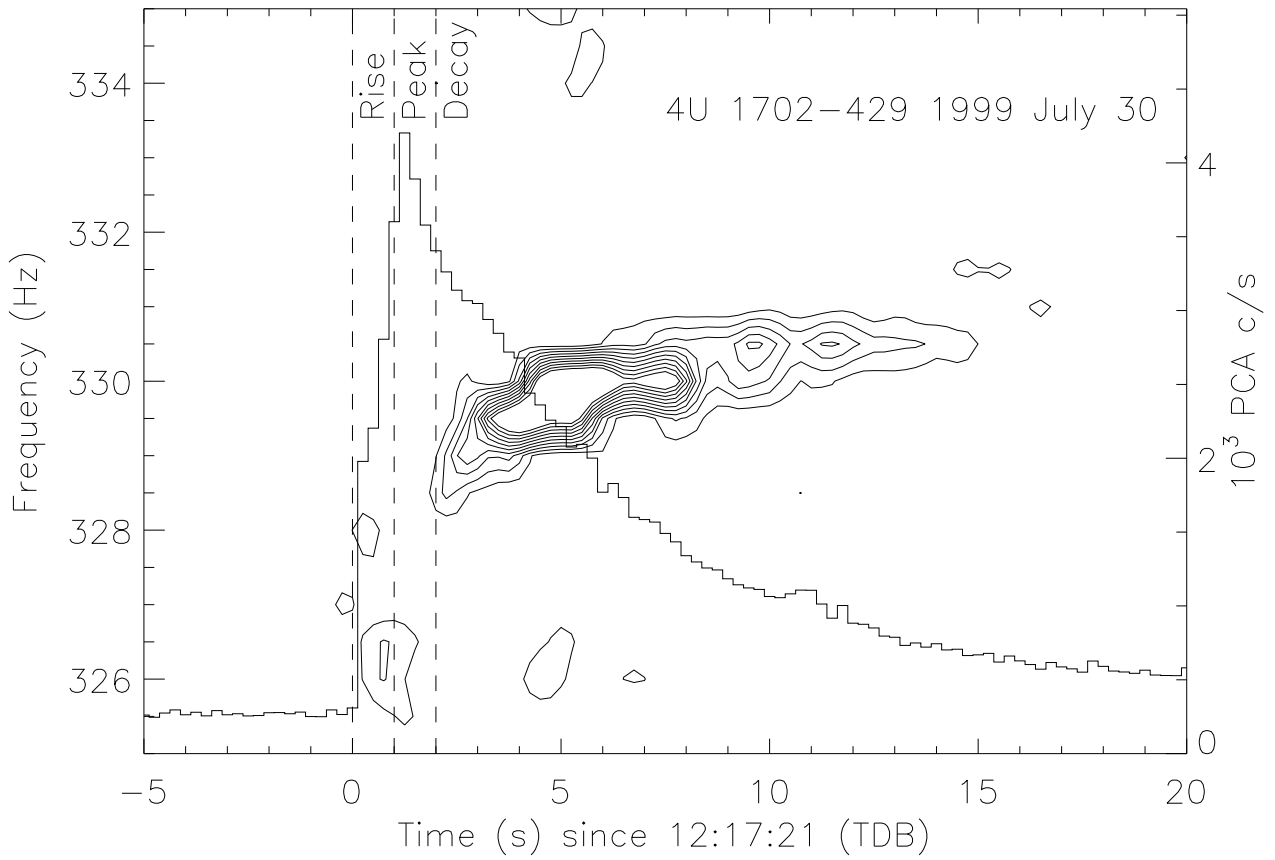

FIG. 3.— A dynamic power spectrum illustrating the typical frequency evolution of a burst oscillation. Contours of power as a function of frequency and time were generated from power spectra of 2 s intervals computed every 0.25 s. A Welch function was used to taper the data to reduce sidebands in the power spectrum due to its finite length (Press et al. 1996). The nth contour level has a single-trial probability of 0.02^n of occurring randomly due to noise. The PCA count rate (histogram) is plotted referenced to the right axis. The time intervals defined in §2.4 as the rise, peak, and decay are indicated with the vertical dashed lines.

Cumming et al. 2002; Heyl 2004; Spitkovsky et al. 2002). The apparent lack of stability in the underlying clock producing these oscillations favors the models in which the brightness asymmetry originates from hydrodynamic instabilities (Spitkovsky et al. 2002) or modes excited in the neutron star ocean (e.g. Heyl 2004).

Few previous observational studies have focussed on the properties of bursts from more than one source. van Paradijs et al. (1988a) compiled 45 measurements in the literature from ten LMXBs, and revealed a global decrease in burst duration with increasing persistent flux, similar to that seen individually for several sources. They also found that α was strongly correlated with the (normalized) persistent flux, more than was predicted by numerical models (e.g. Fujimoto et al. 1981). The normalized fluence depended principally on the burst interval $t_{\rm rec}$, which suggested that continuous stable burning between bursts is a general phenomenon in bursters. Cornelisse et al. (2003) analysed six years of *BeppoSAX* observations of 37 LMXBs, with a combined sample of 1823 bursts, and inferred a transition between long, H-rich bursts (identified as Case 3) to short, pure He bursts (Case 2) with the onset of steady H burning at a persistent luminosity of 2×10^{37} ergs s^{-1} (equivalent to $0.1\dot{M}_{\rm Edd}$, a factor of 10 higher than predicted by theory). Below this level, bursts were long, frequent and occurred quasi-periodically, typified by GS 1826−24 and KS 1731−26. Above 2×10^{37} ergs s^{-1} the burst rate dropped by a factor of five, and the bursts were short and occurred irregularly (although short bursts were also observed in the low accretion rate regime). At even higher luminosities, bursts ceased altogether.

To date, the *Rossi X-ray Timing Explorer* (*RXTE*) has observed ≈ 60 of the known thermonuclear bursters, and discovered several new ones. Additionally, several different classes of kHz variability related to bursts has been discovered in *RXTE* observations, and subsequently found in more than 10 of those sources. While the *RXTE* data are unparalleled for studies of bursts and bursters, thanks to the large instrumental effective area and high timing resolution, the published work to date has fallen short of the detailed comparisons of theory and observations required to understand the discrepancies with the theory which have been identified. Typi-

cally the data for individual sources are inadequate since only a narrow range of accretion rates is spanned, and insufficient exposure time has been accumulated for individual programs, leading to only a small number of bursts in total. New data enters the public archive continually, and published analyses rarely take advantage of all the available bursts in all the public observations, let alone all the bursts from all the known bursters. These shortcomings motivate the present work, which seeks to present a uniform analysis of all thermonuclear bursts from all bursters observed by *RXTE*. By combining the bursts from different sources we achieve much larger burst numbers and a larger range of $\dot{M}$ for global characterization of burst behaviour than is possible for any individual source. We also include information on the presence of burst oscillations, which is only available in the *RXTE* data. While *RXTE* has also observed carbon-burning superbursts, we do not analyse these events in this paper.

We present the contents of the catalog, and the results of our studies, as follows. In §2 we describe the analysis methods and products, and relate to the physical properties of the bursts. We summarise the properties of the catalog and present the results for individual bursters on a case-by-case basis in §3; we constrain the origin for bursts in crowded fields in appendix A. In §4 we combine the bursts from various sources in an attempt to quantify the global burst properties as a function of accretion rate. and compare these properties to predictions from burst theory, Finally, we summarise our results in §5.

2. OBSERVATIONS AND ANALYSIS

Public data from *RXTE* observations of thermonuclear burst sources are available through the High-Energy Astrophysics Science Archive Research Center[8] (HEASARC), dating from shortly after the launch of the satellite on 1995 December 30 to 2005 October 29. *RXTE* carries three instruments sensitive to X-ray photons. The All-Sky Monitor (ASM; Levine et al. 1996) consists of three scanning shadow cameras sensitive to photons between 1.5 and 12 keV with a total effective area of ≈ 100 cm^2, which provide 90 s exposures of most points on the sky every 96 min. The High-Energy X-ray Timing Experiment (HEXTE; Gruber et al. 1996) is comprised of two clusters of NaI/CsI scintillation detectors sensitive to X-rays between 15 and 250 keV with a total effective area of 1600 cm^2. The Proportional Counter Array (PCA; Jahoda et al. 1996). consists of five identical, co-aligned proportional counter units (PCUs), sensitive to photons in the energy range 2–60 keV. The field-of-view of both the PCA and HEXTE is circular with radius $\approx 1^\circ$. Photon counts from the PCA are processed independently by up to 6 Event Analyzers (EAs) in a variety of configurations. Two EAs are permanently set to two standard observing modes, Standard-1 (with 0.125 s time resolution but only one energy channel) and Standard-2 (16 s binned spectra on 129 energy channels between 2–60 keV). The remaining EAs may be configured by the observer to give time resolution down to $1\mu s$ and up to 256 spectral channels.

We extracted 1-s lightcurves covering the full 2–60 keV PCA energy range from Standard-1 mode data of all public observations covering known burst sources. The PCA field of view is approximately 1° in radius, and the effective area drops off approximately linearly as a function of off-axis angle. Thus, we extended our lightcurves to offset pointings of up to 1.°2, which includes the end of the satellite's slew to the source and the beginning of the slew away. We also searched observations of fields centered less than 1° away from known burst sources. We searched each lightcurve for bursts as follows. For each observation we calculated the mean and standard deviation of the 1-s count rate measurements, and identified burst candidates in bins which exceeded the mean by more than 4 standard deviations. We then visually inspected the lightcurves to confirm or reject each candidate. Candidates were rejected if they were attributable to other events which can produce sharp jumps in the count rate, such as detector breakdowns, gamma-ray bursts, or particle events; or ultimately if time-resolved spectral analysis (see below) failed to show any indication of cooling in the tail. This search revealed a total of 1035 thermonuclear bursts.

2.1. *Characterizing the persistent emission*

In order to coarsely characterise the persistent spectrum, we computed hard and soft X-ray colors as the ratio of the background-subtracted detector counts in the (8.6–18.0)/(5.0–8.6) keV and the (3.6–5.0)/(2.2–3.6) keV energy bands, respectively. We used 64 s integrations to calculate the colors when the source intensity was above 100 counts s^{-1}, and 256 s integrations otherwise. We corrected the measured count rates for gain changes over the life of the mission by normalizing count rates from the Crab Nebula in each PCU to constant values for each energy band (totaling 2440 counts s^{-1} PCU^{-1} in the 2.2–18.0 keV band) using linear trends. When this correction is applied, the hard and soft colors from the Crab Nebula have values of 1.358 and 0.679, with standard deviations of only 0.5% and 0.1% respectively.

We show examples of the distribution of source colors (color-color diagrams) in Fig. 4. As $\dot{M}$ onto the neutron star increases, a source moves from the top-left to the bottom-right, roughly tracing a Z-shaped pattern (Hasinger & van der Klis 1989; Muno et al. 2002c; Gierliński & Done 2002). Most bursting LMXBs are classified as "atoll" sources, and trace out their full Z-shaped pattern as they vary in intensity by a factor of $\gtrsim 100$ (see Muno et al. 2002c, for a discussion). Nine atoll sources were observed on both the top and bottom portions of their color-color diagrams: 4U 1608−52, 4U 1636−536, 4U 1702−429, 4U 1705−44, 4U 1728−34, KS 1731−260, 4U 1746−37, XTE J2123−058 and Aql X-1 For those sources, we parameterized the position on the diagram by defining a curve that followed the middle of the Z-shaped track (Fig. 4; Dieters & van der Klis 2000). We first selected several points to define the basic shape of the curve. From these points, we defined a smooth curve using a spline interpolation. We then assigned $S_Z = 1$ to the upper-right vertex of the Z-shape and $S_Z = 2$ to the lower-right vertex, and defined the unit arc-length as the distance along the curve between these two points. The value of S_Z for any given point on the color-color diagram by finding the nearest point on the curve, and finding the value of the arc-length S_Z there. We then defined the mean S_Z value from the mean

[8] \protecthttp://heasarc.gsfc.nasa.gov

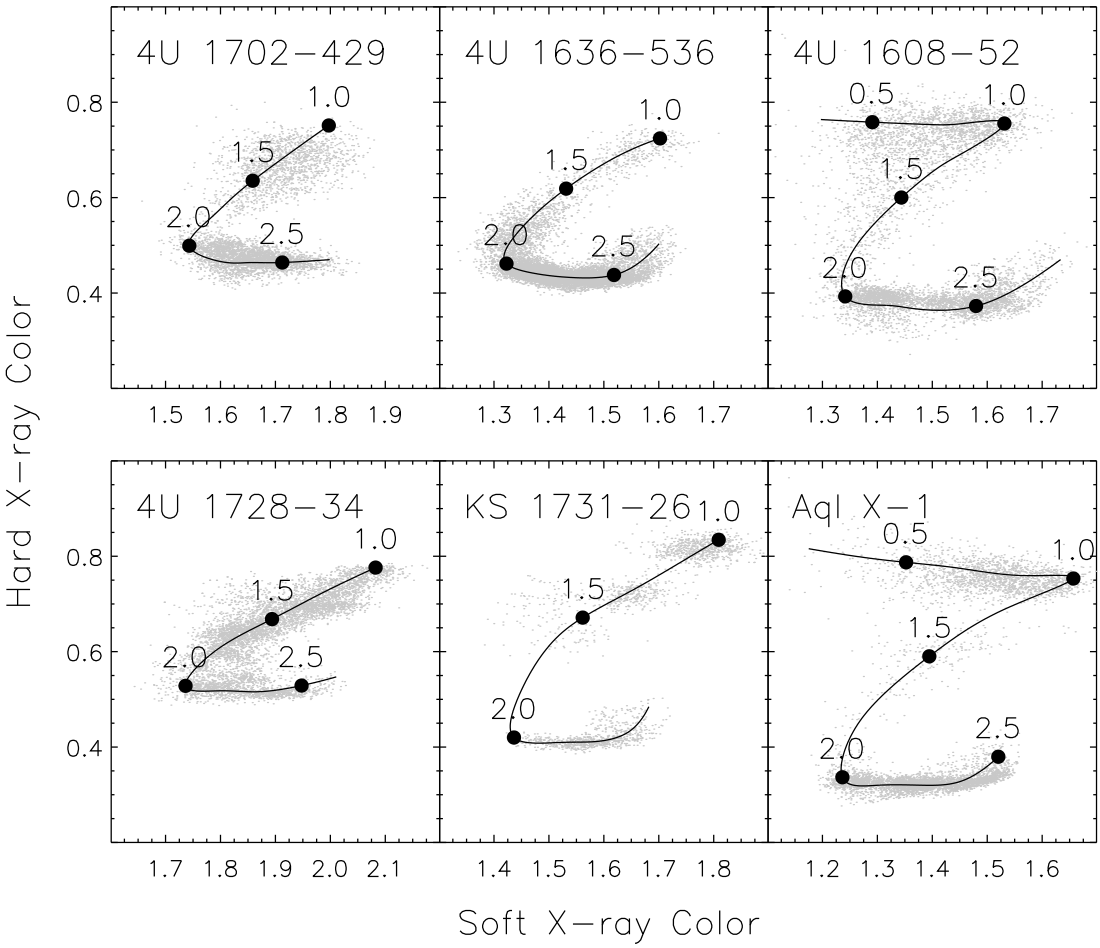

FIG. 4.— Color-color diagrams for six of the nine sources for which it was possible to define the coordinate S_Z locus. The soft color is the ratio of the background-subtracted PCA counts in the energy range 3.6–5.0 keV accumulated in 64 or 256 s, to the counts in the range 2.2–3.6 keV. The hard color is the ratio of counts in the ranges 8.6–18.0 and 5.0–8.6 keV. Colors are corrected for PCU gain variations. Filled circles show the points (labeled with their S_Z values) used to define the overall shape of the curve; solid curves show the spline interpolation between the points. The coordinate S_Z is thought to be proportional to $\dot{M}$.

colors for each observation of the sources listed above. Although S_Z is thought to be proportional to $\dot{M}$ (e.g. Vrtilek et al. 1990), the absolute calibraton is not well determined.

We also estimated the persistent source flux F_p at the time of the bursts from spectra extracted from Standard-2 mode data, separately for each PCU within each observation (excluding a ≈ 300 s interval covering each burst). We fit these spectra over the range 2.5–25 keV with an empirical model consisting of blackbody and power law components, each attenuated by neutral absorption with solar abundances. For many of the spectra, residuals were present around 6.4 keV which we interpreted as fluorescent Fe emission, and where these residuals resulted in a reduced-$\chi^2 \gtrsim 2$ we added a Gaussian component to improve the fit. For particularly bright sources such a model did not give a good fit, and for these we used instead a continuum component describing Comptonisation in a homogeneous environment (`compTT` in XSPEC; Titarchuk 1994a). The particular choice of the continuum was not important so long as the model was qualitatively correct, and possible uncertainties in the flux introduced by a less-than-optimal model are likely to be significantly less than other systematic instrumental uncertainties. We then integrated the model over 2.5–25 keV[9] to estimate the source flux within each PCU. For each source we calculated the mean PCU-to-PCU offset averaged over all the public *RXTE* observations, and renormalized the flux measurements relative to PCU 2. We adopted the mean and standard deviation of the rescaled flux measurements as the flux and error for that observation.

While the majority of the burst flux is emitted in the range 2.5–25 keV, this is generally not true for the persistent emission. In order to estimate the bolometric persistent flux $F_{\rm bol}$ we chose representative (preferably long) observations for selected sources and undertook combined fits of each PCU spectra (as described above) along with HEXTE spectra above 15 keV. We set the upper energy limit for the HEXTE spectra individually depending upon the maximum energy to which the source could be detected (typically 40–80 keV). Persistent spectra from bursters frequently exhibit a spectral cutoff between 15 and 50 keV, and so we fit the broad-

[9] The Crab flux in this band is 3.3×10^{-8} ergs cm^{-2} s^{-1}

band spectra with a Comptonisation continuum component attenuated by neutral absorption, also sometimes with a Gaussian component representing fluorescent Fe emission around 6.4 keV. We generated an idealized response covering the energy range 0.1–200 keV with 200 logarithmically spaced energy bins, and integrated the model flux also over this range. We then calculated a bolometric correction $c_{\rm bol}$ as the ratio between the 0.1–200 and 2.5–25 keV fluxes measured from the broadband spectral fits. The error on the bolometric correction was estimated as the standard deviation of the derived correction over the available PCUs. Altogether we estimated bolometric corrections for observations of 22 bursting sources, ranging between 1.05 (from a 1997 September observation of 4U 1728−34) and 2.14 (for a 2002 October observation of SAX J1808.4−3658). The corrections for the accretion-powered pulsars tended to be larger than for the non-pulsing burst sources, and we found the maximum value for the latter sources to be 1.82. In the mean, $c_{\rm bol} = 1.34$, and we adopt this value except where we calculated a value specifically for that source or observation. The likely error introduced is thus no more than 40%.

Given the persistent flux F_p, we may also estimate the accretion rate per unit area at the neutron star surface, $\dot{m}$. We assume that the X-ray luminosity is

$$L_{X,\infty} = \frac{4\pi R_{\rm NS}^2 \dot{m} Q_{\rm grav}}{(1+z)} = 4\pi d^2 F_{\rm p} c_{\rm bol} \qquad (1)$$

where $R_{\rm NS}$ is the NS radius, $Q_{\rm grav}$ is the energy released per nucleon during accretion ($= c^2 z/(1+z) \approx GM_{\rm NS}/R_{\rm NS}$), and d the distance to the burst source. Here we assume that the accreted fuel covers the neutron star surface evenly, and that the persistent emission is isotropic. Because the neutron star has such a strong gravitational field, the luminosity measured by an distant observer is significantly lower than at the NS surface due to gravitational redshift. Thus, we correct the quantities at the NS surface by a factor $(1+z)$, where z is the surface redshift; $1+z = (1-2GM/R_{\rm NS}c^2)^{-1/2} = 1.31$ for a NS with mass $M_{\rm NS} = 1.4 M_\odot$ and radius $R_{\rm NS} = 10$ km. Both mass measurements (Thorsett & Chakrabarty 1999) and predictions from a range of plausible equations of state (e.g. Lattimer & Prakash 2001) suggest that the masses and radii of neutron stars (and hence the compactness $M_{\rm NS}/R_{\rm NS}$) span relatively narrow ranges. However, a surface redshift has only been tentatively measured via redshifted absorption lines in one burster, EXO 0748−676, at $z = 0.35$ (Cottam et al. 2002). Thus, our assumption of a constant redshift of $z = 0.31$ for all the bursters in our sample unavoidably introduces a small systematic error when combining burst measurements from different sources (see §2.5). Then

$$\dot{m} = 6.7\times10^3 \left(\frac{F_p c_{\rm bol}}{10^{-9}\ {\rm ergs\,cm^{-2}\,s^{-1}}}\right)\left(\frac{d}{10\ {\rm kpc}}\right)^2 \times \left(\frac{M_{\rm NS}}{1.4\ M_\odot}\right)^{-1}\left(\frac{1+z}{1.31}\right)\left(\frac{R_{\rm NS}}{10\ {\rm km}}\right)^{-1} {\rm g\,cm^{-2}\,s^{-1}} \qquad (2)$$

It is generally thought that $L_{X,\infty}$ is proportional to $\dot{m}$ within intervals of days, but that the absolute calibration can shift substantially on longer timescales (e.g. Méndez et al. 2001).

2.2. *Temporal and spectral analysis of individual bursts*

Once each burst was located, high time- and spectral resolution data (where available) from the PCA covering the burst (100–200 s) were downloaded and processed to provide a range of analysis products. For most bursts, multiple spectral channels were available with time resolution of 0.25 s or better. We extracted 2–60 keV spectra within intervals of 0.25–2 s covering the entire burst. We set the initial integration time for the spectra at 0.25, 0.5, 1 or 2 s depending upon the peak count rate of the burst (> 6000, 3000–6000, 1500–3000 or < 1500 count s^{-1} respectively, neglecting the pre-burst persistent emission). Each time the count rate following the peak decreased by a factor of $\sqrt{2}$ we doubled the spectral time bin size. Since the evolution of the burst flux is slower in the tail, this increase in time bin size does not adversely affect the data quality.

We fitted each burst spectrum with a blackbody model multiplied by a low-energy cutoff, representing interstellar absorption using the cross-sections of Morrison & McCammon (1983) and solar abundances from Anders & Ebihara (1982). A spectrum extracted from a (typically) 16 s interval prior to the burst was used as the background; this approach is well-established as a standard procedure in X-ray burst analysis (e.g. van Paradijs & Lewin 1986; Kuulkers et al. 2002). The observations span multiple PCA gain epochs, which are defined by instances where the gain was manually re-set by the instrument team (on 1996 March 21, 1996 April 15, 1999 March 22 and 2000 May 13). In addition to these abrupt changes more gradual variation in the instrumental response is known to occur, due to a number of factors. To take into account these gain variations we generated a separate response matrix for each burst using PCARSP version 10.1[10], which is included as part of LHEASOFT version 5.3 (2003 November 17). The initial fitting was performed with the absorption column density $n_{\rm H}$ free to vary; subsequently it was fixed at the mean value over the entire burst to estimate the bolometric flux. The bolometric flux at each timestep i was calculated according to

$$F_i = \sigma T_{{\rm bb},i}^4 \left(\frac{R}{d}\right)_i^2 = 1.076\times10^{-11}\left(\frac{kT_{{\rm bb},i}}{1\ {\rm keV}}\right)^4 K_{{\rm bb},i}\ {\rm ergs\,cm^{-2}\,s^{-1}} \qquad (3)$$

where $T_{\rm bb}$ is the blackbody temperature, R is the effective radius of the emitter, d is the distance to the source, and $K_{\rm bb}$ is the normalisation of the blackbody component. It is important to note that the apparent blackbody temperature for a distant observer $T_{\rm bb} \equiv T_{{\rm bb},\infty}$ and the apparent temperature measured at the surface differ by a factor of $(1+z)$ in addition to spectral hardening factors arising from radiation transfer in the atmosphere which increases the apparent surface temperature compared to the effective temperature (e.g. London et al. 1986; Titarchuk 1994b).

[10] We note that the geometric area of the PCUs was changed for this release for improved consistency between PCUs and with (e.g.) canonical models of calibration sources, particularly the Crab pulsar. These changes have the effect of reducing the measured flux compared to analyses using previous versions of the response generating tools, by 12–14%. See Jahoda et al. (2006) for more details.

Implicit in equation (3) is the bolometric correction to the burst flux measured in the PCA bandpass; this correction adds $\simeq 7\%$ to the peak 2.5–25 keV PCA flux of radius expansion bursts. Should the emitted spectrum deviate significantly from a blackbody outside the PCA passband, equation (3) will not give the correct bolometric flux. Reassuringly, the blackbody model gave a good fit to the vast majority of the burst spectra (e.g. Fig. 5), although we consider that systematic errors of order as large as the bolometric correction may yet be present in the flux estimates presented here. For bursts observed in slews or offset pointings, we rescaled the measured peak flux and fluence by $1/\Delta\theta$, where θ is the offset between the pointing angle and the source position (see appendix A).

Fixing the $n_{\rm H}$ at the mean $\langle n_{{\rm H},i}\rangle$ derived over each burst may introduce additional errors into the burst flux and fluence, if this value is substantially different from the true column towards the source at the time of the burst. Due to its modest low-energy response, the PCA can generally accurately determine the $n_{\rm H}$ only when it is $\gtrsim 10^{22}$ cm^{-2}. Alternative approaches, such as fixing the absorption at the measured Galactic line-of-sight column density, gave poorer fits overall and hence less reliable fit parameters. Furthermore, the local contribution to the line-of-sight $n_{\rm H}$ can vary with time in LMXBs due to changes in the local distribution of matter, and in the absence of contemporaneous measurements by instruments with better low-energy response we must rely on the values measured by the PCA. Errors in the fluence from incorrect $n_{\rm H}$ values for individual time-resolved spectra are likely to average out in the sum, so that the remaining parameter most likely to be affected by this source of error is the peak flux $F_{\rm pk}$. The magnitude of the introduced error is $\approx 10^{-9}$ ergs cm^{-2} s^{-1} per 10^{22} cm^{-2}; that is, for every 10^{22} cm^{-2} we overestimate the column for the spectral fits, we calculate an unabsorbed flux $\approx 10^{-9}$ ergs cm^{-2} s^{-1} larger. We can estimate the magnitude of the error by comparing the peak flux determined from the spectral fits with $n_{\rm H}$ fixed, to those where it is free to vary. We find that these values are consistent for 90% of the bursts, and for the remainder the peak flux with $n_{\rm H}$ fixed is consistently less than the peak flux with $n_{\rm H}$ free to vary. This is because the fitted $n_{\rm H}$ value for a few low signal-to-noise spectra in some (typically very long) bursts are much higher than the mean, resulting in an erroneously large peak (unabsorbed) flux. Thus, through our approach we eliminate fluxes from these spectra by re-fitting with the $n_{\rm H}$ frozen at the mean, and the additional error introduced to the $F_{\rm pk}$ are likely comparable to our estimated uncertainty on those values.

We defined the burst start time t_0 to be the time when the burst flux first exceeded 25% of the peak flux $F_{\rm pk}$ (see e.g. Fig. 3). The rise time $t_{\rm rise}$ is the interval from t_0 to when the burst flux exceeds 90% of $F_{\rm pk}$. These definitions were chosen for ease of implementation and insensitivity to Poisson or systematic variations in the burst rises during, for example, strong radius expansion bursts. We measured the fluence E_b by summing the measured burst fluxes over the duration of the burst. For some long bursts, we found significant emission over the pre-burst level at the end of the interval over which

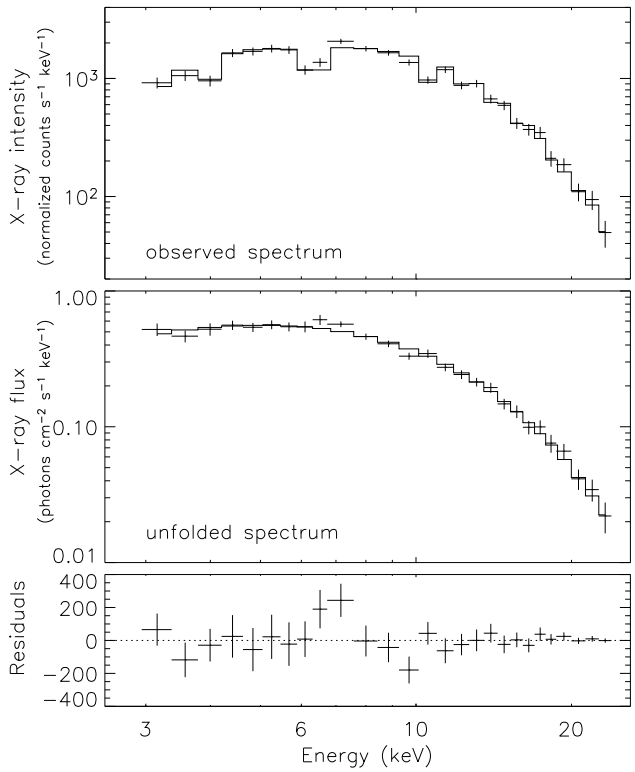

FIG. 5.— Example 0.25-s spectrum from the peak of a burst observed from 4U 1728−34 on 1999 June 30 19:50:14 UT by *RXTE*. The top panel shows the observed spectrum (after subtracting the pre-burst persistent emission), while the middle panel shows the inferred burst spectrum after correcting ("unfolding") for the instrumental response. The histogram in both panels shows the best model fit, in this case a blackbody with color temperature $kT = 2.99 \pm 0.04$ keV and radius $5.09^{+0.13}_{-0.12}$ km (assuming $d = 5.2$ kpc; Table 6) absorbed by neutral material with column density of 6.36×10^{21} cm^{-2} (the mean value derived from spectral fits over the entire burst). The corresponding unabsorbed bolometric flux is $(8.2 \pm 0.2) \times 10^{-8}$ ergs cm^{-2} s^{-1}. Although the measured radius is smaller than expected for a typical neutron-star equation of state, it is important to note that this is an apparent radius which is reduced by biases in the color temperature measurement. The bottom panel shows the residual counts for the fit, with $\chi^2 = 20.5$ for 25 degrees of freedom indicating a statistically good fit. The most noticeable deviations from zero are between 6 and 7 keV, and may originate from fluorescent Fe Kα emission from material surrounding the neutron star.

we extracted burst spectra. In order to extrapolate the burst flux, we fitted a composite exponential curve with decay constant τ_1 throughout the decay from where the burst flux first dropped below 90% of $F_{\rm pk}$. For many bursts, the evolution was not consistent with a single exponential decay, and so we fitted a subsequent exponential curve, with an independent decay constant τ_2 until the end of the burst. We then extrapolated this second decay curve beyond the end of the interval over which we extract burst data, and integrated to estimate the burst flux missed by truncating the high-resolution data. Where this extrapolated contribution to the fluence was greater than the propagated error, we adopted it as the uncertainty instead of the propagated error. Note that the decay curves for most bursts were not statistically consistent with this "broken" exponential model, mainly due to variations on smaller time-scales (for this reason

we do not quote uncertainties for the decay constants τ_1 and τ_2). However, we chose the time ranges to fit the exponential segments so as to qualitatively described the burst decay with as few parameters as possible, even if the actual fit was poor. We also calculated for each burst a simpler, less model-dependent time scale $\tau = E_b/F_{\rm pk}$ traditionally used to characterise burst evolution (e.g. van Paradijs et al. 1988a) for which we estimate the uncertainty by propagating the errors on E_b and $F_{\rm pk}$.

Given the observed (bolometric) integrated burst flux E_b, we estimate the column depth y at which the burst is ignited as

$$y = \frac{L_b d^2 (1+z)}{R_{\rm NS}^2 Q_{\rm nuc}} = 3.0\times10^8 \left(\frac{E_{\rm b}}{10^{-6}\ {\rm ergs\,cm^{-2}}}\right)\left(\frac{Q_{\rm nuc}}{4.4\ {\rm MeV/nucleon}}\right)^{-1} \times \left(\frac{d}{10\ {\rm kpc}}\right)^2 \left(\frac{1+z}{1.31}\right)\left(\frac{R_{\rm NS}}{10\ {\rm km}}\right)^{-2} {\rm g\,cm^{-2}} \quad (4)$$

where $L_b = 4\pi d^2 E_b$ is the total burst luminosity, and $Q_{\rm nuc}$ the energy generation rate (= 4.4 MeV/nucleon for material with solar abundances; e.g. Galloway et al. 2004b). As with the persistent emission, we assume that the burst emission is isotropic.

2.3. *Photospheric radius-expansion*

As a working definition, we considered that radius expansion occurred when 1) the blackbody normalization $K_{\rm bb}$ reached a (local) maximum close to the time of peak flux; 2) lower values of $K_{\rm bb}$ were measured following the maximum, with the decrease significant to 4σ or more; and 3) there was evidence of a (local) decrease in the fitted temperature $T_{\rm bb}$ at the same time as the increase in $K_{\rm bb}$. We examined each of the bursts in the catalog and classified them according to the criteria described above. Bursts where just one or two of these criteria are satisfied represent marginal cases, in which the presence of PRE could not be conclusively established. We note, however, that in the case of 4U 1728−34, the marginal cases have an identical flux distribution as the confirmed radius expansion bursts (Galloway et al. 2003); so this exclusion may be overly conservative.

For spherically symmetric emission, the Eddington luminosity measured by an observer at infinity is given by (Lewin et al. 1993)

$$L_{\rm Edd,\infty} = \frac{8\pi G m_p M_{\rm NS} c[1+(\alpha_{\rm T}T_{\rm e})^{0.86}]}{\sigma_T(1+X)[1+z(R)]} = 2.7\times10^{38}\left(\frac{M_{\rm NS}}{1.4M_\odot}\right)\frac{1+(\alpha_{\rm T}T_{\rm e})^{0.86}}{(1+X)} \times \left[\frac{1+z(R)}{1.31}\right]^{-1} {\rm ergs\,s^{-1}} \quad (5)$$

where $T_{\rm e}$ is the effective temperature of the atmosphere, $\alpha_{\rm T}$ is a coefficient parametrizing the temperature dependence of the electron scattering opacity ($\simeq 2.2\times10^{-9}$ K^{-1}; Lewin et al. 1993), m_p is the mass of the proton, σ_T the Thompson scattering cross-section, and X is the mass fraction of hydrogen in the atmosphere (≈ 0.7 for cosmic abundances). The final factor in square brackets represents the gravitational redshift at the photosphere $1+z(R) = (1-2GM_{\rm NS}/Rc^2)^{-1/2}$, which may be elevated significantly above the NS surface (i.e. $R \geq R_{\rm NS}$). Kuulkers et al. (2003) analysed all bursts detected from the 12 bursters in globular clusters, for which independent distance estimates are available, in order to rigorously test whether the radius-expansion bursts reached a "standard candle" luminosity. They found that for about two-thirds of the sources the radius-expansion bursts reached $3.79\pm0.15\times10^{38}$ ergs s^{-1}. This value is consistent with equation 6 only for H-poor material and where the radius expansion drives the photosphere to very large radii; we note however that the spectral evidence generally does not support the latter condition (e.g. Sugimoto et al. 1984).

Given the observed peak flux of a PRE burst $F_{\rm pk,PRE}$, we estimated the distance as

$$d = \sqrt{\frac{L_{\rm Edd,\infty}}{4\pi F_{\rm pk,RE}}} = 8.6\left(\frac{F_{\rm pk,RE}}{3\times10^{-8}\ {\rm ergs\,cm^{-2}\,s^{-1}}}\right)^{-1/2}\left(\frac{M_{\rm NS}}{1.4M_\odot}\right)^{1/2} \times \left[\frac{1+z(R)}{1.31}\right]^{-1/2}(1+X)^{-1/2}\ {\rm kpc} \quad (6)$$

We discuss the properties of the radius-expansion bursts in §4.4.

2.4. *Burst oscillations*

We searched for burst oscillations in data recorded with 2^{-13} s (122 μs) time resolution. We computed fast Fourier transforms of each 1 s interval of data for the first 15 s of the burst, and searched for signals in bursts from sources known to exhibit burst oscillations within 5 Hz of the oscillation frequencies listed in Table 4. We considered a signal to be a detection if it had less than a 1% chance of occurring due to noise given the 160 trial frequencies searched for each burst. A signal was considered significant if it passed any of three tests: (1) having a probability of $< 6\times10^{-5}$ that it was produced by noise in a single trial, (2) persisting for two adjacent time and frequency bins with a chance probability of $< (6\times10^{-5})^{1/2}/6 = 1.3\times10^{-3}$, or (3) occurring in the first second of a burst with a chance probability of $< 10^{-3}$.

If oscillations were detected during a burst, we then determined whether they were observed during the rise, peak or decay of the burst. We defined these characteristic times during the burst using data with 0.25 s time resolution. The rise of the burst was defined to start 0.25 s before the first time bin in which the count rate rose above 25 % of the peak count rate, and ended in the last time bin for which the count rate was less than 90% of the peak count rate. The peak of the burst was defined to last from the end of the rise until the count rate dropped back below 90% of the peak count rate. The decay of the burst commenced at the end of the peak, and lasted through to the end of the high-time resolution data (typically *la*200 s duration).

Figure 3 illustrates how these times were defined for a burst from 4U 1702–429. Oscillations were detected during the rise and decay of this burst, but not during the peak. Note that the over-sampled dynamic power

spectrum displayed in this figure was not used to search for oscillations; only non-overlapping power spectra were used for the oscillation search. Where oscillations were not detected in any of the 1-s intervals, we also computed FFTs of 4-s intervals covering the burst. We used a probability threshold of 10^{-3} to determine when the oscillations occurred, corresponding to a 1% chance of observing a spurious signal during each 1 s interval (10 trial frequencies).

We computed the amplitudes of the oscillations according to

$$A = \left(\frac{P}{I_\gamma}\right)^{1/2} \frac{I_\gamma}{I_\gamma - B_\gamma}, \quad (7)$$

where P is the power from the Fourier spectrum, I_γ is the total number of counts in the profile, and B_γ is the estimated number of background counts. We estimated the background using the mean count rate 16 seconds prior to the start of the burst. Since the detection threshold is a fixed power, the minimum detectable amplitude depends on the number of counts produced by a burst. We discuss the global properties of the bursts from burst oscillation sources in §4.5.

2.5. *Combined burst samples*

We combined samples of bursts from different sources using two separate measures of the accretion rate $\dot{M}$. First, we calculated the mean peak flux $\langle F_{\rm pk,PRE}\rangle$ of the radius-expansion bursts from each source that exhibited at least one. We identify this value as the flux corresponding to the Eddington luminosity for that source, $F_{\rm Edd}$. For each observation we then calculated the dimensionless persistent flux $\gamma = F_p/F_{\rm Edd}$, rescaling the measured persistent flux (see §2.1) by the $F_{\rm Edd}$ for that source (this approach follows van Paradijs et al. 1988a). We excluded sources for which the PCA field of view contains other active sources, since we cannot reliably estimate the persistent flux in those cases (GRS 1741.9−2853, 2E 1742.9−2929 and SAX J1747.0−2853). Ideally, γ is approximately equal to the accretion rate as a fraction of the Eddington rate, i.e. $\gamma \approx \dot{M}/\dot{M}_{\rm Edd}$. This approach has the advantage of being independent of assumptions about exactly what is the value of the Eddington limit reached by the bursts. The principal drawback is that it is only possible for those sources with at least one detected PRE burst. We also neglect the precise bolometric correction $c_{\rm bol}$ for each observation, which introduces an error up to a factor of two (see §2.1). We also calculated the normalized peak burst flux $U_p = F_{\rm pk}/F_{\rm Edd}$ and fluence $U_b = E_b/F_{\rm Edd}$ in order to measure the combined distribution of those parameters in §4.4. For reference, $\gamma = 0.1$ corresponds to between 1.6–3.5 $\times 10^{37}$ ergs s^{-1} (depending upon the maximum radius R and atmospheric composition X in Equation 5).

There is substantial evidence that F_p may not strictly track $\dot{M}$ (e.g. Hasinger & van der Klis 1989), so that γ may not be the best available measure of $\dot{M}$. Thus, we assembled a second combined sample of bursts from only the sources with a well-defined color-color diagram, and instead adopted the position along the color-color diagram S_Z as a proxy for $\dot{M}$ (see §2.1). We show in Fig. 6 the comparison between the observation-averaged S_Z and γ for eight of the nine sources with well-defined color-color diagrams. For most of the sources, S_Z was proportional to γ when $S_Z < 1$ (upper or "island" horizontal branch in Fig. 4) and $S_Z > 2$ (lower or "banana" branch). However, between these two branches γ is essentially constant at between 0.006 and 0.06, indicating that the transition between the two branches takes place at a roughly constant flux. For two sources, 4U 1608−52 and KS 1731−26, the relationship is more complex, and some observations with very hard spectra ($S_Z \approx 2$) actually have very low γ.

We measured mean burst rates for the combined burst sample as a function of γ (and for selected sources, S_Z). In order to guarantee reasonable statistics, we defined bins such that some minimum number of bursts fell into each bin. We then calculated the mean burst rate within each bin as the number of bursts divided by the total duration of observations which also fell into that bin. We also measured recurrence times $t_{\rm rec}$ from a third sample of successive pairs of bursts, and calculated the instantaneous burst rate as $1/t_{\rm rec}$. In general the measured separation of a pair of bursts is an upper limit on the recurrence time, due to the possibility of missing intervening events in data gaps arising from Earth occultations. Additional gaps arise from satellite passages through the South Atlantic Anomaly (SAA), during which the PCA is turned off to protect the electronics from damage. We can estimate the recurrence time with more confidence when the burst separation is comparable to the typical uninterrupted observation length ($\sim$ 1 hr) or where the source is bursting regularly. We note that this sample omits the bursts with very short recurrence times $<$ 30 min; see §4.2.

We also calculated mean α-values for the combined sample, as a function of γ and S_Z. By substituting expressions 4 and 2 into the simple equality $y = \dot{m}\Delta t$ (assuming implicitly that all the accreted fuel is burnt during the burst) we can calculate α from the measurable quantities:

$$\begin{aligned}\alpha &= F_p c_{\rm bol} \Delta t / E_b \\ &= \frac{Q_{\rm grav}}{Q_{\rm nuc}} (1+z) \\ &= 44 \left(\frac{M}{1.4 M_\odot}\right) \left(\frac{R}{10 \text{ km}}\right)^{-1} \left(\frac{Q_{\rm nuc}}{4.4 \text{ MeV/nucleon}}\right)^{-1} \quad (8)\end{aligned}$$

We estimated the mean α for the bursts arising from observations which fall in a bin j (defined as a range in γ or S_Z, as the case may be) as $\alpha_j = \sum(\gamma_i t_i)/\sum U_b$, where t_i is the duration of each observation i with $\gamma = \gamma_i$. Actually, this α is an underestimate of the true value, since γ is calculated from the 2.5–25 keV flux, which broad-band spectral fits indicate contributes 60–90% of the bolometric persistent flux, depending upon the source and the spectral state. In parallel with the burst rates, we also measured the α values for selected pairs of bursts. For individual measurements, we determined the bolometric correction (see §2.1) and calculated α according to equation 8. We discuss the variations in burst properties, including α, as a function of $\dot{m}$ in §4.1.

3. THERMONUCLEAR X-RAY BURSTS OBSERVED BY RXTE

We summarise the numbers of bursts from individual sources in Table 1. The sky distribution of bursters is

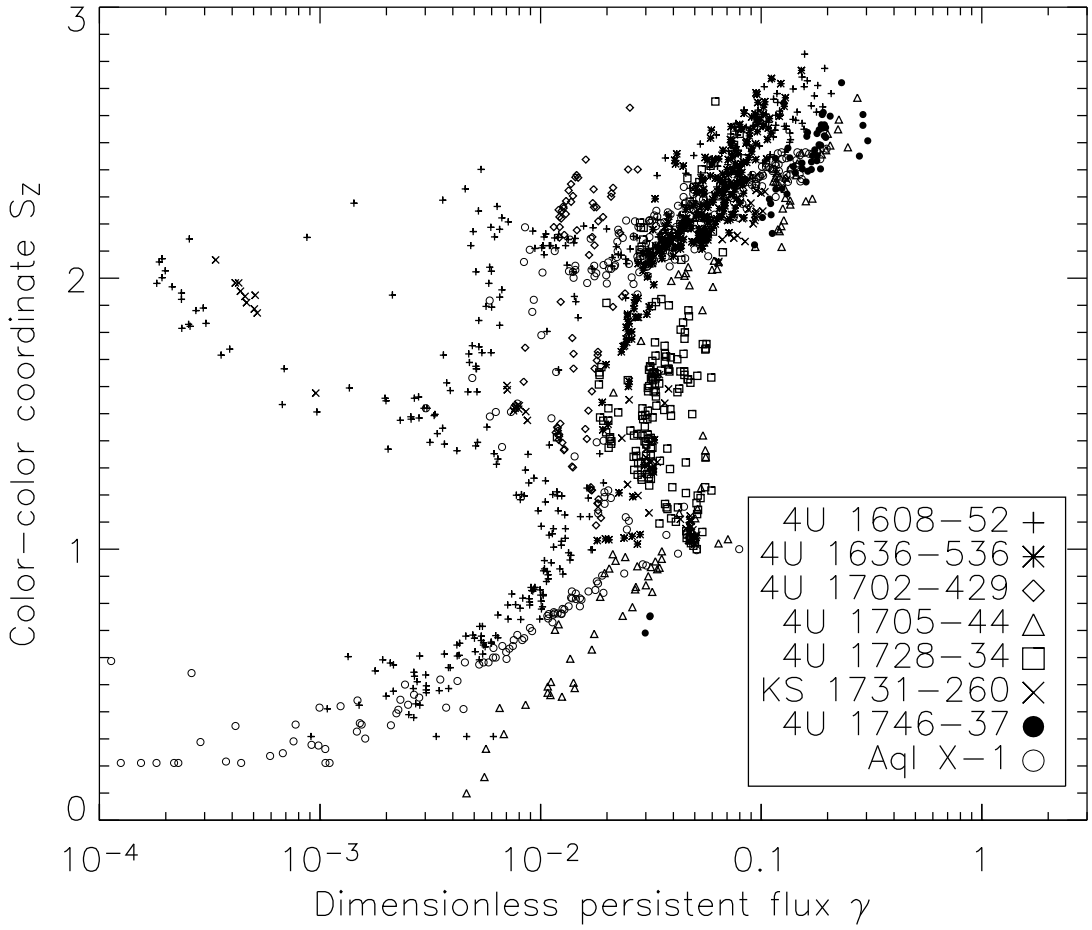

FIG. 6.— Comparison of the two parameters used in §4.1 as proxies for $\dot{M}$ to combine bursts from different sources. The position along the color-color track, S_Z (averaged over each observation) is plotted against the normalised persistent flux $\gamma \equiv F_{\rm p}/F_{\rm Edd}$ for eight of the nine sources with well-defined color-color diagrams. XTE J2123−058 is excluded since no PRE bursts were detected, and thus γ cannot be determined. The two parameters are roughly proportional at high and low S_Z for all sources (in the upper and lower branches of the color-color diagrams in Fig. 4), but in the range $S_Z \simeq 1$–2 γ is approximately constant or varies over a wide range, depending upon the source.

shown in Fig. 7. For each source with bursts observed by *RXTE* we list the relevant analysis results in Table 2. The superscript to the burst number indicates a range of potential analysis issues, as follows:

a The burst was observed during a slew, and thus offset from the source position.

b The observation was offset from the source position. In cases (a) and (b) we scaled the flux and fluence by the mean collimator response appropriate for the position of the source in the field of view, as described in appendix A.

c The origin of the burst is uncertain; the burst may have been from another source in the field-of-view (we rescaled the flux and fluence, if necessary, based upon the assumed origin);

d Buffer overruns (or some other instrumental effect) caused gaps in the data;

e The burst was so faint that only the peak flux could be measured, and not the fluence or other parameters;

f An extremely faint burst or possibly problems with the background subtraction, resulting in no fit results;

g the full burst profile was not observed, so that the event can be considered an unconfirmed burst candidate. Typically in these cases the initial burst rise is missed, so that the measured peak flux and fluence are lower limits only;

h High-time resolution datamodes did not cover the burst.

Column (2) lists the ID for the observation during which the burst was observed; (3) the burst start time in UT and MJD (we neglect corrections to give the time at the solar-system barycenter), in UT (TDB); (4) the peak flux, in units of 10^{-9} ergs cm^{-2} s^{-1}; (5) the fluence, in units of 10^{-6} ergs cm^{-2}; (6) the presence of radius expansion; (7) rise time (s); (8) peak count rate, per PCU; (9,10) the exponential decay constants for the tail of the burst, where available; (11) burst time scale ($E_{\rm b}/F_{\rm pk}$); and (12) burst fluence normalized by the mean peak flux of the PRE bursts $F_{\rm Edd}$, where available (U_b in

TABLE 1
Type-I X-ray burst sources observed by *RXTE*

Source	RA	Dec	Location	$n_{\rm obs}$	Time (ks)	$n_{\rm burst}$	Mean burst rate ($\rm hr^{-1}$)	$n_{\rm RE}$
4U 0513−40	05 14 6.60	-40 02 37.0	NGC 1851	461	1010	6	0.021	
EXO 0748−676	07 48 33.80	-67 45 8.0		364	1140	84	0.26	3
1M 0836−425	08 37 22.70	-42 53 8.0		26	139	17	0.44	
4U 0919−54	09 20 26.80	-55 12 24.0		40	330	4	0.044	1
4U 1254−69	12 57 37.20	-69 17 20.0		26	279	5	0.064	
4U 1323−62	13 26 36.10	-62 08 10.0		12	218	24	0.40	
4U 1608−52	16 12 42.90	-52 25 22.0		485	1590	31	0.070	12
4U 1636−536	16 40 55.50	-53 45 5.0		270	2390	123	0.19	40
MXB 1659−298	17 02 6.30	-29 56 45.0		80	356	26	0.26	12
4U 1702−429	17 06 15.20	-43 02 9.0		181	1220	44	0.13	4
4U 1705−44	17 08 54.60	-44 06 2.0		101	523	39	0.27	3
XTE J1709−267	17 09 30.20	-26 39 27.0		39	145	3	0.075	
XTE J1710−281	17 10 12.40	-28 07 54.0		43	193	15	0.28	1
XTE J1723−376	17 23 38.00	-37 39 42.0		4	34.1	3	0.32	
4U 1724−307	17 27 33.20	-30 48 7.0	Terzan 2	92	510	3	0.021	2
4U 1728−34	17 31 57.30	-33 50 4.0		341[a]	1910[a]	105	0.20	69
Rapid Burster	17 33 24.00	-33 23 16.0	Liller 1	340[a]	1870[a]	65	0.13	
KS 1731−260	17 34 13.00	-26 05 9.0		80	497	27	0.20	4
SLX 1735−269	17 38 16.00	-27 00 18.0		49	252	1	0.014	
4U 1735−44	17 38 58.20	-44 26 59.0		82	454	11	0.087	6
KS 1741−293	17 44 49.20	-29 21 6.0		442[b]	2050[b]	1	0.0018	
GRS 1741.9−2853	17 45 0.56	-28 54 6.5		430[b]	2030[b]	8	0.014	6
2E 1742.9−2929	17 46 6.20	-29 31 5.0		430[b]	2030[b]	84	0.15	2
SAX J1747.0−2853	17 47 2.60	-28 52 58.9		423[b]	2050[b]	17	0.030	10
SLX 1744−300	17 47 25.90	-30 02 30.0		39[b]	290[b]	3	0.037	
GX 3+1	17 47 56.00	-26 33 48.0		95	506	2	0.014	1
SAX J1748.9−2021	17 48 53.40	-20 21 43.0	NGC 6440	18	130	16	0.44	6
EXO 1745−248	17 48 55.70	-24 53 40.0	Terzan 5	51	148	22	0.54	2
4U 1746−37	17 50 12.60	-37 03 8.0	NGC 6441	50	441	30	0.24	3
SAX J1750.8−2900	17 50 24.00	-29 02 18.0		32[b]	118[b]	4	0.12	2
GRS 1747−312	17 50 45.50	-31 17 32.0	Terzan 6	102[a]	651[a]	6	0.033	3
XTE J1759−220	17 59 42.00	-22 01 0.0		17	107	1	0.034	
SAX J1808.4−3658	18 08 27.54	-36 58 44.3		285	1210	4	0.012	4
XTE J1814−338	18 13 40.00	-33 46 0.0		90	447	28	0.23	
GX 17+2	18 16 1.30	-14 02 11.0		140	898	12	0.048	2
3A 1820−303	18 23 40.50	-30 21 40.0	NGC 6624	152	1100	4	0.013	4
GS 1826−24	18 29 27.00	-23 47 29.0		76	574	40	0.25	
XB 1832−330	18 35 44.10	-32 59 29.0	NGC 6652	12	99	1	0.036	1
Ser X-1	18 39 57.50	+05 02 8.0		40	244	7	0.10	2
HETE J1900.1−2455	19 00 8.65	-24 55 13.7		87	278	2	0.026	2
Aql X-1	19 11 15.90	+00 35 6.0		354[a]	1480[a]	40	0.10	9
4U 1916−053	19 18 47.90	-05 14 8.0		51	412	14	0.12	12
XTE J2123−058	21 23 16.10	-05 47 30.0		5	67.2	6	0.32	
4U 2129+12	21 29 58.30	+12 10 2.0	M15	32	343	1	0.010	1
Cyg X-2	21 44 41.20	+38 19 18.0		218	1390	46	0.12	5
Total (45 sources)						1035		234

[a]For sources with a neighbor within 1°, we combine all observations which include this source within the field of view (possibly including observations of the neighbor).
[b]Similarly, for sources towards the Galactic center, we combine all observations which include the source in the field of view to calculate the mean burst rate.

van Paradijs et al. 1988a). From analysis of the persistent spectrum, excluding the bursts (see §2.1) we list in column (13) the persistent flux level prior to the burst (2.5–25 keV, units of 10^{-9} ergs $\rm cm^{-2}\,s^{-1}$); (14) the persistent flux normalised by $F_{\rm Edd}$ (γ in van Paradijs et al. 1988a); (15,16) soft and hard color prior to the burst; and (17) position on the color-color diagram, where available. From estimates of the recurrence times of regular and/or approximately contemporaneous bursts from a subset of 22 sources, we compiled a set of 175 $t_{\rm rec}$ values from which we derived (18) the inferred burst recurrence time Δt; using this value and (19) the correction $c_{\rm bol}$ used to estimate the bolometric flux from the measured 2.5–25 keV persistent flux, we derived (20) the corresponding α-value, calculated according to equation 8. Finally, in column (21) we list references to previously published analyses of the burst. Note that we do not list values for columns 12–17 for those observations where we expect that more than one source is active in the field (see appendix A).

We plot the ASM intensity and burst activity of selected sources in Fig. 8. We also plot individual bursts for all sources with more than one burst in Fig. 9. Note that only the bursts with time-resolved spectral information are plotted; this excludes bursts flagged with superscripts e, f, g, h, and i in Table 2. We have also searched for bursts in the observations of two new transient sources detected by

Table 2. Thermonuclear X-ray bursts observed by *RXTE*

(1)	(2)	(3)		(4)	(5)	(6)	(7)	(8)	(9)	(10)	(11)	(12)	(13)	(14)	(15)	(16)	(17)	(18)	(19)	(20)	(21)
		Start time		Peak flux	Fluence		Rise	Peak count			Time-	Normalized	$F_{\rm per}$ (2.5–25 keV,	Normalized	Soft	Hard		Inferred			
ID	Obs ID	UT	MJD	10^{-9} ergs cm^{-2} s^{-1}	10^{-6} ergs cm^{-2}	PRE?	time (s)	rate (PCU^{-1})	τ_1	τ_2	scale	fluence	10^{-9} ergs cm^{-2} s^{-1})	$F_{\rm per}$	color	color	S_Z	Δt (hr)	$c_{\rm bol}$	α	Refs
4U 0513−40																					
1	10078-02-01-02	1996 Mar 9 14:47:27	50151.61629	11.1 ± 0.6	0.095 ± 0.003	N	1.25 ± 0.18	970	5.25	14.2	8.5 ± 0.5	···	0.336 ± 0.005	···	1.51 ± 0.03	0.540 ± 0.011	···	···	···	···	
2	40404-01-07-05	1999 May 26 06:53:12	51324.28695	13.0 ± 0.5	0.1392 ± 0.0016	N	0.5 ± 0.4	1069	5.18	19.2	10.7 ± 0.4	···	0.201 ± 0.004	···	1.48 ± 0.04	0.452 ± 0.017	···	···	···	···	[1]
3	40404-01-12-11	2000 Feb 7 17:54:18	51581.74605	14.8 ± 0.6	0.195 ± 0.005	?	1.5 ± 0.4	1198	5.90	11.9	13.2 ± 0.7	···	0.268 ± 0.006	···	1.59 ± 0.04	0.529 ± 0.016	···	···	···	···	
4	50403-01-01-00	2000 Mar 19 10:55:49	51622.45543	15.2 ± 0.6	0.144 ± 0.004	N	2.0 ± 0.7	1242	6.57	···	9.5 ± 0.4	···	0.327 ± 0.005	···	1.50 ± 0.04	0.540 ± 0.019	···	···	···	···	
5	70403-01-01-00	2002 Mar 18 13:50:26	52351.57670	13.8 ± 0.4	0.1151 ± 0.0016	N	2.0 ± 0.7	1355	2.98	16.8	8.4 ± 0.3	···	0.650 ± 0.010	···	1.47 ± 0.03	0.552 ± 0.011	···	···	···	···	
6	91402-01-01-00	2005 Mar 13 02:06:01	53442.08752	17.0 ± 0.5	0.125 ± 0.003	?	1.0 ± 0.4	1680	4.43	···	7.4 ± 0.3	···	0.642 ± 0.008	···	1.41 ± 0.07	0.51 ± 0.03	···	···	···	···	
EXO 0748−676																					
1	10108-01-10-00	1996 Aug 15 17:38:54	50310.73536	1.92 ± 0.07	0.0353 ± 0.0007	N	8.0 ± 1.4	254	8.64	···	18.4 ± 0.8	0.85 ± 0.11	0.227 ± 0.008	0.0055 ± 0.0007	3.18 ± 0.18	1.04 ± 0.02	···	···	···	···	
2	10108-01-10-00	1996 Aug 15 17:55:56	50310.74719	5.9 ± 0.2	0.0838 ± 0.0012	N	3.5 ± 0.4	599	8.60	52.6	14.2 ± 0.5	2.0 ± 0.2	0.227 ± 0.008	0.0055 ± 0.0007	2.12 ± 0.06	0.941 ± 0.017	···	0.284	1.93 ± 0.02	5.350 ± 0.010	
3	10108-01-07-01	1996 Aug 15 21:47:35	50310.90805	8.2 ± 0.4	0.259 ± 0.015	N	7.50 ± 0.18	703	12.5	62.7	31 ± 2	6.3 ± 0.9	0.277 ± 0.005	0.0067 ± 0.0008	1.92 ± 0.05	0.938 ± 0.015	···	3.86	1.93 ± 0.02	28.63 ± 0.11	
4	10108-01-12-00	1996 Oct 2 06:04:50	50358.25337	12.9 ± 0.4	0.182 ± 0.002	N	3.5 ± 0.4	1135	8.17	28.6	14.1 ± 0.5	4.4 ± 0.5	0.287 ± 0.005	0.0069 ± 0.0009	2.32 ± 0.13	0.96 ± 0.03	···	···	···	···	
5	10108-01-13-00	1996 Oct 2 09:25:56	50358.39302	9.9 ± 0.3	0.1884 ± 0.0016	N	3.0 ± 0.4	874	5.91	32.9	19.0 ± 0.7	4.5 ± 0.6	0.277 ± 0.003	0.0067 ± 0.0008	2.22 ± 0.06	0.961 ± 0.016	···	3.35	1.93 ± 0.02	34.250 ± 0.010	
6	20069-04-03-00	1997 May 1 19:56:43	50569.83106	16.3 ± 0.7	0.3145 ± 0.0015	N	5.00 ± 0.18	1320	6.65	28.4	19.3 ± 0.8	7.6 ± 0.9	0.187 ± 0.003	0.0045 ± 0.0006	1.74 ± 0.05	0.870 ± 0.019	···	···	···	···	
7	20082-01-01-00	1997 Aug 13 23:05:04	50673.96185	11.4 ± 0.4	0.251 ± 0.004	N	3.5 ± 0.4	1041	9.7	41.0	22.0 ± 0.8	6.1 ± 0.7	0.287 ± 0.004	0.0069 ± 0.0009	1.86 ± 0.05	0.889 ± 0.019	···	···	···	···	
8	20082-01-02-00	1997 Aug 17 15:08:28	50677.63089	14.0 ± 0.5	0.347 ± 0.011	N	5.25 ± 0.18	1142	10.1	46.8	24.8 ± 1.2	8.4 ± 1.1	0.296 ± 0.003	0.0072 ± 0.0009	1.77 ± 0.05	0.91 ± 0.02	···	···	···	···	
9	20082-01-02-00	1997 Aug 18 02:05:55	50678.08744	12.2 ± 0.5	0.288 ± 0.002	N	4.0 ± 0.4	1149	8.23	39.7	23.6 ± 1.0	7.0 ± 0.9	0.296 ± 0.003	0.0072 ± 0.0009	2.08 ± 0.09	0.92 ± 0.02	···	···	···	···	
10	30067-08-01-00	1998 Mar 13 23:22:25	50885.97391	11.3 ± 0.3	0.328 ± 0.005	N	4.5 ± 0.4	1063	11.0	45.5	29.0 ± 1.0	7.9 ± 1.0	0.299 ± 0.017	0.0072 ± 0.0010	1.82 ± 0.06	0.910 ± 0.019	···	···	···	···	
11	30067-09-01-00	1998 Jun 28 15:14:35	50992.63513	14.4 ± 0.5	0.300 ± 0.002	N	4.50 ± 0.18	1302	11.6	37.1	20.9 ± 0.7	7.2 ± 0.9	0.288 ± 0.002	0.0069 ± 0.0009	1.71 ± 0.05	0.850 ± 0.017	···	···	···	···	
12	30067-09-01-00	1998 Jun 28 15:28:18	50992.64466	11.4 ± 0.3	0.1370 ± 0.0014	N	2.0 ± 0.4	984	5.84	20.6	12.0 ± 0.4	3.3 ± 0.4	0.288 ± 0.002	0.0069 ± 0.0009	2.33 ± 0.11	0.93 ± 0.02	···	0.229	1.93 ± 0.02	3.3	
13	30067-12-01-00	1998 Dec 10 06:19:08	51157.26329	10.1 ± 0.4	0.220 ± 0.004	N	4.5 ± 0.4	892	8.02	47.8	21.8 ± 0.9	5.3 ± 0.7	0.277 ± 0.004	0.0067 ± 0.0008	2.19 ± 0.09	0.94 ± 0.02	···	···	···	···	
14	40039-03-04-00	1999 May 11 22:30:37	51309.93793	12.1 ± 0.5	0.1988 ± 0.0018	N	2.0 ± 0.4	1129	6.41	27.7	16.4 ± 0.7	4.8 ± 0.6	0.2973 ± 0.0020	0.0072 ± 0.0009	2.14 ± 0.12	0.90 ± 0.03	···	···	···	···	
15	40039-04-04-00	1999 Jul 5 02:53:29	51364.12049	0.20 ± 0.03	0.0056 ± 0.0006	?	8.0 ± 1.4	57	29.2	···	29 ± 6	0.14 ± 0.02	0.265 ± 0.015	0.0064 ± 0.0009	2.85 ± 0.19	1.00 ± 0.03	···	···	···	···	
16	40039-04-05-00	1999 Jul 5 06:38:48	51364.27694	6.06 ± 0.18	0.173 ± 0.003	N	8.0 ± 0.7	614	11.6	46.2	28.6 ± 1.0	4.2 ± 0.5	0.241 ± 0.005	0.0058 ± 0.0007	2.36 ± 0.11	0.97 ± 0.02	···	3.76	1.93 ± 0.02	36.31 ± 0.03	
17	40039-05-02-00	1999 Aug 21 14:24:48	51411.60057	3.68 ± 0.11	0.0683 ± 0.0011	N	6.0 ± 0.7	405	7.78	32.8	18.6 ± 0.6	1.6 ± 0.2	0.235 ± 0.002	0.0057 ± 0.0007	1.94 ± 0.06	0.845 ± 0.019	···	···	···	···	
18	40039-06-01-00	1999 Oct 17 04:10:57	51468.17428	0.94 ± 0.04	0.094 ± 0.014	N	4.0 ± 1.4	143	98	···	100 ± 16	2.3 ± 0.4	0.238 ± 0.008	0.0057 ± 0.0007	2.7 ± 0.8	0.40 ± 0.09	···	···	···	···	
19[e]	50045-01-04-00	2000 Mar 29 06:56:31	51632.28926	0.61 ± 0.04	···	N	2.0 ± 1.4	102	···	···	···	···	0.360 ± 0.009	0.0087 ± 0.0011	3.1 ± 0.9	0.42 ± 0.10	···	···	···	···	
20	50045-03-02-00	2000 Jul 11 11:47:43	51736.49148	5.86 ± 0.17	0.137 ± 0.015	N	5.5 ± 0.4	641	7.70	31.3	23 ± 3	3.3 ± 0.5	0.41 ± 0.05	0.0099 ± 0.0018	1.85 ± 0.04	0.938 ± 0.015	···	···	···	···	
21	50045-03-05-00	2000 Jul 12 03:06:22	51737.12942	8.2 ± 0.3	0.105 ± 0.012	N	3.0 ± 0.4	757	7.17	···	12.8 ± 1.5	2.5 ± 0.4	0.44 ± 0.02	0.0106 ± 0.0014	1.91 ± 0.05	0.899 ± 0.016	···	···	···	···	
22	50045-04-03-00	2000 Aug 29 09:51:41	51785.41090	0.15 ± 0.02	0.0030 ± 0.0014	?	6.0 ± 1.4	51	14.9	···	20 ± 10	0.07 ± 0.04	0.331 ± 0.004	0.0080 ± 0.0010	2.60 ± 0.11	0.97 ± 0.02	···	···	···	···	
23	50045-06-01-00	2000 Dec 17 20:14:35	51895.84346	9.0 ± 0.3	0.20 ± 0.05	?	7.0 ± 0.4	831	16.6	···	23 ± 6	4.9 ± 1.3	0.247 ± 0.004	0.0060 ± 0.0007	1.92 ± 0.06	0.947 ± 0.020	···	···	···	···	
24	50045-06-02-00	2000 Dec 17 23:53:34	51895.99553	1.88 ± 0.06	0.113 ± 0.011	?	4.0 ± 1.4	237	44.1	77.2	60 ± 6	2.7 ± 0.4	0.204 ± 0.005	0.0049 ± 0.0006	1.0 ± 0.5	1.2 ± 1.0	···	3.65	1.93 ± 0.02	45.9 ± 0.5	
25	50045-06-05-00	2000 Dec 18 15:11:15	51896.63282	0.65 ± 0.04	0.08 ± 0.02	?	12.0 ± 1.4	122	136	···	130 ± 30	2.0 ± 0.6	0.266 ± 0.003	0.0064 ± 0.0008	3.0 ± 1.1	0.51 ± 0.11	···	···	···	···	
26	60047-03-02-00	2001 Jul 8 04:24:21	52098.18359	2.95 ± 0.08	0.0490 ± 0.0009	N	10.0 ± 1.4	373	8.48	18.7	16.6 ± 0.6	1.18 ± 0.15	0.262 ± 0.006	0.0063 ± 0.0008	2.19 ± 0.09	0.89 ± 0.02	···	···	···	···	
27	60047-04-04-00	2001 Aug 31 12:45:43	52152.53175	9.5 ± 0.3	0.193 ± 0.008	N	3.5 ± 0.4	946	7.91	38.9	20.2 ± 1.0	4.7 ± 0.6	0.302 ± 0.003	0.0073 ± 0.0009	1.45 ± 0.05	0.74 ± 0.03	···	···	···	···	
28	60047-05-01-00	2001 Oct 24 20:17:30	52206.84550	2.23 ± 0.11	0.0505 ± 0.0013	N	5.0 ± 0.7	287	11.1	···	22.6 ± 1.3	1.22 ± 0.15	0.293 ± 0.006	0.0071 ± 0.0009	1.81 ± 0.07	0.80 ± 0.02	···	···	···	···	
29	60047-05-04-00	2001 Oct 25 07:54:31	52207.32954	9.9 ± 0.3	0.2046 ± 0.0017	N	3.5 ± 0.4	989	6.95	33.2	20.7 ± 0.7	4.9 ± 0.6	0.244 ± 0.005	0.0059 ± 0.0007	2.48 ± 0.13	0.88 ± 0.03	···	···	···	···	
30[e]	60047-06-01-00	2001 Dec 15 19:03:59	52258.79443	0.30 ± 0.06	···	?	> 2.00	92	···	···	···	···	0.223 ± 0.004	0.0054 ± 0.0007	2.48 ± 0.19	0.97 ± 0.04	···	···	···	···	
31	70048-03-03-00	2002 Apr 20 12:34:20	52384.52385	6.4 ± 0.4	0.127 ± 0.002	N	6.50 ± 0.18	646	5.74	34.6	20.0 ± 1.3	3.1 ± 0.4	0.37 ± 0.08	0.009 ± 0.002	1.2 ± 0.6	1.1 ± 0.2	···	···	···	···	
32	70048-04-04-00	2002 May 21 21:38:43	52415.90190	4.26 ± 0.14	0.0560 ± 0.0013	N	4.0 ± 1.4	457	8.24	···	13.1 ± 0.5	1.35 ± 0.17	0.400 ± 0.005	0.0097 ± 0.0012	2.9 ± 0.5	0.94 ± 0.06	···	···	···	···	
33[d]	70048-05-02-00	2002 Jun 29 18:56:15	52454.78907	0.19 ± 0.04	0.0028 ± 0.0004	N	4.0 ± 1.4	56	7.07	···	14 ± 3	0.067 ± 0.012	0.325 ± 0.011	0.0078 ± 0.0010	1.76 ± 0.14	0.92 ± 0.05	···	···	···	···	
34	70048-06-04-00	2002 Aug 2 02:22:09	52488.09872	5.46 ± 0.17	0.193 ± 0.008	N	7.0 ± 0.7	588	9.6	52.3	35.4 ± 1.8	4.7 ± 0.6	0.29 ± 0.02	0.0071 ± 0.0010	2.12 ± 0.07	0.94 ± 0.02	···	···	···	···	
35	70048-07-01-00	2002 Aug 31 21:24:03	52517.89170	8.9 ± 0.5	0.169 ± 0.018	N	4.25 ± 0.18	772	12.0	25.8	19 ± 2	4.1 ± 0.7	0.306 ± 0.003	0.0074 ± 0.0009	1.9 ± 1.0	0.9 ± 0.2	···	···	···	···	
36	70048-08-02-00	2002 Oct 10 09:17:12	52557.38696	8.9 ± 0.2	0.27 ± 0.04	N	8.0 ± 0.7	853	15.5	33.3	30 ± 5	6.4 ± 1.3	0.304 ± 0.009	0.0073 ± 0.0009	1.7 ± 0.2	0.86 ± 0.09	···	···	···	···	
37	70048-09-02-00	2002 Nov 9 16:08:48	52587.67278	6.5 ± 0.3	0.1015 ± 0.0012	N	5.0 ± 0.7	715	9.6	···	15.6 ± 0.7	2.4 ± 0.3	0.2304 ± 0.0008	0.0056 ± 0.0007	2.14 ± 0.10	0.90 ± 0.03	···	···	···	···	
38	60042-03-01-01	2002 Dec 4 20:17:22	52612.84540	8.2 ± 0.3	0.22 ± 0.04	N	6.0 ± 0.4	761	11.1	40.5	27 ± 5	5.3 ± 1.2	0.28 ± 0.02	0.0067 ± 0.0010	4.0 ± 0.5	1.07 ± 0.03	···	···	···	···	
39	60042-03-01-01	2002 Dec 5 00:48:22	52613.03359	7.6 ± 0.3	0.1050 ± 0.0009	N	2.5 ± 0.4	740	9.26	···	13.7 ± 0.6	2.5 ± 0.3	0.28 ± 0.02	0.0067 ± 0.0010	2.39 ± 0.12	0.90 ± 0.02	···	···	···	···	
40	60042-03-02-04	2002 Dec 6 00:37:28	52614.02603	9.1 ± 0.3	0.178 ± 0.014	N	6.0 ± 0.7	914	4.03	20.2	19.5 ± 1.7	4.3 ± 0.6	0.342 ± 0.006	0.0082 ± 0.0010	1.86 ± 0.06	0.91 ± 0.02	···	···	···	···	
41	60042-03-02-03	2002 Dec 7 01:29:09	52615.06192	14.8 ± 0.6	0.1476 ± 0.0015	N	2.5 ± 0.4	1341	6.89	···	10.0 ± 0.4	3.6 ± 0.4	0.286 ± 0.004	0.0069 ± 0.0009	3.3 ± 0.3	1.03 ± 0.03	···	···	···	···	
42	60042-03-02-02	2002 Dec 7 22:14:13	52615.92655	9.0 ± 0.3	0.21 ± 0.03	N	3.0 ± 0.7	882	7.24	29.8	23 ± 3	5.0 ± 0.9	0.272 ± 0.007	0.0066 ± 0.0008	1.74 ± 0.06	0.84 ± 0.02	···	···	···	···	
43	60042-03-02-01	2002 Dec 9 01:21:34	52617.05664	7.4 ± 0.3	0.20 ± 0.04	N	5.5 ± 0.4	684	11.6	40.9	27 ± 6	4.8 ± 1.1	0.258 ± 0.011	0.0062 ± 0.0008	2.17 ± 0.15	0.89 ± 0.04	···	···	···	···	
44	70048-10-01-00	2002 Dec 12 15:35:50	52620.64988	7.5 ± 0.3	0.20 ± 0.03	N	6.0 ± 0.7	765	10.6	29.4	26 ± 4	4.8 ± 0.9	0.206 ± 0.010	0.0050 ± 0.0007	2.14 ± 0.13	0.86 ± 0.04	···	···	···	···	
45	70047-01-01-11	2003 Feb 15 05:27:01	52685.22711	3.04 ± 0.08	0.0671 ± 0.0010	N	4.0 ± 1.4	386	14.9	···	22.0 ± 0.7	1.62 ± 0.20	0.355 ± 0.007	0.0086 ± 0.0011	1.64 ± 0.08	0.85 ± 0.03	···	···	···	···	

References. — 1. Kuulkers et al. (2003); 2. Chelovekov et al. (2005); 3. Jonker et al. (2001); 4. Barnard et al. (2001); 5. Strohmayer et al. (1998b); 6. Miller (1999); 7. Miller (2000); 8. Giles et al. (2002); 9. Muno et al. (2002); 10. Galloway et al. (2006); 11. Bhattacharyya & Strohmayer (2006); 12. Jonker et al. (2004); 13. Wijnands et al. (2001); 14. Wijnands et al. (2002); 15. Markwardt et al. (1999); 16. Ford et al. (1998); 17. Agrawal et al. (2001); 18. Molkov et al. (2000); 19. Franco (2001); 20. van Straaten et al. (2001); 21. Galloway et al. (2003); 22. Strohmayer et al. (1997b); 23. Strohmayer et al. (1998a); 24. Strohmayer et al. (1996); 25. Fox et al. (2001); 26. Guerriero et al. (1999); 27. Muno et al. (2000); 28. Strohmayer et al. (1997a); 29. Kuulkers & van der Klis (2000); 30. Jonker et al. (2000); 31. Galloway et al. (2004a); 32. Kaaret et al. (2002); 33. in 't Zand et al. (2003a); 34. in 't Zand et al. (2003b); 35. Galloway & Cumming (2006); 36. Chakrabarty et al. (2003); 37. Strohmayer et al. (2003); 38. Watts et al. (2005); 39. Kuulkers et al. (2002); 40. in 't Zand et al. (2004); 41. Galloway et al. (2004b); 42. Kong et al. (2000); 43. Zhang et al. (1998); 44. Galloway et al. (2001); 45. Tomsick et al. (1999); 46. Smale (2001); 47. Smale (1998); 48. Titarchuk & Shaposhnikov (2002);

Note. — The complete version of this table is in the electronic edition of the Journal. The printed edition contains only a sample.

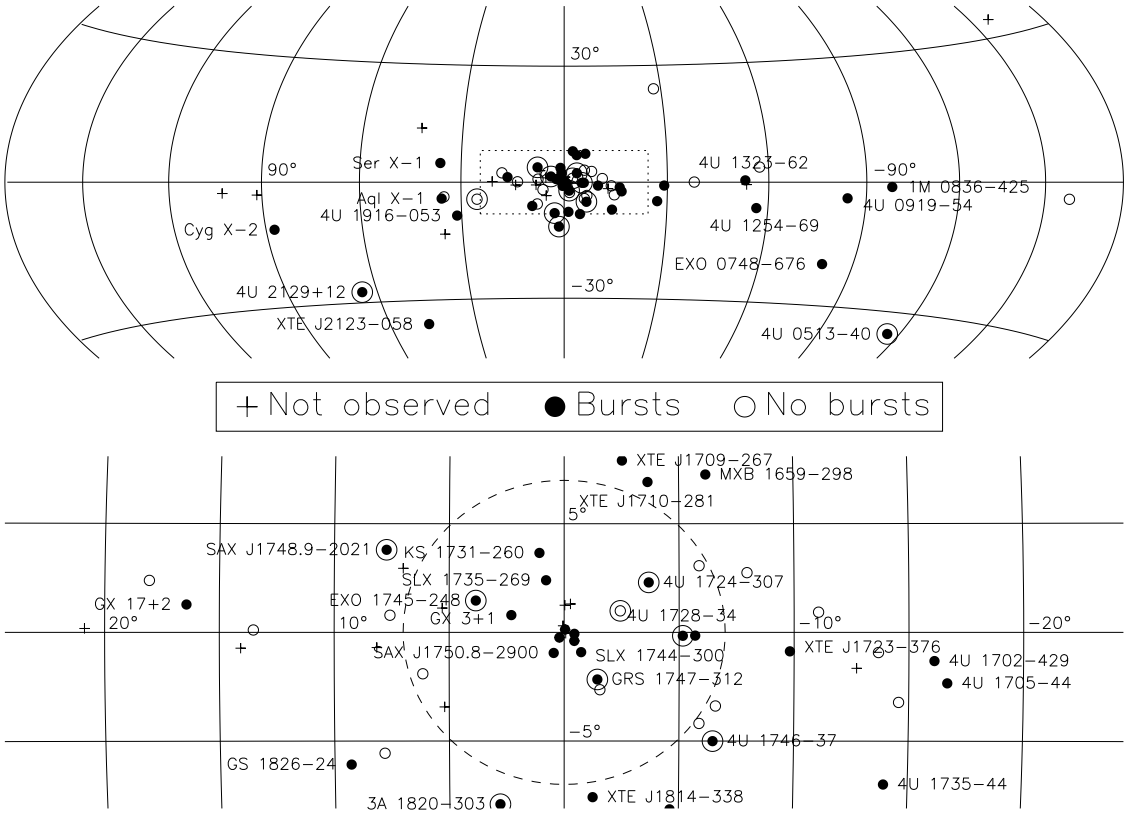

FIG. 7.— Sky distribution of bursters showing those observed by *RXTE*, as well as those from which bursts were detected. Sources within globular clusters are additionally indicated by a larger concentric circle. The lower panel shows the region around the Galactic center. The four (unlabeled) sources closest to the Galactic origin are (clockwise from lower left) are SAX J1747.0−2853, GRS 1741.9−2853, KS 1741−293 and 2E 1742.9−2929. The dashed line shows the approximate projected radius of the Galactic bulge.

RXTE. XTE J1743−363 (Markwardt et al. 1999c) and XTE J1739−285 (Markwardt et al. 1999a). Each was observed for 21 ks, but neither exhibited any X-ray bursts. Seventeen sources previously found to exhibit thermonuclear bursts were observed by *RXTE* but with no detected bursts (Table 3).

We summarise the millisecond oscillation search in Table 4, and list the results for individual bursts in Table 5. Where sufficient signal was available to detect oscillations independently in the rise, peak and decay of the burst, we indicate the detection in the "Location" column (R, P and D, respectively). We also list the maximum Leahy power and the maximum fractional rms for the oscillation.

In the following sections we discuss the properties of bursts observed from individual sources by *RXTE*. For each source, we list the Galactic coordinates, the first detection of thermonuclear bursts, the system properties (where known, including the orbital period and the method of measurement and the NS spin period), and the properties of bursts from previous observations. We describe the type of source (persistent/transient) and the persistent flux history throughout *RXTE*'s lifetime. The burst properties include the presence of PRE and/or double peaked bursts, the corresponding distance, recurrence times and α-values, whether short recurrence time bursts have been found, and the patterns of variation in burst properties with source state (F_p, position on the color-color diagram etc.).

3.1. *4U 0513−40 in NGC 1851*

Thermonuclear bursts from the persistent source (Clark et al. 1975) at $l = 244\overset{\circ}{.}51$, $b = -35\overset{\circ}{.}04$ were first detected by *SAS-3* (Clark & Li 1977) and also possibly *Uhuru* (Forman & Jones 1976). *Chandra* observations of the host cluster NGC 1851 allowed an optical identification (Homer et al. 2001a); while the orbital period has not been measured, the large $L_{\rm X}/L_{\rm opt}$ ratio indicates an ultracompact (i.e. $P_{\rm orb} < 80$ min) system. Additionally, the lack of UV and X-ray modulation at time scales within the expected orbital period range ($\lesssim 1$ hr) suggests low inclination. Only a handful of bursts has ever been observed (see Lewin et al. 1993 and Kuulkers et al. 2003 for summaries); the rather high peak flux of 2×10^{-8} ergs cm^{-2} s^{-1} for a PRE burst observed by *BeppoSAX* is only consistent with the estimated distance to the cluster of 12.1 ± 0.3 kpc if $X = 0$ and the gravitational redshift is negligible (see equation 5) or if the burst flux is beamed preferentially towards us.

Throughout the lifetime of *RXTE* the source has been persistent at a 2.5–25 keV flux of 1.4×10^{-10} ergs cm^{-2} s^{-1}, reaching as high as 8.5×10^{-10} ergs cm^{-2} s^{-1} during a ≈ 50 d transient outburst in 2002. For $d = 12.1$ kpc, this corresponds to an isotropic accretion rate of 2–12% $\dot{M}_{\rm Edd}$. We found six widely-separated bursts in the public *RXTE* data, with rather consistent properties: peak fluxes of $(14 \pm 2) \times 10^{-9}$ ergs cm^{-2} s^{-1}, fluences of $(0.14 \pm 0.03) \times 10^{-6}$ ergs cm^{-2} and $\tau = 10 \pm 2$ s in the mean. None of the bursts exhibited PRE.

3.2. *EXO 0748−676*

This transient at $l = 279\overset{\circ}{.}98$, $b = -19\overset{\circ}{.}81$ was discovered during *EXOSAT* observations in 1995 (Parmar et al. 1986), which also revealed thermonuclear bursts. The source exhibits synchronous X-ray and optical eclipses (Crampton et al. 1986) once every 3.82 hr orbit, and also shows X-ray dipping activity. The bursting behaviour was studied in detail with *EXOSAT*, which revealed that the burst rate was inversely correlated with persistent flux (Gottwald et al. 1986; see also Lewin et al. 1993). In addition, the burst properties varied significantly with F_p; both $F_{\rm pk}$ and E_b increased, and τ decreased when F_p exceeded 7.5×10^{-10} ergs cm^{-2} s^{-1} (0.1–20 keV). That the α-values increased from ~ 10 to ~ 100 confirms that the changes in burst properties resulted from a transition from H/He to He-dominated burst fuel. Bursts with the highest peak fluxes (3–4×10^{-8} ergs cm^{-2} s^{-1}, 0.1–20 keV) exhibited PRE, leading to an estimated distance of $8.3/(1 + X)$ kpc. The combined spectra of bursts observed by *XMM-Newton* exhibited discrete spectral features (Cottam et al. 2001; Bonnet-Bidaud et al. 2001), some of which appeared to be redshifted features from near the neutron star surface ($z = 0.35$; Cottam et al. 2002).

The source was in a low flux state throughout most of the *RXTE* observations, at a mean level of 2.7×10^{-10} ergs cm^{-2} s^{-1} (2.5–25 keV). In 2004 May ongoing monitoring of the source with *RXTE* revealed a radius-expansion burst, which reached a peak flux of 5.2×10^{-8} ergs cm^{-2} s^{-1} (Wolff et al. 2005). Two additional PRE bursts were detected in subsequent observations in 2005 June and August, and the overall range of peak fluxes (following reprocessing with LHEASOFT version 5.3) was $(3.8–4.7) \times 10^{-8}$ ergs cm^{-2} s^{-1}. The short rise times (2 s) and low $\tau = 9.2 \pm 0.9$ s suggest ignition in a He-rich environment, so that the distance inferred from the peak burst fluxes was 7.4 ± 0.9 kpc, implying an accretion rate over the course of the *RXTE* observations of $\approx 2.2\%$ $\dot{M}_{\rm Edd}$ (adopting a bolometric correction of 1.93 ± 0.02). We observed 84 bursts in total, most of which did not exhibit PRE and had properties typical for the low-state bursts observed previously: separations consistent with a recurrence time of 2–5 hr, $F_{\rm pk} = (5–15) \times 10^{-9}$ ergs cm^{-2} s^{-1}, varying fluences typically $\sim 0.2 \times 10^{-6}$ ergs cm^{-2}, and long durations ($\tau \sim 20$ s in the mean). We also found five bursts with much shorter recurrence times in the range 6.5–17 min (see §4.2). Analysis of several of the bursts was complicated due to their occurrence within eclipses, or across an eclipse ingress or egress. For these bursts the flux and fluence measurements are to be treated with caution.

The bursts from most other sources accreting at $\sim 1\%$ $\dot{M}_{\rm Edd}$ are infrequent, bright, and exhibit photospheric radius expansion (e.g. 4U 0919−54, §3.4; SAX J1808.4−3658, §3.33; and 4U 2129+12, §3.44). In particular, our study of the burst properties of SAX J1808.4−3658 confirm that the burst fuel is almost completely helium, the accreted hydrogen having been all but exhausted by steady burning in the 14–30 hr interval prior to burst ignition (Galloway & Cumming 2006). In contrast, many of the bursts from EXO 0748−676 are separated by no more than 5 hours, and both the long timescales and the typical $\alpha \approx 40$ indicate mixed H/He

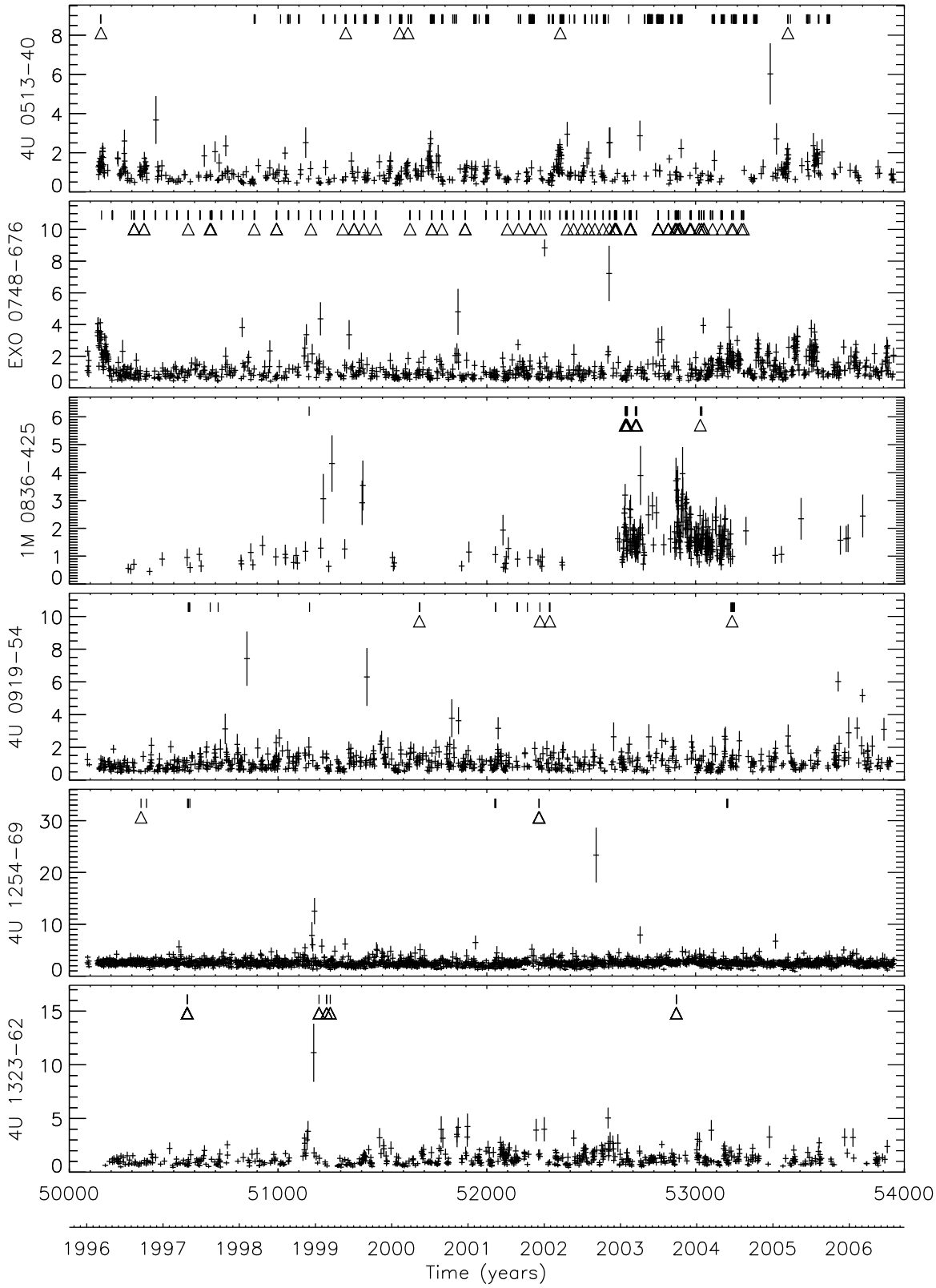

FIG. 8.— 1-d averaged ASM light curves of selected sources for which X-ray bursts have been observed by *RXTE* (see Table 1). The times of the PCA observations are shown by the vertical lines at the top of each plot, while the burst times are shown by the open triangles. The error bars show the 1σ uncertainties on each measurement; we exclude measurements where the significance of the detection is $< 3\sigma$. The complete version of this figure will be made available online. This version contains only a sample.

TABLE 3
Type-I X-ray burst sources observed by *RXTE* with no detected bursts

Source	RA	Dec	Location	$n_{\rm obs}$	Time (ks)	Limit on rate ($\rm hr^{-1}$)	Ref.
4U 0614+09	06 17 7.30	+09 08 13.0		284	1939.8	< 0.002	[1,2]
4U 1246−58	12 49 36.00	-59 07 18.0		1	7.0	< 0.5	[3]
Cen X-4	14 58 22.00	-31 40 7.0		4	10.4	< 0.3	[4,5]
Cir X-1	15 20 40.80	-57 10 0.0		503	2495.7	< 0.001	[6]
4U 1708−40	17 12 23.00	-40 50 36.0		14	61.1	< 0.06	[7]
SAX J1712.6−3739	17 12 34.00	-37 38 36.0		2	3.8	< 0.9	[8]
2S 1711−339	17 14 17.00	-34 03 36.0		10	42.1	< 0.09	[9]
3A 1715−321	17 18 47.30	-32 10 40.0		13	100.2	< 0.04	[10]
GPS 1733−304	17 35 47.60	-30 28 55.0	Terzan 1	7	56.6	< 0.06	[11]
A 1744−36	17 48 14.00	-36 07 30.0		11	26.3	< 0.1	[12]
SAX J1752.3−3138	17 52 24.00	-31 37 42.0		2	2.8	$< 1.$	[13]
SAX J1806.8−2435	18 06 51.00	-24 35 6.0		19	62.9	< 0.06	[14]
GX 13+1	18 14 31.00	-17 09 25.0		62	515.2	< 0.007	[15]
4U 1812−12	18 15 12.00	-12 04 59.0		27	187.6	< 0.02	[16]
SAX J1818.6−1703	18 18 42.00	-17 04 0.0		1	6.9	< 0.5	[17]
AX J1824.5−2451	18 24 30.00	-24 51 0.0		16	146.5	< 0.02	[18]
4U 1850−08	18 53 4.80	-08 42 19.0	NGC 6712	11	65.1	< 0.06	[19,20]
1A 1905+00	19 08 27.00	+00 10 7.0		12	69.8	< 0.05	[21]
Total (18 sources)				999	5800.		

References. — 1. Swank et al. (1978); 2. Brandt et al. (1992); 3. Piro et al. (1997); 4. Belian et al. (1972); 5. Matsuoka et al. (1980); 6. Tennant et al. (1986); 7. Migliari et al. (2003); 8. Cocchi et al. (2001a); 9. Cornelisse et al. (2002b); 10. Makishima et al. (1981a); 11. Makishima et al. (1981b); 12. Emelyanov et al. (2001); 13. Cocchi et al. (2001b); 14. Muller et al. (1998); 15. Matsuba et al. (1995); 16. Murakami et al. (1983); 17. in 't Zand et al. (2004c); 18. Gotthelf & Kulkarni (1997); 19. Swank et al. (1976b); 20. Hoffman et al. (1980); 21. Lewin et al. (1976e).

Note. — This table does not include observations towards the Galactic center which cover multiple sources

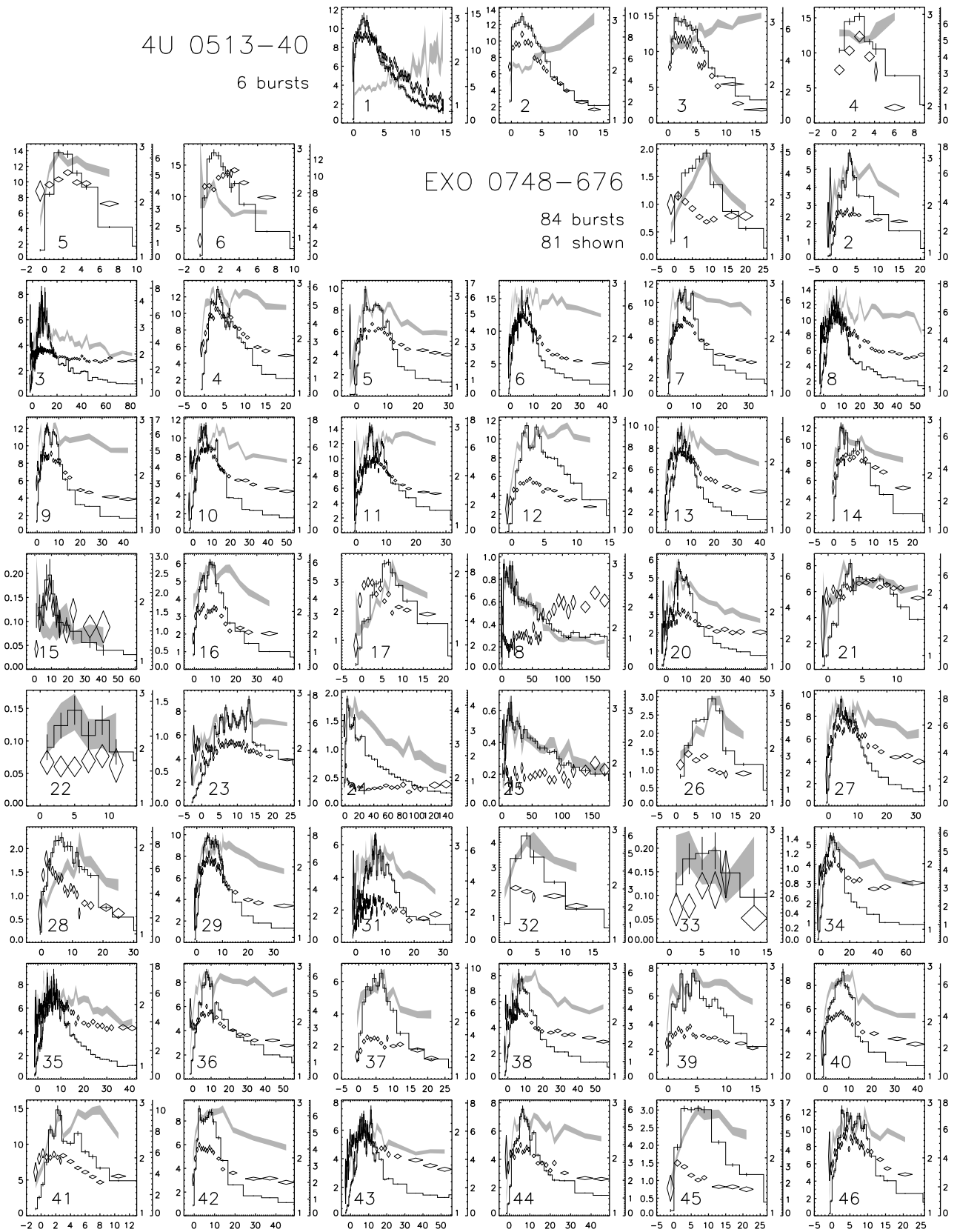

FIG. 9.— Time-resolved spectral parameters for bursts listed in Table 2. The histogram in each panel shows the (bolometric) burst flux (left-hand y-axis) in units of 10^{-9} ergs cm^{-2} s^{-1}, with error bars indicating the 1σ uncertainties. The grey ribbon shows the 1σ limits of the blackbody radius (outer right-hand y-axis) in km/$d_{10\mathrm{kpc}}$. The diamonds show the 1σ error region for the blackbody temperature (inner right-hand y-axis) in keV. Note the data gaps present for bright bursts, which arise from instrument data buffer overruns. The complete version of this figure will be made available online. This version contains only a sample.

TABLE 4
Summary of Burst Oscillations

Source	Number of Bursts[a]	Total	Number of Oscillations 4 s	Rise	R+P	Peak	P+D	Decay	R+D	Cont.
4U 1916−053 (270 Hz)	14(14)	1	···	···	···	···	···	···	···	1
with PRE	12(12)	0	···	···	···	···	···	···	···	···
XTE J1814−338[b] (314 Hz)	28(28)	28	3	···	···	···	2	···	3	20
4U 1702−429 (329 Hz)	44(44)	33	1	2	4	2	9	8	2	5
with PRE	4(4)	0	···	···	···	···	···	···	···	···
4U 1728−34 (363 Hz)	105(103)	37	2	5	1	2	11	9	1	6
with PRE	69(69)	18	2	1	···	···	6	8	···	1
HETE J1900.1−2455[b] (377 Hz)	2(2)	0	···	···	···	···	···	···	···	···
with PRE	2(2)	0	···	···	···	···	···	···	···	···
SAX J1808.4−3658[b] (401 Hz)	6(4)	4	···	1	···	···	···	1	2	···
SAX J1748.9−2021 (410 Hz)	16(16)	1	1	···	···	···	···	···	···	···
with PRE	6(6)	0	···	···	···	···	···	···	···	···
KS 1731−260 (524 Hz)	27(27)	4	···	1	···	···	1	1	1	···
with PRE	4(4)	3	···	···	···	···	1	1	1	···
Aql X-1 (549 Hz)	40(39)	6	···	···	1	2	3	···	···	···
with PRE	9(9)	5	···	···	···	2	3	···	···	···
MXB 1659−298 (567 Hz)	26(25)	6	1	2	···	1	···	1	1	···
with PRE	12(12)	5	1	2	···	···	···	1	1	···
4U 1636−536 (581 Hz)	123(123)	51	4	3	4	1	4	15	11	9
with PRE	40(40)	34	3	1	···	···	4	12	9	5
GRS 1741.9−2853[c] (589 Hz)	8(8)	2	2	···	···	···	···	···	···	···
with PRE	6(6)	2	2	···	···	···	···	···	···	···
SAX J1750.8−2900 (601 Hz)	4(4)	3	···	2	···	···	···	···	1	···
with PRE	2(2)	2	···	1	···	···	···	···	1	···
4U 1608−52 (620 Hz)	31(29)	7	···	2	···	1	1	1	···	2
with PRE	12(12)	7	···	2	···	1	1	1	···	2
Total	474(466)	183	14	18	10	9	31	36	22	43
PRE	183(182)	80	8	8	0	3	15	24	14	8

[a]The first number is the number of bursts observed from this source, while the number in parentheses is the number of bursts which were searched for oscillations.
[b]These sources also exhibit persistent pulsations at the listed frequency. Note that both bursts from HETE J1900.1−2455 exhibited PRE, while for XTE J1814−338, only the last burst observed exhibited marginal evidence for PRE.
[c]We attributed bursts with oscillations from the Galactic center region to this source; see §A.5.

TABLE 5
Bursts with oscillations detected by *RXTE*

Source and frequency	Burst ID	Start time	PRE?	Location	Maximum power	Mean % RMS
4U 1916−053 (270 Hz)	9	1998 Aug 1 18:23:49	N	R P D	28.3	7.5 ± 1.4
XTE J1814−338 (314 Hz)	1	2003 Jun 6 00:58:30	N	R – D	21.2	15 ± 3
	2	2003 Jun 7 06:26:52	N	– P D	40.3	13 ± 2
	3	2003 Jun 7 21:12:21	N	R P D	37.1	11.0 ± 1.8
	4	2003 Jun 9 04:42:35	N	R P D	41.0	10.0 ± 1.6
	5	2003 Jun 10 02:23:00	N	R P D	37.8	11.7 ± 1.9
	6	2003 Jun 11 00:42:02	N	···	36.0	9.5 ± 1.6
	7	2003 Jun 12 11:11:37	N	– P D	44.5	13 ± 2
	8	2003 Jun 12 13:31:06	N	R – D	30.2	17 ± 3
	9	2003 Jun 13 01:25:31	N	···	49.0	8.9 ± 1.3
	10	2003 Jun 13 17:37:13	N	R P D	26.4	10.3 ± 2.0
	11	2003 Jun 14 00:20:54	N	R P D	38.9	11.8 ± 1.9
	12	2003 Jun 15 18:56:50	N	R P D	34.0	12 ± 2
	13	2003 Jun 16 17:56:22	N	R P D	49.0	19 ± 3
	14	2003 Jun 16 19:37:54	N	···	40.0	10.2 ± 1.6
	15	2003 Jun 17 16:00:21	N	R P D	36.0	13 ± 2
	16	2003 Jun 18 19:05:18	N	R P D	35.5	15 ± 2
	17	2003 Jun 19 18:45:29	N	R P D	37.3	14 ± 2
	18	2003 Jun 20 01:38:10	N	R P D	37.4	10.3 ± 1.7
	19	2003 Jun 20 21:38:02	N	R – D	20.9	17 ± 4
	20	2003 Jun 21 15:20:59	N	R P D	27.0	12 ± 2
	21	2003 Jun 22 21:19:41	N	R P D	44.2	14 ± 2
	22	2003 Jun 23 11:15:00	N	R P D	42.0	14 ± 2
	23	2003 Jun 27 16:38:50	N	R P D	42.3	14 ± 2
	24	2003 Jun 27 21:12:01	N	R P D	38.5	15 ± 2
	25	2003 Jun 28 20:29:15	N	R P D	42.1	17 ± 3
	26	2003 Jul 7 06:05:03	N	R P D	41.5	13 ± 2
	27	2003 Jul 8 19:02:33	N	R P D	35.7	16 ± 3
	28	2003 Jul 17 17:42:46	?	R P D	25.1	8.0 ± 1.6
4U 1702−429 (329 Hz)	2	1997 Jul 19 18:40:58	N	– P D	28.5	5.6 ± 1.0
	3	1997 Jul 26 09:03:23	N	– P D	120	11.7 ± 1.1
	4	1997 Jul 26 14:04:18	N	R P D	127	10.7 ± 1.0
	5	1997 Jul 30 07:22:37	N	– P D	49.9	7.4 ± 1.0
	6	1997 Jul 30 12:11:56	N	R – D	87.3	12.1 ± 1.3
	7	1999 Feb 21 23:48:32	N	– P D	28.9	5.1 ± 0.9
	8	1999 Feb 22 04:56:05	N	R P D	22.6	22 ± 5
	9	2000 Jun 22 11:57:46	N	R – –	25.2	4.1 ± 0.8
	10	2000 Jul 23 07:09:42	N	– – D	71.3	10.6 ± 1.3
	14	2001 Feb 4 03:50:29	N	– P D	27.2	4.3 ± 0.8
	15	2001 Apr 1 15:47:17	N	R P –	32.0	4.8 ± 0.8
	16	2001 Apr 1 21:55:53	N	– P D	115	12.3 ± 1.2
	18	2001 Nov 16 17:02:10	N	– – D	21.7	4.7 ± 1.0
	20	2004 Jan 18 01:17:56	N	– P –	15.2	3.1 ± 0.8
	21	2004 Jan 18 21:12:37	N	– – D	18.5	4.9 ± 1.1
	22	2004 Jan 20 00:30:01	N	– P –	29.7	5.2 ± 0.9
	23	2004 Feb 29 01:59:38	N	– – D	34.1	13 ± 2
	24	2004 Feb 29 06:32:16	N	R P D	19.4	5.5 ± 1.2
	26	2004 Mar 1 23:26:40	N	R – –	31.7	6.2 ± 1.1
	27	2004 Mar 2 07:27:52	N	R P –	19.2	4.2 ± 0.9
	28	2004 Apr 8 22:12:46	N	– P D	39.4	6.4 ± 1.0
	29	2004 Apr 9 06:18:07	N	– – D	68.0	14.4 ± 1.7
	30	2004 Apr 9 21:32:20	N	– – D	27.0	5.5 ± 1.1
	31	2004 Apr 11 08:44:45	N	R – D	22.0	5.7 ± 1.2
	32	2004 Apr 12 06:56:34	N	R P –	18.5	3.9 ± 0.9
	35	2004 Apr 13 05:40:02	N	R P D	25.8	9.7 ± 1.9
	36	2004 Apr 13 12:11:53	N	– – D	27.5	9.1 ± 1.7
	37	2004 Apr 13 18:17:23	N	R P –	36.3	5.6 ± 0.9
	38	2004 Apr 14 18:32:01	N	– – D	31.9	7.1 ± 1.2
	39	2004 Apr 15 00:43:14	N	R P D	28.1	5.5 ± 1.0
	40	2004 Apr 16 02:08:57	N	···	30.0	3.8 ± 0.7
	41	2004 Apr 16 20:29:36	N	– P D	56.5	8.0 ± 1.1
	42	2004 Apr 17 02:45:18	N	– P D	67.8	7.3 ± 0.9
4U 1728−34 (363 Hz)	2	1996 Feb 15 21:10:21	Y	– – D	22.8	3.1 ± 0.6
	3	1996 Feb 16 03:57:11	N	R – –	14.2	3.4 ± 0.9
	4	1996 Feb 16 06:51:10	Y	– – D	37.3	4.9 ± 0.8
	5	1996 Feb 16 10:00:47	Y	R P D	55.0	9.1 ± 1.2
	6	1996 Feb 16 19:27:13	Y	– – D	21.9	4.4 ± 0.9
	7	1996 Feb 18 17:31:52	Y	– – D	30.4	4.2 ± 0.8

Note. — The complete version of this table will be made available online. The printed edition contains only a sample.

fuel. As suggested by Gottwald et al. (1986), these properties indicate that the long bursts are ignited by unstable hydrogen ignition rather than the more usual helium ignition which likely triggers the PRE bursts.

3.3. *1M 0836−425*

A Galactic-plane ($l = 261\overset{\circ}{.}95$, $b = -1\overset{\circ}{.}11$) transient discovered during *OSO-7* observations between 1971–74 (Markert et al. 1977; Cominsky et al. 1978), 1M 0836−425 was first observed to exhibit thermonuclear bursts by *Ginga* during an outburst between 1990 November and 1991 February (Aoki et al. 1992). The typical recurrence time for the 28 bursts detected was ≈ 2 hr, but on one occasion was 8 min. No bursts exhibited radius expansion, leading to an upper limit on the distance of 10–20 kpc. The optical counterpart has not been identified, since several stars down to a limiting R-band magnitude of ~ 23.5 are present in the $9''$ *ROSAT* error circle (Belloni et al. 1993).

A new outburst was detected by the ASM aboard *RXTE* on 2003 January, which lasted until May. A second interval of activity commenced around 2003 September, and continued throughout the remainder of 2003–04. Seventeen bursts were observed in total, with rather homogeneous properties; peak fluxes of $(13 \pm 3) \times 10^{-9}$ ergs cm^{-2} s^{-1}, fluence $(0.27 \pm 0.07) \times 10^{-6}$ ergs cm^{-2} and time-scale $\tau = 22 \pm 4$. Recently Chelovekov et al. (2005) analysed 15 of these bursts, in addition to 24 bursts observed by *INTEGRAL*; their maximum peak flux of 1.5×10^{-8} ergs cm^{-2} s^{-1} (3–20 keV) led to a distance upper limit of 8 kpc. The maximum estimated bolometric flux from our analysis was 2×10^{-8} ergs cm^{-2} s^{-1}, which leads to a more conservative upper limit (for $X = 0$) of $d < 11$ kpc. No kHz oscillations were detected in any of the bursts. The peak persistent flux was 1.96×10^{-9} ergs cm^{-2} s^{-1} (2.5–25 keV), corresponding to an accretion rate of $\lesssim 33\%$ $\dot{M}_{\rm Edd}$ (adopting a bolometric correction of 1.82 ± 0.02).

Near the end of 2003 January two pairs of bursts were observed, each separated by just ~ 2 hr. The other bursts in the early part of the outburst occurred at much longer intervals, which were however also consistent with a steady recurrence time of ~ 2 hr, but where the intervening bursts were missed due to data gaps. Assuming the bursts occurred quasi-periodically, the inferred recurrence time was 2.20 ± 0.18 hr on average, similar to that in previous observations (Aoki et al. 1992). The measured α-values were betwen 40 and 100, although the persistent flux measured from the field may be contaminated by emission from the nearby ($\Delta\theta = 0\overset{\circ}{.}4$) 12.3 s X-ray pulsar GS 0834−340. Thus, the derived broad-band flux (and hence α) may be overestimated. Even so, $\alpha \lesssim 40$, the long duration of the bursts, and the ~ 2 hr recurrence times (too short to exhaust the accreted H by steady burning between the bursts, except for an extremely low accreted H fraction; e.g. Fujimoto et al. 1981) all indicate ignition of mixed H/He fuel.

The burst recurrence time decreased slightly from 2.5 hr to 2 hr between January 25 and February 1 (MJD 52664 and 52671), while the persistent flux also decreased, which is the opposite of the trend predicted by theory. Over the same interval the α value decreased systematically from ~ 100 to 40, suggesting a substantial variation in the composition of the burst fuel (although this seems inconsistent with the rather homogeneous properties of the bursts; cf with 4U 1702−429, §3.10). The accretion may be limited to a smaller and smaller area as the accretion rate drops, so that the accretion rate per unit area $\dot{m}$ increases even as the total rate $\dot{M}$ decreases. However, this effect cannot explain the changes in α.

3.4. *4U 0919−54*

This weak, persistent source at $l = 275\overset{\circ}{.}85$, $b = -3\overset{\circ}{.}84$ has been observed by all the major early satellites (*Uhuru*,*OSO-7, Ariel-5, SAS-3, HEAO-1, Einstein*). A $V = 21$ star has been identified as the optical counterpart (Chevalier & Ilovaisky 1987); although the orbital period is unknown, the system is a candidate ultracompact based on the optical properties, and X-ray spectroscopic measurements indicate enhanced abundances (Juett et al. 2001; Juett & Chakrabarty 2003). Observations by *RXTE* led to the first detection of a thermonuclear burst from the source, as well as the discovery of a 1160 Hz QPO (Jonker et al. 2001).

Our analysis of the lone PRE burst, detected by *RXTE* on 2000 May 12 19:50:17 UT (Fig. 9) leads to a distance estimate of 4.0 (5.3) kpc assuming that the burst reaches $L_{\rm Edd,H}$ ($L_{\rm Edd,He}$). We found three other burst candidates, the brightest of which (on 2004 June 18 23:38:17 UT) peaked at $(5.7 \pm 0.2) \times 10^{-9}$ ergs cm^{-2} s^{-1} and exhibited no evidence for PRE. The other two were sufficiently faint that our spectral analysis results did not allow a test for cooling in the burst tail, and thus these three events must remain as merely burst candidates. The 2.5–25 keV PCA flux was between 0.7–4.5×10^{-10} ergs cm^{-2} s^{-1}, which for $d = 5.3$ kpc corresponds to an accretion rate of $\lesssim 1.2\%$ $\dot{M}_{\rm Edd}$.

3.5. *4U 1254−69*

Thermonuclear X-ray bursts and periodic dips were discovered in this 3.9 hr binary ($l = 303\overset{\circ}{.}48$, $b = -6\overset{\circ}{.}42$) during *EXOSAT* observations in 1984 (Courvoisier et al. 1986; Motch et al. 1987). Just two thermonuclear bursts were detected, with rise times of ~ 1 s; durations of ~ 20 s; peak fluxes of $\sim 1.1 \times 10^{-8}$ ergs cm^{-2} s^{-1}; and no evidence of PRE (see also Lewin et al. 1993). in 't Zand et al. (2003b) reported a superburst from this source, as detected by *BeppoSAX* on 1999 January 9. Possible PRE during the type-I burst precursor to the superburst leads to a distance estimate of 13 ± 3 kpc.

RXTE observations in 1996–7 and 2001 detected the source at a persistent level of 8×10^{-10} ergs cm^{-2} s^{-1} (2.5–25 keV), which for $d = 13$ kpc corresponds to an accretion rate of 12% $\dot{M}_{\rm Edd}$ (for a bolometric correction of 1.13 ± 0.03). Four of the five thermonuclear bursts occurred between 2001 December 6–7 and exhibited rather unusual evolution of the blackbody radius. The radius was elevated during the rise and peak of the burst, and was accompanied by a decrease in the blackbody temperature, but not to a sufficient degree to be confirmed as PRE bursts (see Fig. 9). Typically for these bursts the peak flux ($5.6 \pm 0.7 \times 10^{-9}$ ergs cm^{-2} s^{-1} in the mean) was reached at or before the peak radius. The bursts were short (mean $\tau = 5.5 \pm 0.7$ s) and weak, with mean $E_b = (0.028 \pm 0.003) \times 10^{-6}$ ergs cm^{-2}. The recurrence times were 10.7, 4.04 and 9.16 hr; the observations had

sufficient coverage over the final interval to exclude an intermediate burst, although a dip (which could potentially have prevented detection of a burst) was observed at approximately the halfway mark. The measured α-values were 1260 ± 60, 490 ± 20 and 1070 ± 60.

3.6. *4U 1323−62*

Bursting behaviour with a steady recurrence time of 5.3 hr was discovered from 4U 1323−62 ($l = 307\overset{\circ}{.}03$, $b = +0\overset{\circ}{.}46$) in 1984 during *EXOSAT* observations (van der Klis et al. 1984). The bursts were homogeneous, with rise times of 4.0 ± 0.6 s, $F_{\rm pk}$ of $(5.2 \pm 0.9) \times 10^{-9}$ ergs cm^{-2} s^{-1}, $\tau = 14 \pm 2$ s, and no evidence of PRE (Lewin et al. 1993). "Double" bursts, with extremely short ($\lesssim 10$ min) recurrence times, are commonly observed (see e.g. Bałucińska-Church et al. 1999). The source also exhibits 2.93 hr periodic intensity dips (Parmar et al. 1989), and is associated with a faint ($K' = 17.05 \pm 0.20$, $J \sim 20$) IR counterpart (Smale 1995).

RXTE observations found 4U 1323−62 at a persistent, steady flux level of 2.5×10^{-10} ergs cm^{-2} s^{-1} (2.5–25 keV), somewhat higher than the $\sim 1.7 \times 10^{-10}$ ergs cm^{-2} s^{-1} of the *EXOSAT* observations. A total of 24 X-ray bursts were found, in observations taken early in 1997, 1999 and late 2003. Seven bursts were observed between 1997 April 25–28, 5 with a regular recurrence time of 2.7 ± 0.3 hr. Two of these regular bursts were closely (≈ 10 min) followed by extremely faint secondary bursts (see also Barnard et al. 2001). A third double burst was observed by *RXTE* on 1999 Jan 18, during which the recurrence time for the bright, regular bursts was 2.1–2.5 hr. Neglecting the bursts with short recurrence times, the burst properties were roughly consistent with previous observations: $F_{\rm pk} = (3.5 \pm 0.6) \times 10^{-9}$ ergs cm^{-2} s^{-1}, $\tau = 28 \pm 3$ and $E_b = (0.096 \pm 0.012) \times 10^{-6}$ ergs cm^{-2}. The α-values were 38 ± 4 in the mean, which, combined with the long burst duration, strongly suggests mixed H/He fuel in the bursts. Without any radius-expansion bursts, we have only upper limits on the distance, of 11 (15) kpc assuming the bursts do not exceed $L_{\rm Edd,H}$ ($L_{\rm Edd,He}$). For a distance of 11 kpc, the persistent flux indicates an accretion rate of a few percent of $\dot{M}_{\rm Edd}$. At this level, we expect either He-rich bursts with long recurrence times resulting from He-ignition (e.g. SAX J1808.4−3658, §3.33), or mixed H/He bursts with short recurrence times resulting from H ignition (e.g. EXO 0748−676, §3.2). The burst properties of 4U 1323−62 (as well as the presence of faint secondary bursts), strongly suggests the latter regime. We note that the regular occurence of double bursts provides an opportunity to constrain the fuel source for the secondary bursts (see §4.2).

3.7. *4U 1608−52*

Bursts from this Galactic plane ($l = 330\overset{\circ}{.}93$, $b = -0\overset{\circ}{.}85$) transient were first detected by the two *Vela-5* satellites (Belian et al. 1976). *Uhuru* observations confirmed the link between the bursting and persistent source (Tananbaum et al. 1976), and a more precise X-ray position obtained with HEAO-1 (Fabbiano et al. 1978) permitted identification of the $I = 18.2$ optical counterpart QX Nor (Grindlay & Liller 1978). Variations in the persistent X-ray flux as measured by *Vela-5B* have suggested an orbital period of either 4.10 or 5.19 d (Lochner & Roussel-Dupre 1994). Along with 4U 1728−34, 4U 1608−52 was one of the first sources for which the intensity dips at the peak were identified as PRE episodes (Fujimoto & Gottwald 1989). *Hakucho* observations revealed recurrence times as short as 10 min, as well as two separate bursting modes in terms of recurrence time and profile shape, depending upon the persistent flux level (Murakami et al. 1980a,b; see also Lewin et al. 1993). At high F_p, the bursts are bright and fast, with rise times of ~ 2 s and $\tau \approx 8$ s; at low F_p, the rise times exceeded 2 s and the bursts were much longer with $\tau = 10$–30 s.

Two large and several smaller outbursts have occurred during *RXTE*'s lifetime; the most recent observed by *RXTE* in 2005 March. The large outbursts both peaked at $\sim 2.7 \times 10^{-8}$ ergs cm^{-2} s^{-1} (2.5–25 keV), corresponding to an accretion rate of 62% $\dot{M}_{\rm Edd}$ (for a distance of 4.1 kpc, see Table 6; and a bolometric correction of 1.77 ± 0.04). The lowest measured fluxes of $\approx 2.2 \times 10^{-11}$ ergs cm^{-2} s^{-1} provide an upper limit for the quiescent accretion rate of 0.5% $\dot{M}_{\rm Edd}$. We found 32 bursts in public *RXTE* data, of which 12 exhibited PRE. At the lowest F_p values, we found five PRE bursts with long time scales ($\tau = 16 \pm 4$ in the mean). In five of the other 6 PRE bursts we detected burst oscillations at 619 Hz, making this source the most rapidly spinning neutron-star LMXB known to date (Hartman et al. 2006, in preparation). Three bursts exhibited oscillations both before and after the PRE episode, and showed increases in frequency with time of up to 6.6 Hz (1.1%) over 8 s. The oscillations during the burst rise had the largest amplitudes, up to 13% (rms), while detections during the tails were up to 10% but more typically 3–5%.

The bursts from 4U 1608−52 were some of the brightest seen in the entire sample, and peaked between 1.2–1.5×10^{-7} ergs cm^{-2} s^{-1}. As with previous observations, τ appeared to decrease significantly with persistent flux, although there was substantial scatter. For four non-PRE bursts with $\tau = 16$–22 s for which we could confidently measure the recurrence time at between 4.14–7.5 hr, we estimate $\alpha = 41$–54. We observed two instances of extremely short recurrence times for bursts from 4U 1608−52. On 1996 March 22 we observed three bursts in quick succession, two brighter bursts separated by 24 min, with an extremely faint burst ($F_{\rm pk}$= $(1.0 \pm 0.2) \times 10^{-9}$ ergs cm^{-2} s^{-1}) inbetween, just 16 min after the first burst. None of the three bursts exhibited PRE. On 2001 November 21 we observed two bursts separated by at most 6 min (the start of the second burst fell within a data gap). The persistent flux level between these two observations varied by a factor of 2. The bursts with recurrence times < 1000 s, all had atypically low fluences of 0.025–0.27×10^{-6} ergs cm^{-2}; the mean value for the other bursts was $E_b = (1.4 \pm 0.6) \times 10^{-6}$ ergs cm^{-2}.

3.8. *4U 1636−536*

4U 1636−536 ($l = 332\overset{\circ}{.}9$, $b = -4\overset{\circ}{.}8$) is a well-studied LMXB in a 3.8 h orbit with an 18th magnitude blue star, V801 Ara (van Paradijs et al. 1990b). X-ray bursts were first detected from a region containing the previously-known persistent source by *OSO-8* (Swank et al. 1976a),

and were subsequently studied in great detail with observations by *EXOSAT* (see Lewin et al. 1993, for a review). The peak fluxes $F_{\rm pk}$ appeared to be distributed bimodally, with the non-PRE bursts peaking at a factor of 1.7 or more lower in flux than the PRE bursts (Sugimoto et al. 1984). The brighter (PRE) bursts were suggested to result from a He flash in which the outer H-dominated photosphere is ejected in the early stages of the burst, while in the fainter (non-PRE) bursts the peak luminosity is insufficient to eject the photosphere. The measured $F_{\rm pk}$ values of the radius expansion bursts were found to be consistent to within their uncertainties (Ebisuzaki 1987).

RXTE observations revealed burst oscillations at 579.3 Hz (Strohmayer et al. 1998b,a), as well as a possible first detection of a harmonic which has not been confirmed in other bursts from the source (Miller 1999). The properties of the oscillations have been analysed by Muno et al. (2001) and Giles et al. (2002). Three "superbursts" have also been detected, attributed to thermonuclear burning of carbon produced as a by-product of H/He burning (Wijnands 2001; Kuulkers et al. 2004). In one of the superbursts, which was observed with the PCA, Strohmayer & Markwardt (2002) found an ≈ 800 s interval during which oscillations were consistently detected.

The persistent flux of the source varied between 4–6×10^{-9} ergs cm^{-2} s^{-1} (2.5–25 keV) between 1996–2000, but since then it has apparently been declining steadily, reaching 1.25×10^{-9} ergs cm^{-2} s^{-1} during 2004 January. For a distance of 6 kpc (see Table 6), this corresponds to an accretion rate between 3–16% $\dot{M}_{\rm Edd}$. We detected 123 bursts from public *RXTE* observations, of which 40 exhibited PRE. The peak fluxes were bimodally distributed, although we found both PRE and non-PRE bursts with $F_{\rm pk}$ falling within the gap noted by Sugimoto et al. (1984). While the majority of the 40 PRE bursts had peak fluxes distributed about 6.4×10^{-8} ergs cm^{-2} s^{-1}, with a standard deviation of 7.6%, we also found two PRE bursts with much smaller peak fluxes of 38×10^{-9} ergs cm^{-2} s^{-1} (Galloway et al. 2006, see also §4.4). At the highest F_p range the bursts were fast, with $\tau = 6.4 \pm 1.1$ s in the mean; at lower F_p the τ values became both larger and more variable. The burst rate decreased significantly as F_p increased (see Fig. 16 and §4.1), but this was partially compensated by a corresponding increase in the mean E_b. Typical α-values for bursts with $\Delta t = 1.2$–2.2 hr at low F_p were ~ 40, although on occasion were as high as 100 (for somewhat longer $\Delta t = 2.4$ hr); however, at the highest flux range we measured $\alpha = 500$ for a pair of bursts with $\Delta t = 6.3$ hr. We found 4 bursts with distinct double peaks in the bolometric flux, separated by 4–5 s. For three of these bursts (on 2001 September 5 08:15:04, 2001 October 3 00:22:18, and 2002 February 28 23:42:53 UT) the second peak was larger than the first, by 70, 40, and 230% respectively (the lattermost case bore a striking resemblence to a burst from 4U 1709−267; see §3.12 and Jonker et al. 2004). For the other burst, on 2002 January 8 12:22:44 UT, the first peak was very slightly greater than the second, and between the two peaks the flux reached a minimum of around 45% $F_{\rm pk}$. This burst was also analysed by Bhattacharyya & Strohmayer (2006), who interpreted the variation of the blackbody radius as arising from two-phase spreading of the nuclear burning following ignition near the pole.

3.9. *MXB 1659−298*

Regular ($\Delta t = 2.1$–2.6 hr) X-ray bursts were first detected from MXB 1659−298 ($l = 353\overset{\circ}{.}83$, $b = 7\overset{\circ}{.}27$) by *SAS-3* in 1976 (Lewin et al. 1976c). An upper limit on the persistent flux at this time led to a constraint on $\alpha < 25$. Persistent emission at $\sim 5 \times 10^{-10}$ ergs cm^{-2} s^{-1} attributed to the bursting source was detected by *SAS-3* two years later (Lewin et al. 1978), although no bursts were detected at that time (see also Lewin et al. 1993). An improved X-ray position from observations by *HEAO-1* led to the identification of the optical counterpart, V2134 Oph (Doxsey et al. 1979). Irregular X-ray dips as well as 15 min eclipses at the 7.1 hr orbital period were discovered in *HEAO* A-1 scanning observations (Cominsky & Wood 1984).

A new active period which lasted around 2.5 yr began in 1999 April, during which the source was observed extensively by *RXTE* and *BeppoSAX*/WFC. The PCA flux peaked at 10^{-9} ergs cm^{-2} s^{-1} (2.5–25 keV) in 1999 April, but was 4–6×10^{-10} ergs cm^{-2} s^{-1} throughout the remainder of the outburst. For $d = 12$ kpc (see Table 6) this corresponds to a range of accretion rates of 6–15% $\dot{M}_{\rm Edd}$. Burst oscillations at 567 Hz were detected in most of the PRE bursts observed by *RXTE* (Wijnands et al. 2001c); a detailed study of 14 of the 26 bursts observed in total was presented in Wijnands et al. (2002b).

Those authors found no clear correlations between their properties and the accretion rate, although only a limited range of accretion rates were sampled. In the full set of bursts observed by *RXTE* there is a marked division between the PRE bursts, which had $\tau = 4.6 \pm 1.0$ s in the mean and were generally observed at higher F_p, and the non-PRE bursts, for which $\tau = 19 \pm 5$ s (with one exception) and which were observed at somewhat lower F_p. We also found unusually large variations in the peak flux of the PRE bursts (see §4.4); this may be a consequence of the high system inclination, as evidenced from the presence of eclipses. The burst intervals measured by *RXTE* were all > 14 hr, with just two exceptions; for one of those intervals ($\Delta t = 1.82$ hr) we could not exclude intermediate bursts due to a data gap, while for the other (0.53 hr) the high-resolution datamodes did not cover the second burst. Thus, we could not reliably estimate α for any of the burst pairs.

MXB 1659−298 became undetectable by the PCA on 2001 September 7, after which the cooling of the NS was monitored by *Chandra* observations (Wijnands et al. 2004).

3.10. *4U 1702−429*

Bursts from this Galactic plane ($l = 343\overset{\circ}{.}89$, $b = -1\overset{\circ}{.}32$) source were first detected by *OSO-8* (Swank et al. 1976b). Makishima et al. (1982) detected 14 bursts with characteristic recurrence times of 9–12 hr from the region in *Hakucho* observations in 1979, and attributed them to a persistent *Uhuru* source. The peak fluxes were (18–30) $\times 10^{-9}$ ergs cm^{-2} s^{-1} (3–10 keV); rise times a few seconds or less; and $\tau = 10$–15 (see

also Lewin et al. 1993). A distance of ~ 10 kpc was inferred from the similarity of the peak fluxes with those of other Galactic centre sources. A $K = 16.5$ source at the edge of the *Chandra* error circle has been suggested as the counterpart (Wachter et al. 2004). *RXTE* observations in 1997 July 29–30 revealed kHz QPOs as well as 6 type-I bursts with coherent oscillations near 330 Hz (Markwardt et al. 1999b).

4U 1702−429 was persistently active at low levels (0.7–2.3×10^{-9} ergs cm^{-2} s^{-1}, 2.5–25 keV) throughout the lifetime of *RXTE*. For a distance of 5.5 kpc (derived from the mean peak flux of four PRE bursts; Table 6) the accretion rate was 2–6% $\dot{M}_{\rm Edd}$ (where we adopt a bolometric correction for the 2.5–25 keV flux which averages 1.12±0.04 over 6 selected observations). We found 44 bursts in total from 4U 1702−429, with peak fluxes of (28–81) $\times 10^{-9}$ ergs cm^{-2} s^{-1} and fluences typically (0.2–0.6) $\times 10^{-6}$ ergs cm^{-2} for the non-PRE bursts, or $\approx 10^{-6}$ ergs cm^{-2} for the PRE bursts. The burst light curves were quite homogeneous, with $\tau = 8.0$ s and rise time 0.95 s in the mean (see Fig. 9). Unusually, the four PRE bursts had substantially larger $\tau = 12 \pm 3$ s, compared to 7.6 ± 1.4 s for the non-PRE bursts.

The shortest burst interval was 4.5 hr; on 16 separate occasions between 1997 July and 2004 April we detected a pair of bursts separated by no more than 8.1 hr (6.4 ± 1.1 hr in the mean). We tentativelly identify this value as the characteristic burst recurrence time for the *RXTE* observations (although it is possible that intervening bursts were missed in data gaps so that the actual recurrence times were one-half or less of the measured intervals). Even so, these intervals are somewhat lower than the 9–12 hr measured in previous observations (Makishima et al. 1982). The source was quite variable on timescales of a few days, so that the persistent 2.5–25 keV flux during these observations varied between (1.3–2.3) $\times 10^{-9}$ ergs cm^{-2} s^{-1}. Assuming that the measured burst interval is the recurrence time, we derive α-values in the range 74–153. The wide range in α arose mainly from the large variations in E_b, since the burst intervals varied much less. The most notable example was for the pairs of bursts on 1997 July 26 14:04:18 and 1999 Feb 22 04:56:05 (UT), which were preceded by burst intervals agreeing to within 7 min, but exhibited fluences which differed by a factor of 1.8. This inconsistency between the burst fluences for comparable recurrence times and $\dot{M}$ strongly suggests incomplete burning of the accreted fuel in the low-fluence bursts. Residual unburnt fuel may contribute to the ignition column for the subsequent burst, leading to more rapid ignition than might have occurred otherwise. The range of fluences of the bursts within a narrow range of recurrence times is indicative of the maximum fraction of fuel which may be left unburnt, which is almost 50%; this is a much larger fraction than the 10% suggested by studies of other sources (e.g. Gottwald et al. 1987, see also §4.2). The smallest measured α corresponds to the maximum $E_{\rm b}$ for a given $F_{\rm p}$ and Δt, i.e. as close as possible to complete fuel consumption, and thus is a lower limit on the α for complete consumption. We found the three smallest values of α clustered tightly about a mean of 75.3 ± 1.5, suggesting a H-fraction at ignition of less than half the solar value. A low H-fraction is also consistent with the short rise times and low τ-values for the bursts.

3.11. *4U 1705−44*

This persistently bright, variable source ($l = 343\overset{\circ}{.}33$, $b = -2\overset{\circ}{.}33$) was detected initially in *Uhuru* observations (Forman et al. 1978). Bursts were first discovered by *EXOSAT* in 1985, and the bursting behaviour was subsequently studied in detail by that satellite (Langmeier et al. 1987; Gottwald et al. 1989). The burst profile was observed to change from slow (with decay $\tau \sim 100$ s) to fast ($\tau \sim 25$ s) as the intensity increased, similar to EXO 0748−676 (see also §3.2, Lewin et al. 1993). Typical recurrence times were 1.9–2.5 hr, except for occasional faint bursts following brighter events by just 500–1000 s. Model atmosphere fits to spectra of non-PRE bursts observed by *EXOSAT* suggest a distance to the source of $7.5^{+0.8}_{-1.1}$ kpc (Haberl & Titarchuk 1995), and also indicate a H-rich atmosphere; on the other hand, Christian & Swank (1997) derive a distance from the peak flux of PRE bursts of 11 kpc. One (or possibly two) high-frequency QPOs were discovered through *RXTE* observations (Ford et al. 1998). The optical counterpart is unknown.

The persistent flux from the source varies substantially in a quasi-periodic manner on a time-scale of several hundred days (e.g. Priedhorsky 1986, Fig. 8). The 2.5–25 keV flux measured by *RXTE*/PCA varied between 0.18–10.7×10^{-9} ergs cm^{-2} s^{-1}. We found a total of 39 type-I bursts in the public PCA data, including three exhibiting PRE. The distance derived from the PRE bursts is consistent with the closer distance estimate of Haberl & Titarchuk (1995) at between 5.8–7.6 kpc, depending upon the composition (Table 6). The persistent flux range is thus equivalent to an accretion rate of 1.1–70% $\dot{M}_{\rm Edd}$ (for a bolometric correction to the 2.5–25 keV flux which ranged between 1.29–1.75 for 3 selected observations, and was 1.48 in the mean). All but one of the bursts was observed when $F_p \lesssim 2.5 \times 10^{-9}$ ergs cm^{-2} s^{-1} (i.e. $\dot{M} \lesssim 16\%$ $\dot{M}_{\rm Edd}$). The non-PRE bursts had $\tau = 19 \pm 5$ s in the mean, while the PRE bursts, which were all observed at high $F_p = 2.25$–2.5×10^{-9} ergs cm^{-2} s^{-1}, were much faster with $\tau = 5.0 \pm 0.4$ s. The single burst observed at high $F_p = 8.1 \times 10^{-9}$ ergs cm^{-2} s^{-1} on 2002 June 29 19:54:43 UT also had a low $\tau = 6.8 \pm 0.4$ s but did not exhibit PRE.

We found four bursts with short recurrence times of between 7–11 min, which also had unusually small fluences. For the remaining bursts, taking into account the possibility of missed bursts, the recurrence times were 0.76–3.1 hr. Between 1997 May 16–19 ten bursts were detected off-axis during observations of PSR B1706−44, just $0\overset{\circ}{.}41$ away. Assuming that the X-ray flux from the pulsar is negligible, the majority of the bursts for which the recurrence time could be confidently measured had $\Delta t \approx 1$ hr and $\alpha = 34$–75. For three other pairs of bursts with somewhat longer $\Delta t = 1.6$–3 hr, the α-values ere much higher, at 196 ± 16, 186 ± 14, and, for an unusually weak burst, 500 ± 50.

3.12. *XTE J1709−267*

XTE J1709−267 ($l = 357\overset{\circ}{.}47$, $b = +7\overset{\circ}{.}91$) went into a large outburst in 1997 and was discovered by the *RXTE*/PCA during a satellite maneuver (Marshall et al.

1997). An improved position was obtained from *BeppoSAX* observations (Cocchi et al. 1998), also during which bursting behaviour was first observed. Three bursts were observed in total by *BeppoSAX*, with absorption-corrected bolometric peak fluxes of 16×10^{-9} ergs cm^{-2} s^{-1}, leading to a distance upper limit of 10 ± 1 kpc. A second outburst, very similar to the first, was observed with *RXTE* beginning 2001 December (Jonker et al. 2004). The maximum PCA flux was 3.2×10^{-9} ergs cm^{-2} s^{-1} (2.5–25 keV), slightly smaller than for the previous outburst (which peaked at 4.2×10^{-9} ergs cm^{-2} s^{-1}). For $d = 10$ kpc this corresponds to a peak accretion rate of 33–43% $\dot{M}_{\rm Edd}$. PCA observations detected 3 bursts during the 2001–02 outburst with peak fluxes of $(11.6 \pm 0.6) \times 10^{-9}$ ergs cm^{-2} s^{-1} and $\tau = 5.8 \pm 0.5$ s in the mean. All three bursts exhibited low-level flux for 2–3 s prior to the burst, and one (on 2002 January 30 04:16:02 UT) exhibited a precursor event peaking at $\approx 20\%$ of the subsequent maximum, remarkably similar to a burst observed from 4U 1636−536 on 2002 February 28 23:42:53 UT (see Fig. 9). While none of the bursts exhibited evidence for significant radius expansion, the third burst, on 2002 Feb 7 01:12:03 UT, exhibited marginal evidence (although it did not reach a peak flux level significantly higher than the other two). The distance limits derived from these bursts is consistent with that of the *BeppoSAX* observations, at 11 (14) kpc for $X = 0.7$ (0.0).

3.13. *XTE J1710−281*

This nearby source ($l = 356\overset{\circ}{.}36$, $b = +6\overset{\circ}{.}92$) was also detected in outburst by the PCA in 1998, and was identified with the *ROSAT* All-Sky Survey Bright Source Catalog source 1RXS J171012.3−280754 (Markwardt et al. 1998). Low-level activity continued throughout 1999, and recurring $<$ 800 s eclipses with a periodicity of 3.27 h (assumed to be the orbital period) were detected in subsequent observations (Markwardt et al. 1999c; Markwardt & Swank 2002). Bursting activity was also discovered during these *RXTE* observations, with a total of 15 bursts detected since, including one PRE burst and one pair of bursts separated by 10 min. The distance range implied by the peak flux of $(9.2 \pm 0.2) \times 10^{-9}$ ergs cm^{-2} s^{-1} for the single PRE burst is 12–16 kpc (Table 6; see also Markwardt & Swank 2002). The source was also active during 2001–02, at an overall flux range of 0.4–1.4×10^{-10} ergs cm^{-2} s^{-1} (2.5–25 keV). For $d = 16$ kpc this corresponds to 1–4% $\dot{M}_{\rm Edd}$ (assuming a bolometric correction of 1.421 ± 0.126). The non-PRE bursts were exceedingly faint, with peak fluxes of 0.22–3.6×10^{-9} ergs cm^{-2} s^{-1}. The bursts observed when $F_p > 1 \times 10^{-10}$ ergs cm^{-2} s^{-1} had a range of $\tau = 5$–17 s, with the PRE burst having the smallest value of $\tau = 5.7$ s. At lower fluxes all the bursts had $\tau \gtrsim 15$ s. On three occasions we measured burst intervals of ~ 7 hr, which we tentatively identify as the characteristic recurrence time for the bursts. The corresponding α-values varied widely between 22–190.

3.14. *XTE J1723−376*

This transient ($l = 350\overset{\circ}{.}18$, $b = -0\overset{\circ}{.}87$) underwent a moderate outburst on 1999 January and was discovered during an *RXTE*/PCA scan of the region (Marshall & Markwardt 1999). An *ASCA* observation on 1999 March 4 led to an improved position (Marshall et al. 1999), and the source activity continued throughout March (Markwardt et al. 1999c). Thermonuclear bursts were first observed during the *RXTE* observations, and a total of three bursts were observed. The brightest burst reached $(14.1 \pm 0.1) \times 10^{-9}$ ergs cm^{-2} s^{-1}, implying a source distance of at most 13 kpc. The persistent flux reached 1.5×10^{-9} ergs cm^{-2} s^{-1} (2.5–25 keV) in outburst, which for $d \lesssim 13$ kpc corresponds to $\lesssim 20\%$ $\dot{M}_{\rm Edd}$ (for a bolometric correction to the 2.5–25 keV flux of 1.05 ± 0.02). The first of the pair of bursts on 1999 February 3–4 ($\Delta t = 2.7$ hr) exhibited evidence for a double peak in the bolometric flux, and had $\tau = 12$ s. The second burst was faster and somewhat flat-topped, with $\tau = 7.5$ s and $\alpha = 170$.

3.15. *4U 1724−307 in Terzan 2*

A long thermonuclear burst was observed from 4U 1724−307 ($l = 356\overset{\circ}{.}32$, $b = +2\overset{\circ}{.}30$) by *OSO-8* (Swank et al. 1977), reaching a peak flux of 6.2×10^{-8} ergs cm^{-2} s^{-1}. The burst source was identified with the globular cluster Terzan 2 (Grindlay 1978; Grindlay et al. 1980), 7.5–12 kpc away (Kuulkers et al. 2003; although Ortolani et al. 1997 estimated a range of 5–8 kpc). No optical counterpart is known. Bursts are observed from the source relatively infrequently (e.g. Lewin et al. 1993), and the most detailed studies to date have been with *BeppoSAX*/WFC monitoring observations of the Galactic center region which found 24 bursts with inferred PRE reaching 5.4–8.4×10^{-8} ergs cm^{-2} s^{-1} (Kuulkers et al. 2003).

4U 1724−307 was persistently bright although declining during *RXTE* observations; in 1996–98 the persistent flux was $F_p = 1.2 \times 10^{-9}$ ergs cm^{-2} s^{-1} (2.5–25 keV, see also Olive et al. 1998), while in 2001–02 it had declined to 7×10^{-10} ergs cm^{-2} s^{-1}. For a distance of 9.5 kpc this corresponds to an accretion rate of 6–11% $\dot{M}_{\rm Edd}$. A burst observed by *RXTE* on 1996 November 8 07:00:31 UT exhibited sufficiently intense PRE that the color temperature fell below ~ 0.5 keV shortly after the start, so that the burst flux effectively dropped out of the PCA band (see Fig. 10 and Molkov et al. 2000; Kuulkers et al. 2003). Apart from this episode the burst flux was approximately constant at 6×10^{-8} ergs cm^{-2} s^{-1} for the first 25 s; this is substantially above the expected Eddington flux for a source at 9.5 kpc. A second PRE burst observed on 2004 February 23 exhibited much less extreme radius expansion, and reached a peak flux around 30% lower at 4×10^{-8} ergs cm^{-2} s^{-1}. The implied distance from this burst is 7.4 kpc, consistent with the lower limit of the estimated distance range for Terzan 2. The weaker PRE burst lasted only ≈ 20 s, and the fluence was less than a tenth of that of the brighter. The only other burst was similar in profile to the 2004 February burst, reaching a peak of 5×10^{-8} ergs cm^{-2} s^{-1}, but exhibiting only marginal radius expansion. Intense, long duration PRE bursts, as also observed from 4U 2129+12 (see §3.44) and GRS 1747−312 (§3.31), appear to consistently exceed the expected Eddington limit (see §4.4).

3.16. *4U 1728−34 (= GX 354+0)*

4U 1728−34 (GX 354+0; $l = 354\overset{\circ}{.}3$, $b = -0\overset{\circ}{.}15$) was first resolved by *Uhuru* scans of the galactic cen-

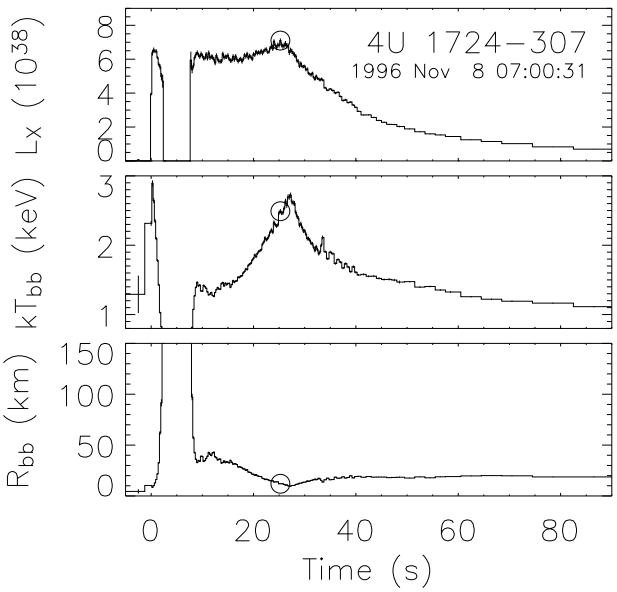

FIG. 10.— An example of an extremely strong photospheric radius-expansion burst observed from 4U 1724−307 in the globular cluster Terzan 2 by *RXTE*. *Top panel* Burst luminosity (in units of 10^{38} ergs s^{-1}; *middle panel* blackbody (color) temperature $kT_{\rm bb}$; and *bottom panel* blackbody radius $R_{\rm bb}$. L_X and $R_{\rm bb}$ are calculated assuming a distance to the host globular cluster Terzan 2 of 9.5 kpc (Kuulkers et al. 2003). The time at which the flux reaches its maximum value is indicated by the open circle. Note the gap in the first 10 s of this burst, preceded by an abrupt increase in the apparent blackbody radius to very large values. This gap was caused not by an interruption in the data but because the radius-expansion was sufficiently extreme to drive the peak of the spectrum below the PCA's energy range. In such cases we expect the luminosity is maintained at approximately the Eddington limit, although it is no longer observable by *RXTE*.

ter region (Forman et al. 1976b). The position of a possible radio counterpart suggested identification with a $K = 15$ infrared counterpart (Martí et al. 1998). Thermonuclear X-ray bursts were discovered during *SAS-3* observations of the Galactic center region (Lewin et al. 1976a; Hoffman et al. 1976). The bursting behaviour was subsequently studied in detail using extensive *SAS-3* observations, which included 96 bursts in total. The burst intervals were moderately regular, varying by a factor of ~ 2, and — along with the burst properties — were apparently not correlated with F_p (Lewin et al. 1993). The average $\tau = 7.8 \pm 2.4$ s, while $\alpha = 110$ with only $\sim 15\%$ variation between observations. Basinska et al. (1984) found evidence for a narrow distribution of peak burst fluxes, as well as a correlation between peak flux and the burst fluence. Assuming that the maximum burst flux is the Eddington limit, the distance to the source is 4.2–6.4 kpc (see also van Paradijs 1978); other measurements are all around these values (e.g. 6 kpc; Kaminker et al. 1989). Early *RXTE* observations of the source led to the discovery of nearly coherent 363 Hz oscillations during the bursts (Strohmayer et al. 1996) that were subsequently observed in 12 other sources (see §2.4). Subsets of the bursts observed during the PCA observations have been studied by van Straaten et al. (2001), Franco (2001), and Muno et al. (2001, 2004), with particular attention to the relationship between the appearance of burst oscillations and the mass accretion rate.

4U 1728−34 was persistently bright during *RXTE*'s lifetime at $F_p = 1$–7×10^{-9} ergs cm^{-2} s^{-1} (2.5–25 keV). We note that these persistent flux levels may be affected by the presence of the nearby transient 4U 1730−335 (the Rapid Burster; see §3.17 and §A.1). For a distance of 5.2 kpc (see also Galloway et al. 2003) this is equivalent to an accretion rate of 3–18% $\dot{M}_{\rm Edd}$ (for a bolometric correction to the 2.5–25 keV flux between 1.05–1.55, or 1.24 ± 0.20 in the mean). We found 105 bursts in total attributable to 4U 1728−34 in public *RXTE* observations. The bursts were all rather homogeneous, with short rise times (≈ 1 s) and time scales ($\tau = 6.3 \pm 1.3$). The shortest measured burst interval was 1.77 hr; Cornelisse et al. (2003) found evidence for clustering of recurrence times in bursts observed by *BeppoSAX* between 2.5–5 hr, which is consistent with the *RXTE* measurements. The α-values for the bursts varied between 91–310, or 150 ± 70 in the mean. The burst properties bear a remarkable resemblence to those of 3A 1820−30 (see §3.36; Cumming 2003), which is an ultracompact binary with an evolved, H-poor mass donor. It seems highly probable that the mass donor in 4U 1738−34 is also H-poor.

A significant fraction ($\approx 2/3$) of the bursts observed by *RXTE* showed evidence for PRE episodes. The peak flux $F_{\rm pk,PRE}$ of these bursts were normally distributed, with a standard deviation of 9%. We found a correlation between the peak PRE burst flux and the persistent emission F_p; both quantities varied quasi-periodically with a time scale of ≈ 40 d (Galloway et al. 2003). Furthermore, the peak flux and burst fluence E_b were strongly correlated. This behaviour is expected if some of the burst flux is reprocessed by material surrounding the neutron star. One possibility is that the accretion disk surrounding the NS is warped, and the warp is precessing on a ≈ 40 d time scale so that the variations in the projected area to our line of sight gives rise to the variable persistent and burst emission as we observe. Shaposhnikov et al. (2003) suggests instead that the variations in $F_{\rm pk,PRE}$ arise from increased visibility of the neutron star following the atmospheric contraction. The expanding atmosphere, it was argued, will effectively remove the inner part of the accretion disk, out to the radius of maximum expansion. When the atmosphere contracts again, a gap will remain between the inner accretion disk and the NS surface, so that the hemisphere of the NS away from the observer (normally obscured by the disk) is exposed, thus boosting the observed flux. This interpretation allows the inclination of the source to be estimated as $\sim 50°$. Model fits to the *RXTE* spectra during PRE also suggest an atmosphere dominated by helium.

3.17. *Rapid Burster (= MXB 1730−335) in Liller 1*

This remarkable Galactic bulge ($l = 354\overset{\circ}{.}84$, $b = -0\overset{\circ}{.}16$) transient was discovered during *SAS-3* observations (Lewin et al. 1976b) to exhibit unusually frequent X-ray bursts, with intervals of 6 s to 5 min. An apparent second class of "anomalous" bursts, with 3 s rise times and lower peak intensities (Ulmer et al. 1977), were later identified as thermonuclear (type-I) bursts; the brighter, more frequent (type II) bursts were attributed instead to episodic accretion (Hoffman et al. 1978). Thermonuclear bursts occur in the Rapid Burster at intervals of

$\sim$ 1.5–4 hr (Lewin et al. 1993), in the same range as other bursters, and are almost always observed alongside type-II bursts. No PRE bursts have been reported; the peak flux of the brightest thermonuclear bursts is 1.7×10^{-8} ergs cm^{-2} s^{-1} (Kuulkers et al. 2003; see also Lewin et al. 1993). The type-I bursts have long durations, suggesting that substantial amounts of H is present at ignition. Historically, the source has exhibited approximately periodic outbursts every $\sim$ 200 d (Guerriero et al. 1999); thermonuclear bursts are seen preferentially in the first 15–20 d of the outburst. Located in the globular cluster Liller 1 (Liller 1977), no conclusive optical counterpart has been found despite *Chandra* and *HST* observations of the field (Homer et al. 2001b), and a confirmed radio counterpart (Moore et al. 2000).

RXTE observations have detected ≈ 25 outbursts (as of 2006 March), and indicate that the outburst recurrence time has decreased to $\sim$ 100 d (Masetti 2002; see also Fig. 8). The peak 2.5–25 keV flux typical for outbursts prior to 2000 was 1.2×10^{-8} ergs cm^{-2} s^{-1}, which for a distance to the host cluster of 8.8 kpc (Kuulkers et al. 2003) corresponds to an accretion rate of 95% $\dot{M}_{\rm Edd}$. Outbursts occuring in 2000 and later appeared to peak at a significantly smaller flux of $\approx 5 \times 10^{-9}$ ergs cm^{-2} s^{-1}, or $\approx 40\%$ $\dot{M}_{\rm Edd}$. The minimum detectable F_p was 1.6×10^{-10} ergs cm^{-2} s^{-1}, or 1.2% $\dot{M}_{\rm Edd}$. We note that these F_p measurements may include a contribution from the nearby source 4U 1728−34 (see §3.16, §A.1). In the public *RXTE* observations of the Rapid Burster we found 65 type-I bursts, none of which exhibited PRE. Analysis of a subset of the thermonuclear bursts by Fox et al. (2001) revealed a possible burst oscillation at 306.5 Hz. The signal was detected by combining the power density spectra of 31 individual bursts, and is not detected in any single burst. As also noted by Fox et al. (2001), the bursts exhibit a range of profiles, with τ = 5–40; some bursts appear to last for more than 100 s. A few bursts appear to be followed by an increase in the persistent flux level, which makes the fluence difficult to constrain. The peak flux was $\sim 10^{-8}$ ergs cm^{-2} s^{-1}, similar to previous observations. The burst rate was 0.43 ± 0.06 hr^{-1} on average, and increased significantly with persistent flux (although it is possible that some faint thermonuclear bursts are in fact mis-identified type-II bursts). Interestingly, the Rapid Burster appears to be "rapid" both in the sense of type-I and type-II bursts.

3.18. *KS 1731−260*

A transient located near the Galactic center (l = 1.°07, b = +3.°66), KS 1731−26 was discovered in August 1989 using the imaging spectrometer aboard the *Mir-Kvant* observatory (Sunyaev et al. 1990). Type I X-ray bursts were also first seen during these observations, lasting 10–20 s and reaching $\sim$ 0.6 Crab (3×10^{-8} ergs cm^{-2} s^{-1}). An improved X-ray position from *Chandra* observations (Wijnands et al. 2001a) led to the identification of the $J = 17.32 \pm 0.2$, $K' = 16.36 \pm 0.18$ counterpart (Revnivtsev & Sunyaev 2002; Mignani et al. 2002). *RXTE* observations revealed 524 Hz burst oscillations which occurred preferentially in PRE bursts (Smith et al. 1997; Muno et al. 2000)

The source was active at 1–6 $\times 10^{-9}$ ergs cm^{-2} s^{-1} (2.5–25 keV) although declining steadily in intensity between 1996–2000, before transitioning to quiescence early in 2001 (Wijnands et al. 2001b). After this time the source became undetectable by *RXTE*, and no more bursts were detected We found 27 bursts from KS 1731−26, with 4 PRE bursts observed at relatively high $F_p \gtrsim 3.9 \times 10^{-9}$ ergs cm^{-2} s^{-1} (see also Muno et al. 2004); oscillations were found preferentially in the PRE bursts (Muno et al. 2001; see also §4.5). The PRE bursts reached peak fluxes indicating a source distance of 7.2 ± 1.0 kpc (assuming the bursts reach $L_{\rm Edd,He}$; Table 6). Thus, the accretion rate while the source was active was 6–38% $\dot{M}_{\rm Edd}$ (for a bolometric correction averaging 1.62 over two observations). The PRE bursts were of short duration, with $\tau = 8.7 \pm 1.4$ s in the mean. In observations between 2000 August–September, during which $F_p = (2.12 \pm 0.07) \times 10^{-9}$ ergs cm^{-2} s^{-1} (i.e. 14% $\dot{M}_{\rm Edd}$), the bursts were much longer duration ($\tau = 23.8 \pm 0.7$ s, rise time 4.8 ± 0.6 s) and occurred regularly at $\Delta t = 2.59 \pm 0.06$ hr. The α-values were 46.9 ± 1.4 in the mean; in many respects these bursts were remarkably similar to those observed from GS 1826−24 (Galloway et al. 2004b; see also §3.37, §4.1). At both higher and lower F_p this regular bursting ceased (also noted by Cornelisse et al. 2003).

3.19. *SLX 1735−269*

This persistent Galactic-center (l = 0.°79, b = +2.°40) source was discovered in observations with a coded-mask X-ray telescope aboard *Spacelab 2* (Skinner et al. 1987), and a single X-ray burst detected later by *BeppoSAX*/WFC was attributed to the source (Bazzano et al. 1997). The burst lasted 30 s, and had a peak flux of 1.8×10^{-8} ergs cm^{-2} s^{-1}. Molkov et al. (2004) detected six bursts in *INTEGRAL* observations between 2003 April and September, one with a brief precursor, an unusually long duration of $\sim$ 600 s, and indications of PRE. The peak flux of 6×10^{-8} ergs cm^{-2} s^{-1} for the long burst suggests a distance of 5–6 kpc, depending upon the composition. The five bursts in 2003 September were consistent with a steady recurrence time of 12.3 hr; the estimated α-values were 100–200, and the inferred accretion rate was $\approx 1.7\%$ $\dot{M}_{\rm Edd}$ (for $d = 8.5$ kpc). An improved X-ray position has been determined from *Chandra* observations by Wilson et al. (2003), although this position did not match that of any IR counterpart (to an upper limit of $J > 19.4$).

The persistent flux measured by the *RXTE*/PCA during 1997 and 2001–02 was 2.5–6.5×10^{-10} ergs cm^{-2} s^{-1} (2.5–25 keV); the timing behaviour during these observations was studied by Wijnands & van der Klis (1999). We found just one burst, on 2002 January 23, with a peak flux of $(43.0 \pm 1.3) \times 10^{-9}$ ergs cm^{-2} s^{-1} and $\tau = 12.5$, and with no evidence for PRE. This implies an upper limit to the distance of 7.3 kpc (Table 6). The inferred accretion rate during the *RXTE* observations was then 1–4% $\dot{M}_{\rm Edd}$.

3.20. *4U 1735−44*

This bright, persistent atoll source at l = 17.°7, b = 17.°5 was first detected by *Uhuru*, while thermonuclear bursts were discovered during *SAS-3* observations

(Lewin et al. 1977). The 20–30″ position from *SAS-3* (Jernigan et al. 1977) led to the identification of the $V \sim 17.5$ optical counterpart, V926 Sco (McClintock et al. 1977), with optical and UV properties very similar to those of the counterpart of Sco X-1 (e.g McClintock et al. 1978). Delayed optical bursts have been observed from the counterpart (Grindlay et al. 1978), and periodic photometric variations indicate an orbital period of 4.65 hr (McClintock & Petro 1981; Corbet et al. 1986; note that Lewin et al. 1993 erroneously lists the $P_{\rm orb}$ as 3.65 hr). The bursts are notable for their rapid time scales ($\tau = 4.4$ s), irregular recurrence times and consequently extremely variable α-values (from 250 to ~ 8000; van Paradijs et al. 1988b; Lewin et al. 1993). The source is one of a growing number which exhibit extremely long "superbursts", detected in *BeppoSAX* observations (Cornelisse et al. 2000).

The persistent flux measured by *RXTE* varied between 3–8 $\times 10^{-9}$ ergs cm^{-2} s^{-1} (2.5–25 keV), with evidence for a long ($\sim$ 1000 d) time scale (see Fig. 8). We detected 11 bursts in total from the PCA observations, 6 of which exhibited evidence for PRE with a mean peak flux of $(31 \pm 5) \times 10^{-9}$ ergs cm^{-2} s^{-1}. Assuming these bursts reach $L_{\rm Edd,He}$, the distance to the source is 8.5 kpc, implying a range of accretion rates of 19–50% $\dot{M}_{\rm Edd}$ (adopting a bolometric correction of 1.137, the mean of values from two observations). All the bursts were observed when $F_p \lesssim 5.4 \times 10^{-9}$ ergs cm^{-2} s^{-1}, i.e. $\dot{M} \lesssim 34\%\ \dot{M}_{\rm Edd}$. The majority were fast, with $\tau = 3.4 \pm 0.4$ s. We found four pairs of bursts with recurrence times of 1.1–1.5 hr, and one pair with $\Delta t = 0.46$ hr; the alpha values varied from 150–270. These properties are all consistent with pure He fuel.

3.21. *KS 1741−293 (= AX J1744.8-2921)*

This Galactic center ($l = 359\overset{\circ}{.}55$, $b = -0\overset{\circ}{.}07$) source was discovered in 1989 August with TTM/Kvant aboard *Mir* (in 't Zand et al. 1991); it is within the error boxes of both MXB 1742−29 & MXB 1743−29 (Lewin et al. 1976d). Two single-peaked X-ray bursts were observed, with estimated peak fluxes of 12 and 16×10^{-9} ergs cm^{-2} s^{-1}. KS 1741−293 was visible to *RXTE* in all the Galactic center fields in which bursts were observed (see §A.4), as well as the field centered on GRO J1744−28 (§A.5), although none of those bursts were conclusively attributable to this source. Because the source density is so high in this region, it was not possible to independently measure the source flux with the PCA observations. Furthermore, because the source position is only known to $\approx 1'$, KS 1741−293 is not included in the list of sources for which the ASM routinely provides intensity measurements.

An extremely faint burst was observed on 1998 Sep 24 00:22:24 UT during pointings towards 1E 1740.7−2942, with an intrinsic peak flux of $(1.6 \pm 0.3) \times 10^{-9}$ ergs cm^{-2} s^{-1}. KS 1741−293, 2E 1742.9−2929 and SLX 1744−300 are all $\approx 1^\circ$ from the center of this field, with KS 1741−293 the closest by a small margin. Since the scaling factor due to the collimator response is extremely sensitive to offset angles around this value, we attribute this burst to the closest source, KS 1741−293. The resulting scaled peak flux was $(41 \pm 9) \times 10^{-9}$ ergs cm^{-2} s^{-1}, which is a factor of ≈ 2 larger than previously observed bursts from the source. While 2E 1742.9−2929 exhibited other bursts soon after, on 1998 September 30, the rescaled flux assuming the burst originated from that source instead would be almost a factor of two higher, which would be in excess of the Eddington limit for a Galactic center source.

3.22. *GRS 1741.9−2853 (= AX J1745.0−2855)*

This Galactic center ($l = 359\overset{\circ}{.}96$, $b = +0\overset{\circ}{.}13$) transient was discovered during observations with the ART-P coded-mask X-ray telescope aboard the *GRANAT* observatory (Pavlinsky et al. 1994). Bursts (with indications of PRE) were first detected from this source by *BeppoSAX* in August and September 1996 (Cocchi et al. 1999); the peak flux indicates a distance of ~ 8 kpc, consistent with the distance to the Galactic center.

We attributed 8 bursts in observations covering GRS 1741.9−2853 to this source; we note that Strohmayer et al. (1997a) reported millisecond oscillations in 3 of the 8, originally attributed to MXB 1743−29 (see also §A.5). The two shortest burst intervals were 35.6 hr and 39.4 hr, similar to the recurrence time of 1.46 d observed for MXB 1743−29 (Lewin et al. 1993), although it is possible that intermediate bursts were missed during the *RXTE* observations. Six of the 8 bursts exhibited PRE, with peak fluxes varying significantly between 22–52 $\times 10^{-9}$ ergs cm^{-2} s^{-1}. This range of peak PRE burst fluxes implies a range of distances of 5–10 kpc, consistent with the distance to the Galactic center (see also Table 6). The two brightest bursts, on 1996 July 8 01:57:47 UT and July 23 04:13:56 UT, had unusual profiles with broad maxima, long durations ($\tau = 20.8$ and 46.4 s, respectively; see Fig. 9) and PRE to large radii, similar as has been observed recently for GRS 1747−312 (in 't Zand et al. 2003c) as well as a few other sources. The remaining bursts had much shorter durations, $\tau = 11 \pm 2$ s in the mean.

3.23. *2E 1742.9−2929 (= GC X-1/1A 1742−294)*

Bursts from this Galactic center ($l = 359\overset{\circ}{.}56$, $b = -0\overset{\circ}{.}39$) source were probably first observed with *SAS-3*, and attributed to a source designated MXB 1742−29 (Lewin et al. 1976d). 2E 1742.9−2929 was subsequently observed with *Ariel-5* and *Einstein*, among others. The most detailed study of the bursts were of 26 observed with ART-P/*Granat* Lutovinov et al. (2001). Both "weak" and "strong" bursts were observed; the brightest of the latter class reached a maximum of 3.5–4 $\times 10^{-8}$ ergs cm^{-2} s^{-1} (3–20 keV).

2E 1742.9−2929 was the most active Galactic center burster during the period covered by the *RXTE* observations. In the ASM the source was persistently bright at ≈ 2 counts s^{-1} (25 mCrab, or 6×10^{-10} ergs cm^{-2} s^{-1} in 2–10 keV; see Fig. 8). We attributed more than 80 bursts to this source in total, the majority from 2001 September 26 to October 8 (see §A.4.3). All but two of the bursts were faint, with inferred peak fluxes of $(7 \pm 3) \times 10^{-9}$ ergs cm^{-2} s^{-1} in the mean, $\tau = 10$–40 s, and no evidence for PRE. The other two bursts, observed in the field centered on $\alpha = 17\overset{\rm h}{.}44\overset{\rm m}{.}02.6$, $\delta = -29^\circ 43' 26''$ (J2000.0; see §A.4.1) on 1997 March 20 and 1998 November 12, were of shorter duration with $\tau \approx 8$ s and exhibited strong PRE with rescaled peak fluxes of

4×10^{-8} ergs cm^{-2} s^{-1}, consistent with the brightest bursts previously observed from this source by *Granat*. About 20% of the bursts had recurrence times $\lesssim 0.5$ hr (0.31 ± 0.09 hr in the mean), while 35% had $\Delta t = 1.5$–3 hr.

3.24. *SAX J1747.0−2853*

This transient was first detected in 1998 (in 't Zand et al. 1998a) at a position ($l = 0\overset{\circ}{.}21$, $b = -0\overset{\circ}{.}24$) consistent with a source detected in the 1970s by rocket-borne coded-mask/*Ariel-5* observations, GX .2−.2 (also known as 1A 1743-288; Proctor et al. 1978). Bursting behaviour was first observed by *BeppoSAX* (Sidoli et al. 1998). Followup observations revealed at least one radius-expansion burst, indicating a source distance of ~ 9 kpc (Natalucci et al. 2000).

The source appeared in outburst on several subsequent occasions, including 2000 February-June and 2001 September (Natalucci et al. 2004). During *RXTE* observations in 2001 September–October, 15 bursts were detected which we attributed to this source (see §A.4.3). The bursts were relatively long, with $\tau = 11 \pm 2$ s in the mean; 10 of the 15 exhibited PRE, and 7 bursts also exhibited a distinct double-peaked morphology. If the PRE bursts reached $L_{\rm Edd,He}$, the estimated mean peak flux implies a distance of 6.7 kpc (see Table 6). Assuming that SAX J1747.0−2853 was the only active source in the field during the 2001 September observations, the persistent flux was 1.5–1.7×10^{-9} ergs cm^{-2} s^{-1}, equivalent to an accretion rate of 7–8% $\dot{M}_{\rm Edd}$. The shortest recurrence times measured for the bursts was 3–4.2 hr.

3.25. *SLX 1744−299/300*

This close ($2\overset{'}{.}8$ separation) pair of Galactic center ($l = 359\overset{\circ}{.}26$, $b = -0\overset{\circ}{.}91$) sources was discovered during mapping observations with the SL2-XRT instrument aboard *Spacelab-2* (Skinner et al. 1987). Their dual nature was revealed when a burst was observed from the southern source, with a peak flux of 1.4×10^{-8} ergs cm^{-2} s^{-1} (including a 20% correction for absorption; Skinner et al. 1990). Bursts from this region were also observed by *EXOSAT*, TTM/*Kvant* and *SAS-3* (Lewin et al. 1993).

The source was persistently active in the ASM at $\approx$ 2 counts s^{-1} (equivalent to 25 mCrab, or 6×10^{-10} ergs cm^{-2} s^{-1} in 2–10 keV; see Fig. 8). The source was only observed with the PCA well off-axis in a field containing a number of other sources (see §A.4.1), so it was not possible to measure the flux more precisely. We found 3 bursts in public observations attributable to this pair of sources. The bursts were short, with $\tau = 6$–7.6 s, and with peak fluxes between 1.4–1.9×10^{-8} ergs cm^{-2} s^{-1}, roughly consistent with earlier observations.

3.26. *GX 3+1*

This persistent Galactic center source ($l = 2\overset{\circ}{.}29$, $b = +0\overset{\circ}{.}79$) was discovered during a rocket flight in 1964 (Bowyer et al. 1965), and subsequently proved to be one of the brightest persistent sources in the Galaxy. A detailed study of low-frequency QPOs in this and other sources led to the introduction of the atoll/Z-source classification (Hasinger & van der Klis 1989). No optical counterpart is known (e.g. Naylor et al. 1991). Thermonuclear X-ray bursts were discovered during *Hakucho* observations (Makishima et al. 1983). The bursts were observed at a particularly low F_p level, and reached peak fluxes of 4–8×10^{-8} ergs cm^{-2} s^{-1} (see also Lewin et al. 1993). Kuulkers (2002) also found evidence for a possible "superburst" from *RXTE*/ASM monitoring. The most detailed study of the thermonuclear bursts to date was by den Hartog et al. (2003), who detected 61 bursts with *BeppoSAX*/WFC and found them remarkably homogeneous with a weighted mean $\tau = 3.63 \pm 0.10$ s. The burst rate dropped by a factor of ≈ 6 as the persistent flux increased through a relatively small range.

Long-term flux measurements suggest that F_p varies on a time scale of a few years (e.g. Fig. 8). At the peak in 2001–03 the PCA flux was 8–12×10^{-9} ergs cm^{-2} s^{-1}, while during the minimum was 4–7×10^{-9} ergs cm^{-2} s^{-1}. *RXTE* observations revealed the first radius expansion burst from the source on 1999 August 10 18:35:54 UT (Kuulkers & van der Klis 2000), leading to a distance estimate of $\sim$ 4.5 kpc with estimated uncertainty of up to 30%. The rapid rise (0.75 s) and short duration ($\tau = 4.96 \pm 0.13$ s) of the burst suggests He-rich fuel, and assuming the flux reaches $L_{\rm Edd,He}$ a somewhat larger value of 6.5 kpc is indicated (see Table 6 and den Hartog et al. 2003). In that case, the persistent flux range corresponds to accretion rates of 17–50% $\dot{M}_{\rm Edd}$. Just one other burst was observed, on 2001 Aug 7 16:38:46 UT, with $\tau = 11.6 \pm 1.0$ s and no evidence for PRE. While the $F_{\rm pk}$ was significantly lower than for the PRE burst, the fluence was significantly larger.

3.27. *SAX J1748.9−2021 in NGC 6440*

SAX J1748.9−2021 is one of an estimated 4–5 LMXBs (Pooley et al. 2002) in the globular cluster NGC 6440 ($l = 7\overset{\circ}{.}73$, $b = +3\overset{\circ}{.}80$, $d = 8.4^{+1.5}_{-1.3}$ kpc; Kuulkers et al. 2003). Transient X-ray emission was detected from the cluster in 1971 (Markert et al. 1975; Forman et al. 1976a), 1998 (in 't Zand et al. 1999b), and 2001 (in 't Zand et al. 2001b), although it is not certain that the outbursts were all from the same source. A possible optical counterpart was identified during the 1998 outburst (Verbunt et al. 2000). Thermonuclear bursts were also first detected during this outburst (in 't Zand et al. 1999b). Three bursts were detected in the WFC, with recurrence times of ≈ 2.8 hr. A similar burst observed with the narrow-field instruments reached a peak flux of 1.7×10^{-8} ergs cm^{-2} s^{-1}.

No bursts were detected by *RXTE* during the 1998 outburst, but observations during the 2001 outburst revealed 16 bursts, one of which (#16, Table 2) exhibited burst oscillations at 409.7 Hz (Kaaret et al. 2003). Six bursts exhibited PRE, most with a pronounced double-peaked maximum (see Fig. 9) which varied in flux between 28–40×10^{-9} ergs cm^{-2} s^{-1}. The inferred distance (assuming, based on the short PRE burst duration of $\tau = 6.9 \pm 1.3$ s, that the bursts reached $L_{\rm Edd,He}$) is 8.1 kpc (see Table 6). The range of F_p measured by *RXTE*, from 6×10^{-10} ergs cm^{-2} s^{-1} prior to the 2001 outburst to 4.4×10^{-9} ergs cm^{-2} s^{-1} (2.5–25 keV) at the peak, thus translates to an inferred accretion rate range of 3–25% $\dot{M}_{\rm Edd}$ (with a bolometric correction averaging 1.157 ± 0.015 over four observations).

The non-PRE bursts bursts had longer durations, $\tau = 15 \pm 4$ on average, and peaked in the range 1.9–

2.2×10^{-8} ergs cm^{-2} s^{-1} (roughly consistent with the burst observed by the *BeppoSAX*/NFI; in 't Zand et al. 1999b). The inferred burst recurrence times varied between 1.02–1.90 hr, rather faster than in previous observations (in 't Zand et al. 1999b). While the measured α was not correlated with F_p (which only varied by about 9% rms over the observations with bursts), it was strongly anticorrelated with τ, with $\alpha = 100$–150 for the fast bursts and $\alpha = 50$–65 for the slow bursts. This is consistent with the fast bursts arising primarily from He burning, while in the slow bursts the fuel is a mixture of H/He (see also Fig. 21). Perhaps most interestingly, the long and short bursts appeared to alternate independently of the persistent flux.

A new outburst was detected in PCA scans of the Galactic bulge region on 2005 May 12–16 (Markwardt & Swank 2005).

3.28. *EXO 1745−248 in Terzan 5*

EXO 1745−248, in the Galactic bulge ($l = 3\overset{\circ}{.}84$, $b = +1\overset{\circ}{.}46$) globular cluster Terzan 5 ($d = 8.7^{+3.3}_{-2.4}$ Kuulkers et al. 2003), was discovered during *Hakucho* observations of the region (Makishima et al. 1981b). The source has been noted for episodic burst behaviour, as well as burst intervals as short as 8 min (Inoue et al. 1984; see also Lewin et al. 1993). PCA/*RXTE* scans of the bulge detected a new transient outburst in 2000 July (Markwardt & Swank 2000). Followup pointed observations revealed 15 X-ray bursts with an average separation of 25 min, as well as dipping activity and QPOs around 65 and 134 mHz (Markwardt et al. 2000).

The 2000 outburst lightcurve was strongly asymmetric, with an initial interval of variable intensity (2.5–25 keV flux of 1–5 $\times 10^{-9}$ ergs cm^{-2} s^{-1}) interrupted by an abrupt increase between August 15–18 to a peak on August 24 (MJD 51780) of 14×10^{-9} ergs cm^{-2} s^{-1} (2.5–25 keV; Fig. 11). Following the peak, the flux decreased more or less smoothly to $\lesssim 10^{-9}$ ergs cm^{-2} s^{-1} (2.5–25 keV) on October 16. For $d = 8.7$ kpc this corresponds to an accretion rate at the peak of $\gtrsim \dot{M}_{\rm Edd}$ (for a bolometric correction averaging 1.42 ± 0.13 over three observations). Prior to the outburst maximum we detected 21 type-I bursts with peak fluxes of 3–19×10^{-9} ergs cm^{-2} s^{-1}. For those observations where we saw more than one burst, the typical recurrence times were 17–49 min. We found no correlation between the recurrence time and the burst fluence. Some of these faint bursts exhibited ~ 1 Hz quasi-periodic intensity variations superimposed on the burst lightcurve (Fig. 9). The estimated α-values were rather low at 20–46 which (along with the long burst durations $\tau \approx 25$ s) can typically only be achieved with high $Q_{\rm nuc}$ values indicative of H-rich fuel. At higher accretion rates He burning is stabilized, which is likely the cause of the cessation of bursting following the increase on August 15–18.

Following the abrupt increase in intensity between August 15–18, the bursting behaviour ceased until September 24. By this time the persistent intensity had decreased to around 4×10^{-9} ergs cm^{-2} s^{-1} (2.5–25 keV), similar to the level at which bursts were observed prior to the outburst peak. During this observation one burst was observed, followed by a second on October 2. These two bursts were of markedly different character to those prior to the intensity peak, with peak fluxes of $\approx 6 \times 10^{-8}$ ergs cm^{-2} s^{-1}, shorter durations of $\tau = 6.6$ and 7.3 s, and both exhibiting strong PRE (see Fig. 9; Kuulkers et al. 2003). For the known distance of 8.7 kpc for Terzan 5, we expect an Eddington flux for cosmic abundances of 1.7×10^{-8} ergs cm^{-2} s^{-1}, or 3×10^{-8} ergs cm^{-2} s^{-1} for pure He; thus, the two PRE bursts appear to be super-Eddington by a factor of at least 2 (see §4.4). This discrepancy was also noted by Kuulkers et al. (2003); furthermore, the peak fluxes for all PRE bursts from this source measured by different instruments exhibited a large (factor of ~ 3) variation.

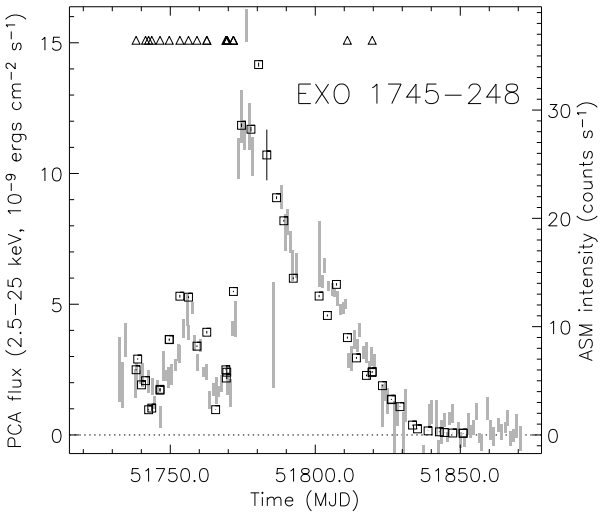

FIG. 11.— Flux evolution of EXO 1745−248 throughout the 2000 outburst. The PCA flux (open squares) is calculated from spectra covering 2.5–25 keV, and is averaged over those PCUs which are operating, correcting for systemic biases between individual PCUs. Error bars indicate the 1σ uncertainties. Also shown are the 1σ confidence regions for ASM intensity measurements (grey rectangles, right-hand y-axis). The triangles at the top of the plot indicate the times of type-I bursts. The properties of the bursts were markedly different before and after the outburst maximum, although they occurred at similar persistent flux levels. The bursts before 2000 August 24 (MJD 51780) were frequent and faint, while the two bursts observed afterwards were bright and exhibited radius expansion.

3.29. *4U 1746−37 in NGC 6441*

Persistent emission from 4U 1746−37 ($l = 353\overset{\circ}{.}53$, $b = -5\overset{\circ}{.}01$) was first recorded in the 3rd *Uhuru* catalog (Giacconi et al. 1974); thermonuclear X-ray bursts were probably first observed during *SAS-3* observations (Li & Clark 1977). PRE bursts have previously been observed by *EXOSAT* (Sztajno et al. 1987) with peak fluxes of $(1 \pm 0.1) \times 10^{-8}$ ergs cm^{-2} s^{-1} (see also Lewin et al. 1993; Kuulkers et al. 2003). Periodic intensity dips every 5.7 hr were reported from *Ginga* observations (Sansom et al. 1993); more recent analysis of *RXTE* data indicate a somewhat shorter dip period of 5.16 ± 0.01 hr (Bałucińska-Church et al. 2004). The optical counterpart, identified from an *HST* image following *Chandra* observations, also shows variations which are consistent with a period of ≈ 5 hr (Homer et al. 2002).

4U 1746−37 was active but variable at between 0.16–1.6×10^{-9} ergs cm^{-2} s^{-1} (2.5–25 keV) throughout the *RXTE* observations. For the distance to the cluster of

$11.0^{+0.9}_{-0.8}$ kpc (Kuulkers et al. 2003) this corresponds to a range of accretion rates of 2–16% $\dot{M}_{\rm Edd}$ (for a bolometric correction of between 1.09–1.45, depending upon the epoch). The catalog contains a total of 30 bursts from 4U 1746−37. The burst properties were clustered into three groups, depending upon the persistent flux level; at $F_p \approx 1.6 \times 10^{-10}$ ergs cm^{-2} s^{-1} (2.5–25 keV), we detected long-duration bursts with $\tau = 13 \pm 2$ s in the mean, while at higher F_p the bursts fell into two groups, one even longer duration with $\tau = 31 \pm 3$ s and the other very short with $\tau = 4.5 \pm 0.9$ s. This latter group included three PRE bursts, which reached peak fluxes a factor of two lower than previous PRE bursts from the source, at $(5.3 \pm 0.9) \times 10^{-9}$ ergs cm^{-2} s^{-1} (see also §4.4 and Table 6). We note that Kuulkers et al. (2003) did not categorize these three bursts as PRE. Overall the peak fluxes were approximately bimodally distributed, with 15 bursts reaching fluxes between (0.4–2.8) $\times 10^{-9}$ ergs cm^{-2} s^{-1}, and the rest peaking at between (3.8–6.3) $\times 10^{-9}$ ergs cm^{-2} s^{-1}. The characteristic α-values for the bright bursts ($\tau \approx 12$ s) was 35–50, while for the faint bursts ($\tau \approx 32$ s) was 140–180 (we note that 4U 1705−44 was the only other source with bursts with $\tau > 20$ s and $\alpha > 100$).

On two separate occasions (1996 October 25–27 and 1998 November 7th), a train of regular bright (faint) bursts was interrupted by an out-of-phase faint (bright) burst. As discussed by Galloway et al. (2004a), such interrupted regular bursting has not been previously observed, and is difficult to understand in the context of standard burst models. An alternative possibility is the presence of *two* sources in the cluster, bursting independently. From the stellar encounter rate for the host cluster NGC 6441 (which is the second-highest of all Galactic globular clusters), we expect around 6 LMXBs in the cluster (Pooley et al. 2003; Heinke et al. 2003). High spatial resolution observations during intervals of burst activity are required in order to independently localize individual bursts and confirm this hypothesis.

3.30. *SAX J1750.8−2900*

This Galactic center ($l = 0.^\circ45$, $b = -0.^\circ95$) source was first detected by *BeppoSAX* in 1997 as a weak, bursting transient (Natalucci et al. 1999). The source was detected in outburst once more in 2001 March, exhibiting an initial rise and steep fall early in March, followed by a second peak around April 21.

We found four bursts between 2001 April 6–15 attributable to the source, three of which were bright with $F_{\rm peak} \approx 5 \times 10^{-8}$ ergs cm^{-2} s^{-1} and two of those with evidence for PRE. The corresponding distance estimate (assuming, given the short durations $\tau = 5$–7.3 s of the bursts, that they reach $L_{\rm Edd,He}$) is 6.79 ± 0.14 kpc (see Table 6). Burst oscillations at 600.75 Hz were detected in the second burst on 2001 April 12, which also exhibited PRE implying a distance 6.3 ± 0.7 kpc (Kaaret et al. 2002). The peak flux measured by the PCA during the 2001 outburst was 2.7×10^{-9} ergs cm^{-2} s^{-1} (2.5–25 keV), which corresponds to 13% $\dot{M}_{\rm Edd}$; during the secondary peak the source reached 2.4×10^{-9} ergs cm^{-2} s^{-1}, while the persistent level was $\approx 3 \times 10^{-10}$ ergs cm^{-2} s^{-1} (1.4% $\dot{M}_{\rm Edd}$, although the flux may contain contribution from other souces in the field; see §A.2). The shortest recurrence time measured, between one of the PRE bursts and the final, faint burst ($F_{\rm peak} = 7.2 \times 10^{-9}$ ergs cm^{-2} s^{-1}, 2.5–25 keV) was 1.58 hr.

3.31. *GRS 1747−312 in Terzan 6*

GRS 1747−312 ($l = 358.^\circ56$, $b = -2.^\circ17$), in the globular cluster Terzan 6, was discovered by ART-P/*GRANAT* in 1990–1992 (Pavlinsky et al. 1994). *RXTE* observations revealed quasi-periodic outbursts every $\approx$ 4.5 months, as well as thermonuclear bursts, eclipses and dips (in 't Zand et al. 2003a). The orbital period is 12.36 hr.

RXTE/PCA observations of two successive outbursts in 2001 May-June and October found a maximum persistent flux of 8–9 $\times 10^{-10}$ ergs cm^{-2} s^{-1} (2.5–25 keV); the minimum flux measured following the first outburst was 0.6×10^{-10} ergs cm^{-2} s^{-1}. At the distance to the host cluster of $9.5^{+3.3}_{-2.5}$ kpc (Kuulkers et al. 2003), this corresponds to a range of accretion rates of 0.6–8% $\dot{M}_{\rm Edd}$. Of the six bursts from public *RXTE* observations towards GRS 1747−312, four have been previously discussed by in 't Zand et al. (2003a). The bursts had short durations, of 5.5 ± 1.2 s on average. Two of the bursts exhibited PRE, and despite their similar profiles reached distinctly different peak fluxes of 1.0 and 1.7×10^{-8} ergs cm^{-2} s^{-1} respectively (see also §4.4 and Kuulkers et al. 2003). The first PRE burst may have been fainter because it actually originated from the nearby ($\Delta\theta = 0.^\circ485$) source SAX J1752.3−3138 (Cocchi et al. 2001b) instead. If that was the case, the corrected peak flux would be consistent with the earlier PRE burst observed from that source by *BeppoSAX*. With only 4 PCUs on during that observation, and rather low count rate at the peak of the burst, it was not possible to rule out either source as the origin. Furthermore, for none of the other 3 bursts can we rule out an origin at GRS 1747−312, so that we can attribute none of the bursts concusively to SAX J1752.3−3138. Thus, we attribute all the bursts to GRS 1747−312.

One additional PRE burst was observed in the field of the millisecond X-ray pulsar XTE J1751−305, but was subsequently attributed to GRS 1747−312 (in 't Zand et al. 2003c). This burst exhibited approximately constant flux for $\approx$ 50 s, interrupted between 10–30 s by an excursion up to a maximum flux of almost a factor of two higher (see Fig. 9). During this excursion, however, the blackbody radius reached a maximum, and the color temperature reached a minimum of ≈ 0.6 keV, at which level extrapolating the blackbody spectra outside the PCA bandpass becomes particularly error-prone. Thus, for this burst we exclude the data during the radius maximum for the purposes of calculating the peak flux, and instead adopt the mean peak flux between 5–10 and 30–50 s as the peak, i.e. $(22.4 \pm 0.7) \times 10^{-9}$ ergs cm^{-2} s^{-1}. Even with this correction, the peak flux significantly exceeds than that of the other two PRE bursts, leading to a fractional standard deviation of peak PRE burst flux of 38%, the largest of any of the sources with PRE bursts (see §4.4). The estimated fluence for the brightest PRE burst was almost thirty times larger than the next most energetic PRE burst; the profile was similar to other extreme bursts from 4U 1724−307 (see §3.15) and 4U 2129+12 (§3.44).

3.32. *XTE J1759−220*

This quasi-persistent source towards the Galactic bulge ($l = 7.^\circ58$, $b = 0.^\circ78$) was detected by *INTEGRAL* between 2003 March–April (Lutovinov et al. 2003), and was subsequently identified with a new source detected by *RXTE* since 2001 February (Markwardt & Swank 2003a). Significant spectral variability was measured during the *INTEGRAL* observations between 2003 and 2004, suggestive of transitions between low/hard and soft/high states (Lutovinov et al. 2005). In addition, there was evidence of dipping behaviour in the *RXTE* observations, suggesting high inclination. A single X-ray burst was detected in an *RXTE* observation on 2004 September 13. The burst was faint, reaching a peak flux of just $(5.07 \pm 0.16) \times 10^{-9}$ ergs cm^{-2} s^{-1}. Both the slow (4 s) rise and long $\tau = 24.8$ s indicate a H-rich burst; the upper limit on the distance (assuming $X = 0.7$) is 16 kpc. Assuming that the source is equidistant with the Galactic bulge, the distance is ~ 8.5 kpc. The X-ray flux measured by *RXTE* during 2004 Mar–September was between 2–4 $\times 10^{-10}$ ergs cm^{-2} s^{-1} (2.5–25 keV). For a distance of 8.5 kpc, this corresponds to an accretion rate of a few percent $\dot{M}_{\rm Edd}$.

3.33. *SAX J1808.4−3658*

The first accreting millisecond X-ray pulsar, SAX J1808.4−3658 ($l = 355.^\circ38$, $b = -8.^\circ15$) was discovered during *BeppoSAX*/WFC observations (in 't Zand et al. 1998b). Two bright thermonuclear bursts were also observed from the source, separated by 14 hr. *RXTE* observations during a subsequent outburst in 1998 revealed persistent millisecond pulsations at 401 Hz (Wijnands & van der Klis 1998), modulated by Doppler shifts arising from a 2.1 hr binary orbit (Chakrabarty & Morgan 1998). Giles et al. (1999) made observations of the $V \sim 20$ (in quiescence) optical counterpart as it faded following the outburst peak. Reanalysis of the 1996 *BeppoSAX* discovery observations revealed a third, previously undetected, brighter burst, leading to a revised distance estimate of 2.5 kpc (in 't Zand et al. 2001a). The source has continued to exhibit outbursts every ~ 2 yr; the latest was in 2005 June (Markwardt et al. 2005; see also Wijnands 2004). At the peak of the October 2002 outburst four bursts were observed by *RXTE*/PCA, each with burst oscillations also at 401 Hz, confirming the link with the NS spin (Chakrabarty et al. 2003).

The 2002 outburst was the best sampled so far by *RXTE*, and reached a maximum persistent flux of 2.6×10^{-9} ergs cm^{-2} s^{-1} (2.5–25 keV). The four bursts were all observed within a 100 hr interval just after the outburst peak, and the last three were separated by 21.1 and 29.8 hr, respectively. The bursts were quite homogeneous, all exhibiting strong PRE; the fluence increased steadily by 30%, and τ by 20% (total) as F_p decreased. The peak fluxes exhibited little variation and indicate a distance of 2.77 (3.61) kpc assuming the bursts reach $L_{\rm Edd,H}$ ($L_{\rm Edd,He}$; see also Table 6). For $d = 3.61$ kpc the peak persistent flux corresponds to a maximum accretion rate of just 5.5% $\dot{M}_{\rm Edd}$ (adopting a bolometric correction averaging 2.12 ± 0.04 over four observations near the peak). The estimated α-values for the last two burst intervals were $\alpha = 148$ and 167, respectively.

The α-values, as well as the fast rise times (≈ 0.5 s) suggest almost pure He fuel. A comparison of the burst properties with an igition model (Cumming & Bildsten 2000) indicates that the mean H-fraction at ignition is ≈ 0.1 (Galloway & Cumming 2006). These are the first He-rich bursts which have been securely observationally identified. The ignition model comparison allowed an estimate of the distance, which was consistent with the estimate derived by equating the long-term time-averaged X-ray flux with the expected mass transfer rate due to gravitational radiation, as well as the peak flux of the bursts. The derived distance range for the source is 3.4–3.6 kpc.

3.34. *XTE J1814−338*

XTE J1814−338 ($l = 358.^\circ75$, $b = -7.^\circ59$) was discovered in outburst during *RXTE*/PCA scans of the Galactic center region (Markwardt & Swank 2003b). Subsequent PCA observations revealed persistent pulsations at 314.4 Hz, making this source the fifth known accretion-powered millisecond pulsar (Strohmayer et al. 2003). Doppler variations in the persistent pulsation frequency indicate an orbital period of 4.28 hr. A total of 28 bursts were observed throughout the outburst, all with burst oscillations at the pulsar frequency (see e.g. Watts et al. 2005), and all without conclusive evidence of PRE. From the maximum peak flux of the bursts, an upper limit to the distance of ≈ 8 kpc is derived.

The persistent flux level while the source was bursting was 0.4–0.5 $\times 10^{-9}$ ergs cm^{-2} s^{-1}, equivalent to 3.6–4.5% $\dot{M}_{\rm Edd}$ averaged over the NS surface (for $d = 8$ kpc and a bolometric correction of 1.86 ± 0.3). We found five bursts separated by < 10 hr. The burst times were not consistent with a constant Δt, and instead suggest irregular reccurence times of 4–6 hr (with longer intervals resulting from missed bursts in data gaps). The two bursts with shorter recurrence times (1.7 and 2.3 hr) both had fluences around 1×10^{-7} ergs cm^{-2} (as did three others), while the remainder had fluences of $(2.6 \pm 0.3) \times 10^{-7}$ ergs cm^{-2} in the mean. Thus, the burst behaviour appears to consist of irregular bursts with recurrence times of 4–6 hr and roughly constant fluence interrupted occasionally by bursts with approximately half the fluence, occurring after approximately half the usual interval. The measured alpha values from the bursts with recurrence times $\lesssim 10$ hr ranged between 55–100. The low α values, coupled with the relatively long burst time scales of $\tau = 30 \pm 6$ in the mean indicate that mixed H/He makes up the burst fuel.

The burst behaviour of XTE J1814−338 is in marked contrast to the infrequent, He-rich bursts observed at similar accretion rates from the other accretion-powered millisecond X-ray pulsars, SAX J1808.4−3658 (see §3.33) and HETE J1900.1−2455 (§3.40). The long bursts in XTE J1814−338 may arise instead from H-ignition, as is seen in EXO 0748−676 (§3.2).

3.35. *GX 17+2*

One of the first cosmic X-ray sources ever detected (e.g. Bradt et al. 1968), GX 17+2 ($l = 16.^\circ43$, $b = +1.^\circ28$) is one of the few Z-sources which exhibits thermonuclear bursts (Hasinger & van der Klis 1989). Despite a precise position from radio detection (Hjellming 1978) the

optical counterpart long eluded observers; HST observations finally led to identification of a variable IR counterpart (Deutsch et al. 1999; Callanan et al. 2002) with ~ 4 mag modulation on a time scale of days to weeks (Bandyopadhyay et al. 2002). Bursting behaviour was discovered with *Hakucho* (Oda et al. 1981); the unique features of the characteristic long bursts unique to this source (rise time 1.5 s, duration 3–15 min) were subsequently discussed by Tawara et al. (1984). Difficulties for the "standard" burst analysis presented by these long (as well as short ~ 10 s) bursts were explored by Sztajno et al. (1986), who concluded they were indeed type-I (thermonuclear) bursts. A search for superbursts in *BeppoSAX*/WFC data was presented by in 't Zand et al. (2004b).

GX 17+2 was persistently bright during the *RXTE* observations at $15–33 \times 10^{-9}$ ergs cm^{-2} s^{-1}. *RXTE* observed 12 thermonuclear bursts from the source, 10 of which were studied in detail previously by Kuulkers et al. (2002). One additional event, on 1998 Nov 19 03:39:10 UT, was not discussed by those authors; however, the lack of spectral softening during this event appears to rule out a thermonuclear burst. Instead, this event, along with the four other "flares" noted by Kuulkers et al. (2002) may be type-II bursts (i.e. accretion instability events), analogous to those observed in the Rapid Burster and previously observed from GX 17+2 during *Einstein* observations (Kahn & Grindlay 1984). Two of the short ($\tau \lesssim 10$ s) and six of the long ($\tau \sim 100$–300 s) bursts exhibited indications of PRE, with peak fluxes of 14.8×10^{-9} ergs cm^{-2} s^{-1} in the mean. Neglecting the persistent emission, this suggests a distance of 9.8 (12.8) kpc, assuming the bursts reach $L_{\rm Edd,H}$ ($L_{\rm Edd,He}$). In GX 17+2, as distinct from almost all the other bursters, the persistent flux is comparable to the peak burst flux; even for a distance of 10 kpc, the persistent flux level suggests accretion rates consistently $\gtrsim \dot{M}_{\rm Edd}$ (for a bolometric correction of 1.083 ± 0.017). Thus, the estimated distance will be significantly closer if we sum the two contributions for our estimate of the Eddington flux. However, we note that detailed spectral studies seem to indicate that the two are truly independent, so that combining them may not be correct (Kuulkers et al. 2002). We found three pairs of bursts with relatively short intervals of 5.77, 13.0 and 11.5 hr, and assuming that this represents the recurrence time, we derive $\alpha = 7200 \pm 600$, 6000 ± 1000 and 580 ± 60, respectively. The first two bursts were of short duration, while the third was long with $\tau = 92.1$ s, and followed another long ($\tau = 113$ s) burst.

3.36. *3A 1820−303 (= Sgr X-4) in NGC 6624*

Thermonuclear bursts from this globular cluster source at $l = 19\overset{\circ}{.}06$, $b = 18\overset{\circ}{.}81$ were first discovered by *ANS* (Grindlay et al. 1976), although some bursts were actually observed earlier by *SAS-3* but not initially detected (Clark et al. 1976). The $B = 18.7$ UV/optical counterpart detected by King et al. (1993) was later confirmed by the detection of periodic variations at $P_{\rm orb} = 685$ s (King & Watson 1986; Stella et al. 1987; see also Anderson et al. 1997). The NS is thus in an ultra-compact binary with one of the shortest orbital periods known. The source is also notable for a steady long-term (176 d) periodicity in the persistent X-ray intensity, detected initially with *Vela 5-B* observations (Priedhorsky & Terrell 1984a, see also Fig. 8). Long-term observations indicate that regular motions throughout the color-color diagram of this atoll source also reflect the 176 d period (Bloser et al. 2000). Some authors have suggested that this periodicity indicates that the source is in fact a heirarchical triple (e.g. Chou & Grindlay 2001).

X-ray burst activity appears to be confined to within ± 23 d of the minima in the long-term periodicity. A 20 hr *EXOSAT* observation found 7 extremely regular ($\Delta t = 3.21 \pm 0.04$ hr) PRE bursts (Haberl et al. 1987); PRE bursts were also detected by *SAS-3* (Vacca et al. 1986). The Δt was found to decrease with increasing F_p (Clark et al. 1977), up to a critical level of around 2×10^{-9} ergs cm^{-2} s^{-1} (i.e. $\sim 9\%$ $\dot{M}_{\rm Edd}$ for $d = 7.6$ kpc; Kuulkers et al. 2003) at which the bursts stopped completely. A comparison of the burst properties with theoretical ignition models indicates pure He fuel, which is consistent with the expected H-poor nature of the donor (Cumming 2003).

The *RXTE* observations of 3A 1820−303 were almost always made when the source was above the critical threshold for burst activity; the persistent flux level was $3–16 \times 10^{-9}$ ergs cm^{-2} s^{-1} (2.5–25 keV). For $d = 7.6$ kpc this is equivalent to 18–95% $\dot{M}_{\rm Edd}$. As a result, only four thermonuclear bursts were detected, when the source was between $F_p = 2.7–3.7 \times 10^{-9}$ ergs cm^{-2} s^{-1}. All four bursts exhibited extreme PRE and reached fluxes of around 55×10^{-9} ergs cm^{-2} s^{-1}, leading to a distance estimate only consistent with that of NGC 6624 if the gravitational redshift is neglected. However, as with most of the PRE bursts observed by *RXTE*, the peak flux was consistently achieved after the radius expansion had ended (see also Kuulkers et al. 2003), suggesting that the photosphere had already settled back onto the NS surface. *RXTE* observations also revealed a "superburst" with 3 hr duration (Strohmayer & Brown 2002).

3.37. *GS 1826−238*

This quasi-persistent source ($l = 9\overset{\circ}{.}27$, $b = -6\overset{\circ}{.}09$) was discovered during *Ginga* observations (Tanaka 1989). Thermonuclear bursts were first conclusively detected by *BeppoSAX* (Ubertini et al. 1997), although this source may also have been the origin of X-ray bursts observed much earlier by *OSO-8* (Becker et al. 1976). Optical photometry of the $V \approx 19$ counterpart (Motch et al. 1994; Barret et al. 1995) revealed a 2.1 hr modulation, as well as optical bursts (Homer et al. 1998). The delay time measured between the X-ray and optical bursts is consistent with the binary separation for a 2.1 hr orbit (see also Kong et al. 2000). Based on optical measurements, the distance to the source is at least 4 kpc (Barret et al. 1995); since no PRE bursts have been observed, an upper limit of 8 kpc has been derived from the peak fluxes of bursts measured by *BeppoSAX*, *ASCA* and *RXTE* (in 't Zand et al. 1999a; Kong et al. 2000), placing the source just outside the Galactic bulge. Analysis of the ≈ 260 bursts observed by the *BeppoSAX*/WFC revealed that the source consistently exhibits approximately periodic bursts, with a recurrence time which decreases significantly as the persistent flux increases (Ubertini et al. 1999; Cornelisse et al. 2003).

RXTE observations revealed that the source intensity steadily increased between 1997–2003, from 1.1–1.9×10^{-9} ergs cm^{-2} s^{-1} (2.5–25 keV). For $d = 6$ kpc, this corresponds to a range of accretion rates of 5–9% $\dot{M}_{\rm Edd}$ (for a bolometric correction of 1.653 ± 0.009). We detected a total of 40 remarkably homogeneous, long ($\tau = 39 \pm 3$ s, rise time 6.0 ± 0.8 s) bursts in the *RXTE* observations, with regular recurrence times that decreased proportionately with the increase in F_p (Galloway et al. 2004b; see also §4.1). The mean α-value was 37.5 ± 1.2[11], indicating a high proportion of H in the burst fuel. None of the bursts exhibited any evidence for PRE.

3.38. *XB 1832−330 in NGC 6652*

This globular-cluster source at $l = 1\overset{\circ}{.}53$, $b = -11\overset{\circ}{.}37$ was discovered by *ROSAT* during a probable transient outburst (Predehl et al. 1991); the first thermonuclear bursts were observed by *BeppoSAX* (in 't Zand et al. 1998c). The bursts were long, with exponential decay times of 16 and 27 s, and peak fluxes of $\sim 8 \times 10^{-9}$ ergs cm^{-2} s^{-1} (bolometric). A third burst was detected by *ASCA*, reaching a peak flux of 2×10^{-9} ergs cm^{-2} s^{-1} (Mukai & Smale 2000). A *Chandra* observation reavealed 3 new sources in the cluster, and the improved position for XB 1832−330 allowed identification of the blue variable $M_V = 3.7$ optical counterpart from archival *HST* observations (Heinke et al. 2001). Sparse optical data suggest a 43.6 min periodic intensity modulation with semiamplitude 30% (Deutsch et al. 2000), although no periodic modulation of the X-rays was seen in 2001 by *BeppoSAX* (Parmar et al. 2001). A 43.6 min period would indicate an ultracompact binary with an evolved, likely H-poor companion similar to 3A 1820−30 (see §3.36).

RXTE/PCA measurements in 1998 and 2001–2 indicate a flux of $2–3.5 \times 10^{-10}$ ergs cm^{-2} s^{-1} (2.5–25 keV), although this may include contributions from the other (typically quiescent) LMXBs in the cluster. For $d = 9.6 \pm 0.4$ kpc (Kuulkers et al. 2003), this gives an upper limit to the accretion rate in XB 1832−330 of 2–3% $\dot{M}_{\rm Edd}$. We found just one burst in public *RXTE* observations, on 1998 November 27 05:45:15 UT. The blackbody radius reached local maxima during the rise and near the flux maximum, and the simultaneous inflection of the blackbody temperature suggests that this burst may have experienced modest PRE (although see Kuulkers et al. 2003). The peak flux suggests a distance consistent with that of the host cluster, assuming the burst reached $L_{\rm Edd,He}$ (see Table 6). The burst exhibited a steep initial decay, but then a long ≈ 100 s tail (Fig. 9), so that the overall τ was long at 21.4 s.

3.39. *3A 1837+049 (= Ser X-1)*

This persistent source at $l = 36\overset{\circ}{.}12$, $b = +4\overset{\circ}{.}84$ was first detected in early rocket flights (Bowyer et al. 1965). A more precise position from *SAS-3* observations (Doxsey 1975) led to a suggested optical counterpart (Davidsen 1975); later observations revealed that this candidate was actually two stars, one of which (with HeII 4686 Å emission) was the counterpart (Thorstensen et al. 1980). The inferred L_X/L_O ratio is > 100. X-ray bursts were discovered more or less simultaneously by *OSO-8* (Swank et al. 1976c) and *SAS-3* (Li et al. 1977). The bursts exhibited irregular recurrence times of 1–38 hr, average $\tau = 6.8 \pm 2.1$ s, and showed no indications of PRE (Sztajno et al. 1983; see also Lewin et al. 1993). The variations in burst interval were apparently independent of F_p, although $F_{\rm pk}$ increased with F_p. A "superburst" was detected by *BeppoSAX* (Cornelisse et al. 2002a), which apparently quenched the regular thermonuclear bursting for 34 d afterwards.

The source was persistently bright at $4–6 \times 10^{-9}$ ergs cm^{-2} s^{-1} (2.5–25 keV) in *RXTE*/PCA observations. We found 7 bursts in public data, two of which exhibited weak PRE indicating a distance of 7.7 (10) kpc assuming the bursts reached $L_{\rm Edd,H}$ ($L_{\rm Edd,He}$; see Table 6). We note that one other burst exceeded the peak flux of the two PRE bursts by $\approx 30\%$ but did not itself exhibit PRE. The corresponding accretion rate range is 38–56% $\dot{M}_{\rm Edd}$ (for a bolometric correction of 1.24 ± 0.08). The bursts were of short duration, with mean $\tau = 4.8 \pm 0.6$ s. We found one pair of bursts separated by 7.99 hr, from which we derived $\alpha = 1590 \pm 150$ (although there may have been intermediate bursts which were missed during Earth occultations).

3.40. *HETE J1900.1−2455*

This source ($l = 0\overset{\circ}{.}00$, $b = -12\overset{\circ}{.}87$) was discovered on 2005 June 14 when a strong thermonuclear (type-I) burst was detected by *HETE-II* (Vanderspek et al. 2005). A subsequent PCA observation of the field on 2005 June 16 revealed 2% rms pulsations at 377.3 Hz, confirming the bursting source as the seventh accretion-powered millisecond pulsar (Morgan et al. 2005). A series of followup PCA observations allowed measurements of Doppler shifts of the apparent pulsar frequency on the is 83.25 min orbital period (Kaaret et al. 2005). The optical counterpart was identified by its brightening to $R \sim 18.4$ during outburst (Fox 2005). Based on the peak flux of the burst observed by *HETE-II*, the distance was estimated at 5 kpc (Kawai et al. 2005).

Two bursts were detected during followup PCA observations, the first on 2005 July 21. The burst profile was complex, with a precursor lasting 2 s, followed by a slower rise to a maximum of $(110.7 \pm 1.5) \times 10^{-9}$ ergs cm^{-2} s^{-1} lasting approximately 20 s. While the burst flux was close to maximum, the blackbody radius reached two successive local maxima, each accompanied by local minima in the blackbody temperature. The second burst was much less energetic, reaching a peak flux $\approx 20\%$ lower, and with a total fluence only a quarter of the first burst. Assuming both bursts reached the Eddington limit for pure He material, the distance to the source is 4.7 ± 0.6 kpc, consistent with the earlier estimate from the first burst observed by *HETE-II* by Kawai et al. (2005).

The source activity continued for more than 1 yr after the outburst began (e.g. Galloway et al. 2005). This is much longer than the typical outburst duration for the other accretion-powered millisecond pulsars (≈ 2 weeks), and a factor of three longer than the previous record-holder, XTE J1814−338, at 50 d (see §3.34). The inferred accretion rate (for a bolometric correction of

[11] Note that this is slightly smaller than the value quoted by Galloway et al. (2004b) of 41.7 ± 1.6, due to an improved estimate of the burst fluence. The fractional variation in α with F_p is unchanged.

1.96 ± 0.02) was 2–3% $\dot{M}_{\rm Edd}$. Should activity persist at this level indefinitely, HETE J1900.1−2455 will have the highest time-averaged accretion rate of all the millisecond pulsars.

3.41. *Aql X-1*

One of the earliest cosmic X-ray sources detected (e.g. Friedman et al. 1967), Aql X-1 ($l = 35\overset{\circ}{.}72$, $b = -4\overset{\circ}{.}14$) is a recurrent transient with a quasi-regular outburst interval variously reported as ≈ 230 d (e.g. Kaluzienski et al. 1977), 122–125 d (Priedhorsky & Terrell 1984b), or 309 d (Kitamoto et al. 1993). Optical photometry of the highly variable (B = 20–17) K0 counterpart (Thorstensen et al. 1978) throughout an outburst revealed a 19 hr period, assumed initially to be the binary period (Chevalier & Ilovaisky 1991). The I-band periodicity is twice this value (Shahbaz et al. 1998). Thermonuclear bursts were probably first detected by *SAS-3* (Lewin et al. 1976e), but were confirmed during *Hakucho* observations in the declining phase of an outburst (Koyama et al. 1981). The bursts reached peak fluxes between 7–11 × 10^{-8} ergs cm^{-2} s^{-1}, with time scales $\tau \sim$ 10–18 s (e.g. Lewin et al. 1993). *RXTE* observations during an outburst in 1997 February–March revealed a QPO in the frequency range 740–830 Hz as well as burst oscillations around 549 Hz (Zhang et al. 1998). Note the nearby source 1A 1905+00 ($\Delta\theta = 0\overset{\circ}{.}82$), which has also exhibited bursts (Lewin et al. 1976e, see also Table 3). While bursts were detected during *RXTE* observations centered on this source, we attributed them all to Aql X-1 instead (see §A.3).

RXTE has observed around 8 outbursts since 1996 (Fig. 8). The 2.5–25 keV flux reached 2–18 × 10^{-9} ergs cm^{-2} s^{-1} at the peak of these outbursts. The 40 bursts detected by *RXTE* occurred at F_p levels which span more than an order of magnitude. The burst properties were diverse, and indicate three approximately distinct groups: one with short time scales (τ = 5–10) and rather low fluences, another of non-radius expansion bursts with $\tau \approx$ 15–30 and a third group which have $\tau \approx$ 8–15. It is this third group in which all the bursts which exhibit PRE and oscillations occur. The peak flux of the PRE bursts indicates a distance of 3.5 (4.5) kpc, assuming the bursts reach $L_{\rm Edd,H}$ ($L_{\rm Edd,He}$). The peak accretion rate reached during the outbursts is thus 6–56% $\dot{M}_{\rm Edd}$ (for d = 5 kpc and a bolometric correction of 1.65 ± 0.05). We found three instances of short recurrence times, between 10–22 min. As is typical for short-Δt bursts, the fluence of these bursts was significantly smaller than the mean value (see §4.2).

3.42. *4U 1916−053*

This source at $l = 31\overset{\circ}{.}36$, $b = -8\overset{\circ}{.}46$ was discovered by the *Uhuru* satellite (Giacconi et al. 1972). *EXOSAT* observations revealed irregular X-ray dipping behaviour with a period of ≈ 50 min (Walter et al. 1982; White & Swank 1982), which optical observations of the $V = 21$ companion confirmed was approximately the orbital period (Grindlay et al. 1988). The source is thus an "ultracompact" system, which cannot accommodate a H-rich mass donor. Bursts were first observed from the source by *OSO-8* (Becker et al. 1977), and were subsequently detected by *SAS-3*, *HEAO-1* and *EXOSAT* (see Lewin et al. 1993). The typical burst interval is 4–6 hr, although bursts may sometimes occur at longer intervals or not at all. Bursts exhibiting PRE suggest a source distance of 8.4–10.8 kpc (Smale et al. 1988). Measured α-values vary between 120–170; burst durations are typically $\tau \sim 5$ s, but may be up to a factor of two longer. A burst oscillation at 270 Hz was discovered in a single burst observed by *RXTE*, on 1998 August 1 (Galloway et al. 2001). This source is the only one in which the burst oscillation frequency is significantly below the kHz QPO peak separation.

The persistent flux of the source was between 0.2-1 × 10^{-9} ergs cm^{-2} s^{-1} (2.5–25 keV) throughout the *RXTE* observations, although we note that these values are not corrected for the presence of dips. We found a total of 14 bursts from the source, with 12 exhibiting PRE. The inferred distance is 7–9 kpc (see Table 6), giving a range of accretion rates of 1.5–8% $\dot{M}_{\rm Edd}$ (for d = 9 kpc and a bolometric correction of 1.37 ± 0.09). The bursts were short, with $\tau = 6.5 \pm 1.3$ s, although one burst (which also had the largest fluence) exhibited a much broader peak, resulting in τ = 10.2 s. Just one pair of bursts were separated by < 10 hr, on 1998 July 23, with Δt = 6.33 hr; from these two bursts we calculate $\alpha = 78.8 \pm 0.3$, equivalent to a mean H-fraction at ignition of $X \approx 0.2$ (equation 8).

3.43. *XTE J2123−058*

This source ($l = 46\overset{\circ}{.}48$, $b = -36\overset{\circ}{.}20$) was discovered as an X-ray transient by *RXTE* in late June 1998 (Levine et al. 1998). The optical counterpart was identified and found to have a 5.96 hr periodic optical modulation, identical to the spectroscopic period (Tomsick et al. 1999). The counterpart was monitored extensively throughout the outburst (e.g. Soria et al. 1999), and into quiescence. Keck measurements resulted in a narrowing of the distance range to 8.5 ± 2.5 kpc (Tomsick et al. 2001; see also Tomsick et al. 2002). *RXTE* observations revealed thermonuclear X-ray bursts and high-frequency QPOs (Homan et al. 1999); optical bursts have also been detected.

The peak PCA flux during the 1998 outburst was 1.74×10^{-9} ergs cm^{-2} s^{-1} (2.5–25 keV). At $d = 8.5$ kpc, this corresponds to 11% $\dot{M}_{\rm Edd}$ (for a bolometric correction of 1.19 ± 0.06). We found a total of 6 weak bursts from the source, the two brightest (on 1998 July 22) reaching a peak of just ≈ 6 × 10^{-9} ergs cm^{-2} s^{-1}. The remaining four bursts all reached peak fluxes below 3 × 10^{-9} ergs cm^{-2} s^{-1}. None of the bursts exhibited PRE; the peak fluxes were all well below the expected value for bursts reaching $L_{\rm Edd,H}$ at 8.5 kpc. The two brightest bursts were separated by just 6.5 hr, which for the persistent flux level measured during the observation leads to an $\alpha = 370 \pm 40$. Such a large value suggests that intervening bursts may have been missed in data gaps, or that only a fraction of the accreted material was burned.

3.44. *4U 2129+12 (= AC 211) in M15*

This source ($l = 65\overset{\circ}{.}01$, $b = -27\overset{\circ}{.}31$) is one of two bright LMXBs in the globular cluster M15 ($d = 10.3 \pm 0.4$ kpc; Kuulkers et al. 2003), separated by just $2\overset{''}{.}7$ (White & Angelini 2001). Originally

the x-ray source was identified with the 17.1 hr binary AC 211 (Ilovaisky et al. 1993; Auriere et al. 1984; Charles et al. 1986); the other source, M15 X-2, is the suggested origin of the strong PRE bursts observed by *Ginga* (Dotani et al. 1990; van Paradijs et al. 1990a), *RXTE*/PCA (Smale 2001), *BeppoSAX*/WFC (Kuulkers et al. 2003) and *RXTE*/ASM (Charles et al. 2002). The latter work also identified 15 burst candidates in the ASM data, leading to a lower limit on the burst recurrence time of 1.9 d.

The PCA flux of the source in observations in 1997 and 2000 was $2\text{–}4 \times 10^{-10}$ ergs cm^{-2} s^{-1} (2.5–25 keV). Although this flux contains contributions from both LMXBs, White & Angelini (2001) found M15 X-2 (the suggested origin of the bursts) to be 2.5 times brighter than M15 X-1, so that the inferred range of accretion rate of 2–4% $\dot{M}_{\rm Edd}$ should be approximately correct. The inferred $\dot{M}$ is also consistent with the long burst recurrence times of $\gtrsim$ 1.9 d. The single burst observed by *RXTE*/PCA, on 2000 September 22, peaked at 4×10^{-8} ergs cm^{-2} s^{-1} (note that the higher value of 5×10^{-8} ergs cm^{-2} s^{-1} quoted by Smale 2001 was derived using the older response matrices), which agrees well with the peak flux of the burst observed by *Ginga* of 4.2×10^{-8} ergs cm^{-2} s^{-1}. Although the burst duration was long, with $\tau = 30$ s (see Fig. 9), the *Ginga* burst was even longer. The burst exhibited very strong radius expansion, similar to that seen in the bursts from 4U 1724−307 (§3.15, Fig. 10) and GRS 1747−312 (§3.31) although insufficient to drive the emission at the radius peak completely out of the PCA band (the minimum blackbody temperature reached was 0.8 keV). As noted by Kuulkers et al. (2003), the peak fluxes of these bursts are substantially in excess of the expected range of $L_{\rm Edd,He}$ for $d = 10.3$ kpc.

3.45. *Cyg X-2*

This source ($l = 87\overset{\circ}{.}33$, $b = -11\overset{\circ}{.}32$) was detected in the very first observations which indicated the existence of cosmic X-ray sources (Giacconi et al. 1962). A $V = 14.7$ optical counterpart was identified shortly afterwards (Giacconi et al. 1967); the binary orbit is very wide, with $P_{\rm orb} = 236.2$ hr (Cowley et al. 1979). An event resembling a thermonuclear burst was first observed during *Einstein* observations (Kahn & Grindlay 1984; see also Lewin et al. 1993). In their analysis of an event observed by *RXTE*, Smale (1998) detected a decrease in color temperature late in the burst, following an apparent PRE episode. This appeared to confirm the thermonuclear nature of these events, as well as allowing a distance estimate of 11.6 ± 0.3 kpc to be made. At accretion rates comparable to the Eddington limit, which is typical for this Z source, it is expected that bursts should be extremely infrequent or absent altogether since the temperature in the accreted layer may be sufficient for the accreted fuel to burn stably, instead. That the bursts have such short time-scales presents an additional puzzle, since in other sources such bursts are identified with pure He fuel, whereas at the high $\dot{M}$ typical for Cyg X-2 it is expected that a substantial H-fraction remains at ignition (see also Kuulkers et al. 2002).

Cyg X-2 was persistently bright in *RXTE*/PCA observations at $6\text{–}21 \times 10^{-9}$ ergs cm^{-2} s^{-1}, with a mean level of 11×10^{-9} ergs cm^{-2} s^{-1}. For $d = 11.6$ kpc, this corresponds to a range of accretion rates of > 0.8 $\dot{M}_{\rm Edd}$, and for much of the time well in excess of $\dot{M}_{\rm Edd}$. We found 46 burst-like events from Cyg X-2 in public data from *RXTE*, including five apparently exhibiting PRE (similar to the burst on 1996 Mar 27 14:29:07 UT analysed by Smale 1998). The mean peak flux of these bursts suggests a distance of 10 (14) kpc, assuming the bursts reach $L_{\rm Edd,H}$ ($L_{\rm Edd,He}$; see Table 6). However, some of the PRE bursts did not exhibit any decrease in $T_{\rm bb}$ following the peak. Furthermore, only a handful of the other events showed a decrease in $T_{\rm bb}$ following the maximum flux. In many bursts, $T_{\rm bb}$ was constant or even *increased* with time throughout the burst. One particularly notable event occurred on 1997 Jul 3 04:41:03 UT, just 14 min after the previous burst. These two bursts were similar in profile for the typical ≈ 2 s duration, but after the second burst the flux did not decrease back to the pre-burst persistent level for at least 8 min (Fig. 12). One possibility is that the enhanced emission following the second burst resulted from continuing thermonuclear burning. Alternatively, it may be that the enhancement is indicative of an abrupt change in $\dot{M}$, occurring as a consequence of the burst. It is difficult to understand this link if the burst arose from thermonuclear burning of accreted fuel, but not if the burst instead arose from the same type of accretion instability which is thought to give rise to type-II bursts. In the latter case it is perfectly plausible that the transient accretion causing the burst may induce subtle changes in the magnetospheric configuration, leading to a slight change in $\dot{M}$ as a side-effect. The short recurrence time, as well as the lack of evidence for a decrease in $T_{\rm bb}$ during the burst, all support the interpretation as a type-II burst. Furthermore, we note that several of the short burst-like events in GX 17+2 also appear similar to type-II bursts (see §3.35). Given the unusual properties of the bursts from Cyg X-2, and the lack of consistent detections of spectral softening in the (often abbreviated) decay, it seems plausible that most (if not all) of the bursts from this source arise from accretion instabilities, and not from thermonuclear burning as has previously been thought.

4. RESULTS AND DISCUSSION

4.1. *Burst rates and energetics*

The mean burst rate for the combined sample of bursts from 28 sources (for which we can calculate the normalized persistent flux γ; see §2.5) reached a maximum of around 0.2–0.3 hr^{-1} in the range $\gamma \approx 0.02\text{–}0.06$. This range corresponds to a source luminosity of $0.3\text{–}2 \times 10^{37}$ ergs s^{-1} (Fig. 13, top panel). Above and below this range, the mean burst rate was in the range 0.06–0.1 hr^{-1}, extending up to $\gamma \approx 1$ (where the only sources bursting were GX 17+2 and Cyg X-2). The recurrence time for individual pairs of bursts, interpreted as an instantaneous burst rate, are also shown in Fig. 13. In the regime where the burst rate is rising, the individual measurements loosely follow the mean rate. However, above the range of γ where the mean burst rate peaks, the individual measurements continue to increase, up to rates as high as ≈ 2 hr^{-1}. We note that there are substantial selection biases in this set of measurements towards regular bursts with short recurrence times, and the locus

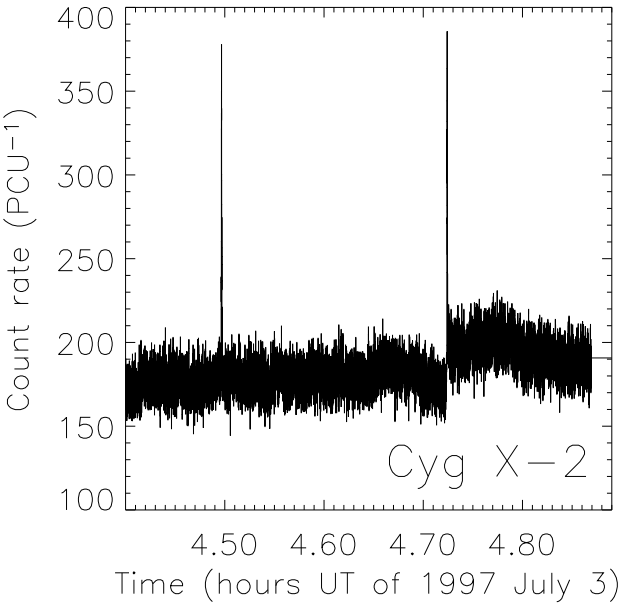

FIG. 12.— Two of the three bursts observed by *RXTE* from Cyg X-2 on 1997 July 3rd. Note the apparent increase in the persistent flux level following the second burst. This increase may be interpreted as an increase in $\dot{M}$ following a rearrangement of the accretion geometry, in which case the burst which preceded it may originate from an accretion instability (similar to the frequent events observed from the Rapid Burster; Lewin et al. 1993) instead of thermonuclear burning of accreting fuel.

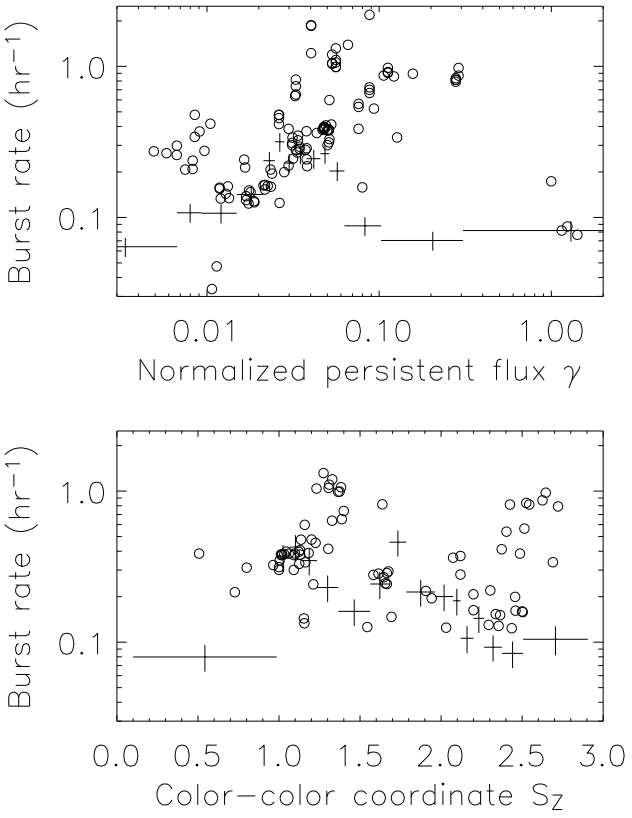

FIG. 13.— Burst rates for sources observed by *RXTE* as a function of normalized persistent flux γ (*upper panel*) and color-color coordinate S_Z (*lower panel*). Bursts were combined in groups of ≈ 50 to calculate the ensemble average (*crosses*); the vertical error bars indicate the 1σ uncertainties. Instantaneous burst rates ($1/t_{\rm rec}$) for pairs of bursts are also shown (*open circles*). The ensemble-averaged burst rate increased with γ/S_Z and reached a broad maximum around $\gamma \simeq 0.04$ (equivalent to $\approx 10^{37}$ ergs s^{-1}) or $S_Z \simeq 1$. This behaviour is qualitatively consistent with burst ignition models, although the decrease in burst rate above these levels is not. At the highest persistent flux levels $\gamma \sim 1$ the bursts all come from two sources: GX 17+2 and Cyg X-2. The individual measurements exhibited significant scatter and deviated in some cases by up to an order of magnitude from the ensemble average. We note that these measurements are biased towards frequent, regular bursts, and thus not representative of the overall distribution.

of individual measurements cannot be considered representative. Nevertheless, it is interesting how far the burst rates for individual sources can deviate from the ensemble-averaged value. At least one source of dispersion likely arises from the inclusion of bursts identified as resulting from both H- and He-ignition at $\gamma \lesssim 0.01$, since these two types have markedly different recurrence times for the same accretion rate. At higher accretion rates $\gamma \gtrsim 0.08$ two kinds of burst behavior are also apparent: very frequent bursting (evidenced by the measurements from individual burst pairs), whereas the much lower average rate suggests that for many other sources bursts are far less frequent, or perhaps have ceased completely. Sources with frequent (> 0.5 hr^{-1}) bursts in the range $\gamma > 0.08$ include SAX J1748.9−2021, EXO 1745−248, 4U 1735−44 and 4U 1746−37.

We also show the burst rates as a function of S_Z (Fig. 13, lower panel). The burst rate increased from 0.1 to ≈ 0.3 hr^{-1} as S_Z increased through 1, but then decreased gradually back to 0.1 hr^{-1} as S_Z increased from 1 to 3, with additional bin-to-bin variations of smaller amplitude superimposed upon this trend. Note that the set of bursts that contributed to the measured rates in the lower panel of Fig 13 was somewhat different than for the upper panel, since not all the bursts for which we measure S_Z come from sources with a measured $F_{\rm Edd}$, and vice versa. However, the sample of bursts which contributes to the mean rates in the lower panel, when binned instead as a function of γ, exhibited the same variations as found for the larger sample used for the top panel of Fig. 13. Thus, the two samples are equivalent, at least in terms of the variation in burst rate as a function of γ. As with the mean rates as a function of γ, the inferred rates for individual bursts as a function of S_Z correspond only loosely to the mean values. We found variations of up to an order of magnitude compared to the mean rates over all sources.

Assuming ideal conditions (constant area over which accretion takes place, complete consumption of the accreted fuel) and neglecting possible transitions between H- and He-ignition, we expect the burst rate to increase with $\dot{M}$. The source which best meets this theoretical ideal is GS 1826−24, the "Clocked Burster", so-called because it consistently exhibits extremely regular bursts (e.g. Ubertini et al. 1999, Cornelisse et al. 2003; see also §3.37). The burst recurrence time decreased significantly over the course of the *RXTE* observations, in response to a gradually increasing F_p (Fig. 14; Galloway et al. 2004b). The decrease in the burst recurrence time was proportional to $F_p^{-1.05\pm0.02}$, precisely the variation we

expect as a response to increasing $\dot{M}$ (which we assume is $\propto F_p$), for constant fuel composition. Without any radius-expansion bursts or a well-defined color-color diagram, γ and S_Z values could not be calculated for bursts from GS 1826−24, and thus these bursts were not included in the combined sample used to produce Fig. 13. The equivalent $\dot{M}$ was estimated from comparisons with theoretical ignition models at $\sim 0.1\dot{M}_{\rm Edd}$ (i.e. $\gamma \sim 0.1$). Both the long burst durations and the low $\alpha \approx 40$ indicate that hydrogen makes up a significant fraction of the fuel for these bursts. We found $\approx 10\%$ variations in α over the observed range of F_p, indicating that hydrogen burns stably between bursts via the hot CNO cycle, leading to slight changes in the composition of the fuel layer at ignition (and hence α) as F_p increased. Since H-burning is stable between the bursts, unstable He-burning must trigger the burst ignition, i.e. Case 1 of Fujimoto et al. (1981).

Since hot CNO burning plays a role in determining the properties of the bursts, the detailed variation of burst rate with $\dot{M}$ also depends upon the CNO metallicity $Z_{\rm CNO}$ in the accreted material. Solar metallicity ($Z_{\rm CNO} \sim 0.02$) ignition models (Cumming & Bildsten 2000) naturally reproduce the observed variation in α for bursts from GS 1826−24, as well as the burst energies, but do not match the variations in recurrence time and burst fluence (Fig. 14). On the other hand, low metallicity models ($Z_{\rm CNO} \sim 0.001$) reproduce the observed trends in recurrence time and fluence, but are ruled out by the variation in α. Amongst a number of ways to reconcile these observations is the possibility that the fraction of the neutron star covered by the accreted fuel increases with $\dot{M}$. The blackbody radius $R_{\rm bb}$ in the tail of the bursts decreased by ≈20% between the observed epochs, which if interpreted as a change in covering fraction, would almost be enough to explain the discrepancy. We note that a decrease in the covering fraction with $\dot{M}$ is opposite to the increase suggested by Bildsten (2000) to explain trends in burst properties in other sources.

The decrease in burst rate observed for the combined sample above $\gamma = 0.05$ (which may be identified with the corresponding decrease between $S_Z = 1$ and 3; Fig. 13) is contrary to the theoretically predicted trend, and is at a much lower $\dot{M}$ level than expected for the onset of stable He burning. A drop in burst rate at roughly the same persistent flux level was found by Cornelisse et al. (2003) for bursters observed by *BeppoSAX*, and was attributed by those authors to the onset of stable H burning (i.e. the transition between Case 3 to Case 2 of Fujimoto et al. 1981). However, our analysis of the bursts from GS 1826−24 at $\gamma \sim 0.1$ confirm that these arise from Case 1 ignition (this discrepancy was also noted by in 't Zand et al. 2004c), so that the transition must take place at lower $\dot{M}$ (γ). Although we found no evidence for an additional peak in the mean burst rate at very low γ, we observed bursts consistent with H-ignition (Case 3) from EXO 0748−676 at $\gamma = 0.005$–0.01 (see §3.2), and possibly a few others.

While the properties of bursts from GS 1826−24 do not vary much as a function of accretion rate, this is far from true for the combined sample, and here we must also consider the variation of α with γ ($\dot{M}$). A comparison of the mean and individual α measurements is shown in Fig. 15. In the mean, α reached a minimum of ~ 100 at $\gamma = 0.05$, within the range where the burst rate peaked (Fig. 15, upper panel), so that for the most part α and the burst rate were roughly anticorrelated. Below this γ range the mean α varied between 100 and 500, while above $\gamma \approx 0.05$ α increased steadily up to ~ 1000. In the highest γ range $\alpha \sim 100$ once more. The variation in the mean α between adjacent bins was much greater than for the burst rates, and (as with the burst rates) the individual α measurements differed from the binned values by up to an order of magnitude. In fact, we detected no discernable trend in the individual α-values as a function of γ. This scatter may be attributable in part to variations of the kind seen in 1M 0836−425 (§3.3), and possibly also incomplete burning as seen in 4U 1702−429 (§3.10) as well as the inclusion of both H- and He-triggered bursts at $\gamma \lesssim 0.01$. Both sets of values, however, are inconsistent with the monotonic re-

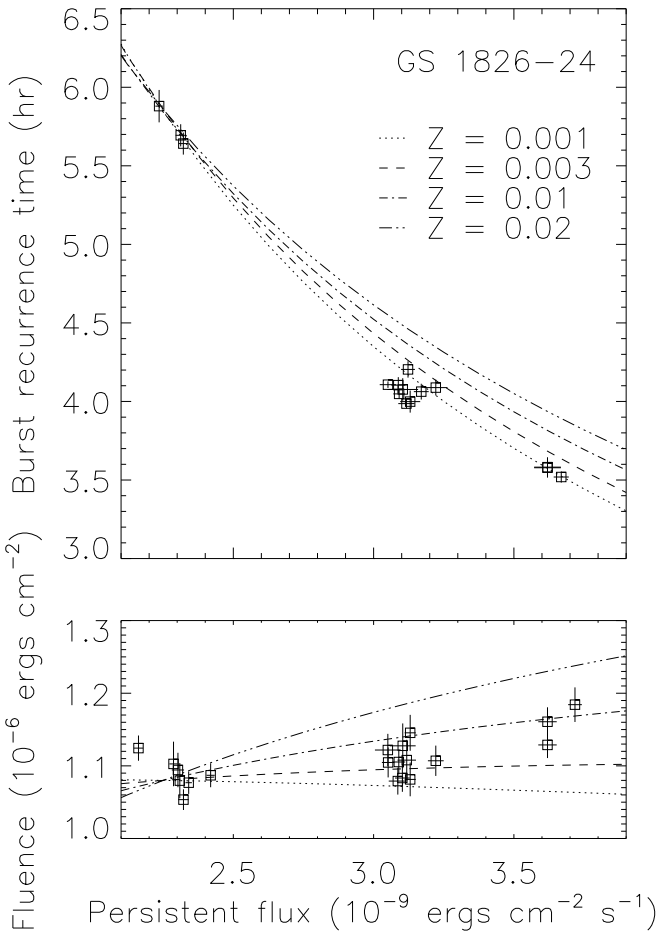

FIG. 14.— Variation of the burst recurrence time (*upper panel*) and the burst fluence (*lower panel*) as a function of the estimated bolometric persistent flux in GS 1826−24, from *RXTE* measurements between 1997–2002. Error bars indicate the 1σ errors. The curves show theoretical calculations for a range of metallicities: $Z = 0.02, 0.01, 0.003$, and 0.001. The solid angle (R/d) and gravitational energy have been chosen in each case to match the observed fluence and recurrence time at $F_{\rm p} = 2.25 \times 10^{-9}$ erg cm^{-2} s^{-1}. For $Z = 0.02, 0.01, 0.003$, and 0.001, this gives $R/d = 13, 10, 8, 6$ km @ 10 kpc, and $Q_{\rm grav} = 175, 196, 211, 215$ MeV per nucleon. Adapted from Galloway et al. (2004b).

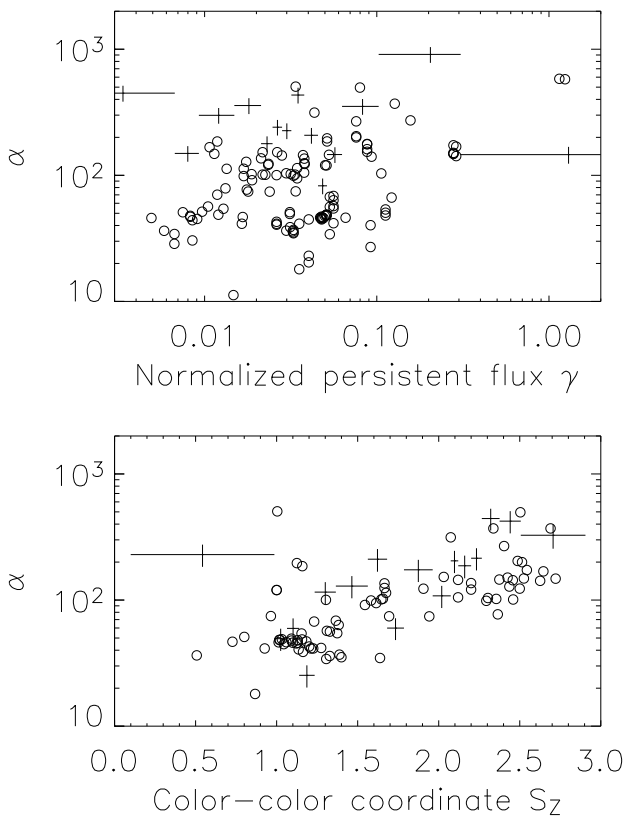

FIG. 15.— Measured α-values for bursters observed by *RXTE* as a function of normalized persistent flux γ (*upper panel*) and color-color coordinate S_Z (*lower panel*). Bursts were combined in groups of ≈ 50 for binning, as for Fig. 13. Error bars indicate the 1σ uncertainties. Also shown are measured α-values for pairs of closely-spaced bursts from a range of sources (*open circles*). The fractional energy in the bursts ($1/\alpha$) peaks where the burst rate is also the highest, around $\gamma \approx 0.04$ or $S_Z \approx 1$, decreasing above and below. Again, the deviations between the measurements for pairs of bursts and the ensemble average can be significant, although the agreement appears to be better when plotted as a function of S_Z than γ.

lation found by van Paradijs et al. (1988a), in which α increased systematically from ~ 10 at $\gamma = 0.01$ to $\sim 10^3$ at $\gamma = 0.3$. This is roughly how the mean α measurements from the *RXTE* data increased above $\gamma = 0.05$, but the individual measurements show that the instantaneous α measurements for individual sources may be very different to the mean value. Conspicuously absent from the van Paradijs et al. (1988a) sample are low-α bursts at intermediate $\gamma = 0.03$–0.1, typified by the regular bursts from KS 1731−26 (see §3.18; the bursts from GS 1826−24 will also fall in this part of the γ-α diagram). The variation of α with S_Z is somewhat more consistent between the mean and individual measurements (Fig. 15, lower panel), with α increasing rather steadily from ~ 30 to ~ 300 as S_Z increases from 1 to 2.5. Below $S_Z = 1$, $\alpha \sim 200$.

Based on the measurements of burst rate and α as a function of γ and S_Z, we attempted to identify the boundaries between the different classes of ignition. Ignition in mixed H/He (Cases 1 and 3) and pure He (Case 2) environments should be distinguishable by small and large values of α respectively, since H nuclei contribute much more energy per nucleon than He (i.e. $Q_{\rm nuc}$ is larger in equation 8). The transition to steady H-burning expected around $\dot{M} \sim 0.01\dot{M}_{\rm Edd}$ (between Case 3 and 2), will also result in a substantial drop in burst rate. As the accretion rate increases further, the recurrence time is expected to decrease so that eventually steady H-burning will not be complete (the transition between Case 2 and Case 1 expected at $\sim 0.1\dot{M}_{\rm Edd}$) and α will steadily decrease. This behavior is almost the opposite of what we observe in Fig. 15; the mean α is high at low $\gamma < 0.01$, decreases initially, and then increases. The pattern of variation with S_Z is very similar. Comparison of the ensemble mean and individual burst rate and α measurements suggests that the sample is rather too diverse to be described by a global mean behaviour. We identified bursts arising from H-ignition from EXO 0748−676 at $\gamma = 0.005$-0.01 and perhaps from a few other sources at slightly higher γ. Beginning at $\gamma \gtrsim 0.01$ we also observed infrequent, He-rich bursts in which the hydrogen had been all but exhausted from steady burning. While the increasing α and decreasing burst rate at rather higher γ values, above ≈ 0.04 are also qualitatively consistent with the behavior we expect at the onset of steady H-burning (as suggested by Cornelisse et al. 2003), results from individual bursters indicate that He ignition in a mixed H/He environment is already occurring at this persistent flux level. Thus, we confirm the theoretical prediction that the boundary between H- and He-ignition (Case 3 and Case 2) is at $\gamma \approx 0.01$ (i.e. $\approx 1\%$ $\dot{M}_{\rm Edd}$). The transition between Case 2 and Case 1 bursting (He-ignition in He-rich and H-rich environments, respectively) likely results in more subtle variations of burst rate and α, and the *RXTE* data suggests that this occurs between $\gamma \approx 0.01$ and where the burst rate peaks at ≈ 0.05. The other distinct feature we observe is the increase in α and decrease in burst rate above $\gamma = 0.05$, which may be related to the cessation of bursting activity expected at high $\dot{M}$. Another explanation is the "delayed mixed bursts" of Narayan & Heyl (2003), in which the available fuel (He as well as H) is reduced prior to ignition by steady burning, reducing the fluences and resulting in increased α-values and decreased burst rate. The previously mentioned sources which show frequent bursts at $\gamma > 0.08$ are a notable exception to this pattern.

One possible contributing factor to the disagreement between the sample mean and individual burst rate and α-values is that the behaviour as a function of γ/S_Z is not the same for all sources. This possibility has already been alluded to in reference to the sources bursting frequently above $\gamma > 0.08$, in marked contrast to the ensemble average. While our limited statistics for most sources prohibits rigorously testing this hypothesis with all sources in the *RXTE* sample, it is illustrative to plot the inferred rates for the two sources with the most bursts, 4U 1636−536 and 4U 1728−34 (Fig. 16, upper panels). These sources exhibit very different burst rate behaviour over a similar range of γ/S_Z values. For 4U 1636−536 we find a decrease in burst rate as a function of γ/S_Z, significant to greater than 5σ in either case. (This is in stark contrast to the behaviour of GS 1826−24 within approximately the same $\dot{M}$ range). For 4U 1728−34, on the other hand, the burst rate appears to increase with γ

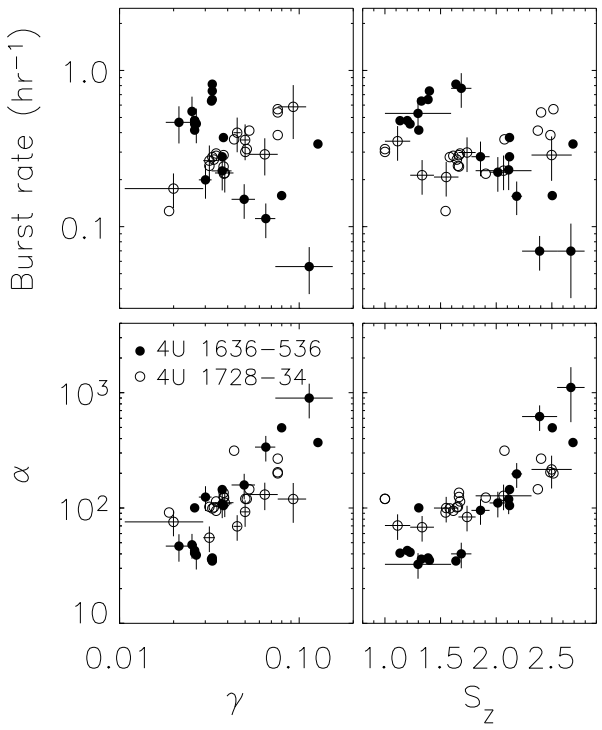

FIG. 16.— Mean burst rates (*upper panels*) and α-values (*lower panels*) for 4U 1636−536 (*filled circles*) and 4U 1728−34 (*open circles*) plotted as a function of γ (*left-hand panels*) and S_Z (*right-hand panels*). Bursts are combined in groups of ≈ 16 for binning. Also shown are the instantaneous burst rates ($1/t_{\rm rec}$) and α-values for selected pairs bursts from these two sources. While the γ/S_Z range spanned by the two sources is almost identical, the variation of the burst rate and α is distinctly different. Error bars indicate the 1σ uncertainties.

but not with S_Z. We also see very different behaviour in the measured α-values for these two sources as a function of γ/S_Z (Fig. 16, lower panels). For 4U 1636−536, α increases significantly with γ/S_Z, most dramatically as a function of S_Z where it increases from ≈ 20 to ≈ 1000 between $S_Z = 1.4$–2.5 (significance of 6σ). 4U 1728−34, on the other hand, consistently has $\alpha \approx 70$–200, and does not show significant variations as a function of γ or S_Z ($< 2\sigma$ in each case). This is in contrast to the results of Cornelisse et al. (2003), who inferred consistent burst rate behaviour from a much larger sample of bursts observed by *BeppoSAX* from 9 sources (including 4U 1728−34 and 4U 1636−536). The burst properties of 4U 1728−34 closely resemble those of 4U 1820−30 (Cumming 2003), indicating that it may also be a He accretor. Since this is the most frequent burster in our sample, this is a critical caveat on interpreting results where we combine bursts from different sources including 4U 1728−34. While the differences between the burst behaviours of 4U 1728−34 and 4U 1636−536 may be attributable to differences in the composition of the accreted material, this still does not explain why the behaviour of the latter source is so at odds with theoretical predictions.

4.2. *"Double" bursts*

Thermonuclear bursts with extremely short recurrence times ("double" or "prompt" bursts) have long presented a challenge to our understanding of burst physics. Their recurrence times of $\gtrsim 5$ min are too short for sufficient fuel to accumulate to allow ignition by unstable thermonuclear burning. The classical double burst consists of an initial bright burst followed by a much fainter event. An important question is whether the fuel for the second burst is residual material left unburnt by the first (the *truncated* model), or if it is newly accreted (*premature* model). It has been previously suggested that residual fuel leftover from the first burst reaches ignition conditions by mixing deeper into the atmosphere of the NS (Woosley & Weaver 1984; Fujimoto et al. 1987). For example, bursts from EXO 0748−676 span a relatively large range of recurrence times (as short as 23 min), and the burst fluence $E_{\rm b}$ has been demonstrated to be linearly proportional to the recurrence time (Gottwald et al. 1987). The line of best fit does not go through the origin, so that in principle a burst with zero recurrence time will have a finite, non-zero fluence. This result suggests that in that source some small fraction ($\approx 10\%$) of the fuel left over from the previous burst contributes to the fluence of subsequent bursts. We note also that there are cases of weak burst-like events *preceeding* otherwise normal bursts by only a few seconds, in 4U 1636−536 (see §3.8) and 4U 1709−267 (see §3.12 and Jonker et al. 2004). For these bursts, as well as those with prononounced double peaks in the flux, it is much less clear that the peak arise from distinct ignition events.

We plot the small-Δt end of the burst recurrence time distribution in Fig. 17. The distribution exhibits a deficit of bursts with $\Delta t = 40$–100 min; the 90 min satellite orbit falls within this range, so that this deficit is likely a consequence of the regular data gaps (the typical duty cycle is ≈ 0.65) due to Earth occultations of bursters. For $\Delta t > 100$ min it is not possible to be confident that intermediate bursts have not been missed, so that the actual recurrence time is 1/2 or 1/3 the measured value; however this is less a problem for the bursts with $\Delta t \lesssim 30$ min, which is shorter than the typical on-source duration per orbit. Thus, we extract this subsample for our analysis of short recurrence time bursts.

Of the 75 pairs of bursts with $\Delta t \leq 30$ min, we found 11 cases where short-recurrence time pairs immediately followed each other, i.e. a series of three bursts with recurrence times < 30 min. Sources contributing to this subset were 4U 1705−44, Rapid Burster (4), 4U 1636−536, 2E 1742.9−2929 (3), EXO 1745−248 and 4U 1608−52. We also found two instances of four bursts following each other, all with recurrence times < 30 min, from the Rapid Burster and 4U 1636−536. This leaves 47 cases of no more than two bursts following each other with short recurrence times. With several examples of three and even four bursts following each other in rapid succession, we hypothesize that many of the short-recurrence time bursts from the Rapid Burster may be type-II bursts instead of type-I. Type-II bursts are thought to arise from accretion instabilities rather than thermonuclear ignition, and may occur regularly with recurrence times as short as a few tens of seconds. Type-II bursts may be distinguished from thermonuclear bursts by their rapidity and their lack of spectral variation with time. In few of the bursts in the sample from the Rapid Burster are

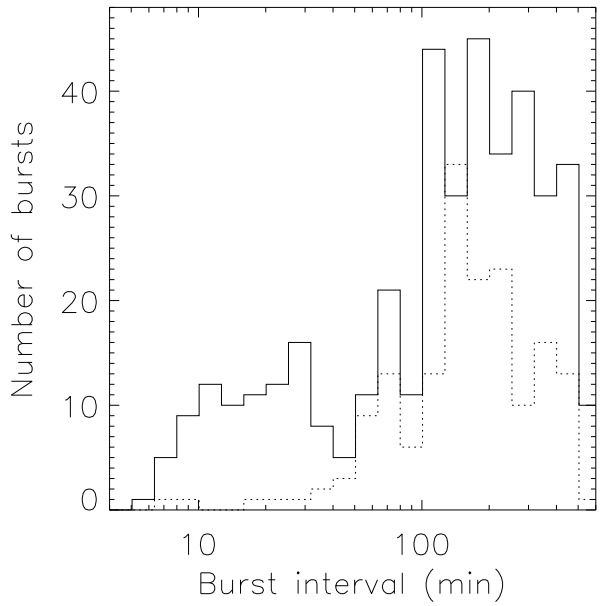

FIG. 17.— Distribution of observed burst recurrence times Δt below 10 hours. The solid histogram shows the distribution for all the bursts observed by *RXTE*; the dotted histogram shows the distribution for those pairs of bursts with measured α-values (see §2.5). The majority of the latter subset of bursts are regular, and so represent conventional burst behaviour. Regular bursting with recurrence times $\lesssim 30$ min is not observed; these close pairs of bursts are only observed episodically.

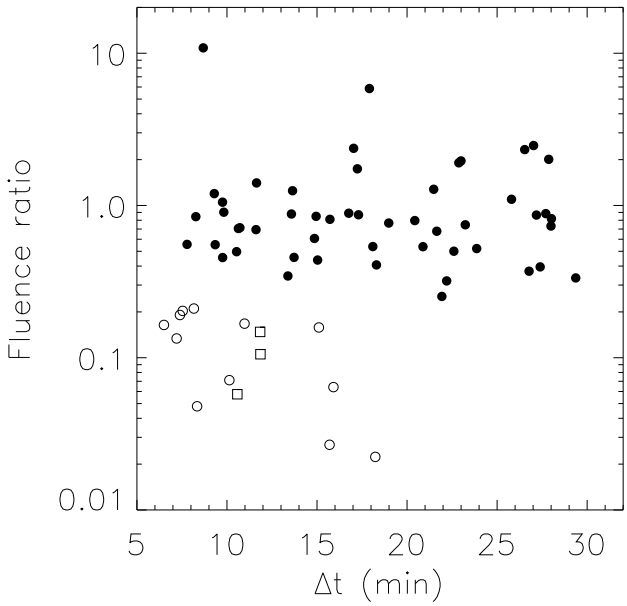

FIG. 18.— Ratio of fluences $E_{b,1}/E_{b,0}$ of pairs of bursts plotted as a function of their separation Δt. We found evidence for two distinct groups of short-recurrence time bursts, one with comparable fluences (mean ratio of the fluences was 0.77; *filled symbols*), and a second with a much fainter second burst $E_{b,1} \lesssim 0.24 E_{b,0}$ (resembling more closely the "classical" double bursts; *open symbols*). The dashed line shows the log-linear line of best fit for the pairs of bursts with fluence ratio < 0.24. The open squares are from the three short bursts from 4U 1323−62 (§3.6).

temperature variations present at a significance of more than 3σ, so that we cannot confirm these bursts as arising from thermonuclear ignition.

We show the ratio of fluences for pairs of bursts with $\Delta t < 30$ min in Fig. 18. For 9 pairs we could not measure the fluence for one of the pairs, because either the high time-resolution data did not cover the burst, or because the burst was too faint to reliably measure the fluence. These burst pairs occurred primarily between $\gamma = 0.01$ and 0.3, or $S_Z = 1.0$ and 2.9. A significant fraction of the bursts pairs have comparable fluences, i.e. $E_{b,1}/E_{b,0} \approx 1$. Approximately 1/3 of these burst pairs are from the Rapid Burster, and may be mis-identified type-II bursts, as discussed above. Other sources with bursts in this group (filled circles in Fig. 18) are EXO 0748−676, 4U 1608−52, 4U 1636−536, 4U 1705−44, 4U 1735−44, 2E 1742.9−2929, EXO 1745−248, 4U 1746−37, Aql X-1 and Cyg X-2. The median fluence ratio for these bursts was 0.77; the minimum recurrence time was 7.8 min (for a pair of bursts from 2E 1742.9−2929). We also found a somewhat distinct group with a median fluence ratio of 0.064 and $\Delta t = 6.1$–18 min (open symbols in Fig. 18). This group more closely resembles the "classic" double bursts, and includes bursts from EXO 0748−676, 4U 1323−62, 4U 1608−52, 4U 1636−536, 4U 1705−44, XTE J1710−291 and 4U 1746−37. Fig. 18 suggests an anticorrelation between the fluence ratio and Δt for these bursts; the longer the waiting time, the smaller the fluence (as a fraction of the previous burst's fluence). We found none of these bursts with recurrence time longer than 18 min, whereas the distribution of recurrence times for bursts pairs with comparable fluences was essentially uniform up to 30 min.

One particularly interesting source with bursts in this latter group was 4U 1323−62 (see also §3.6). Five of the 24 bursts observed from this source by *RXTE* occurred between 1997 April 25–28 and exhibited a roughly constant recurrence time of 2.7 hr. Two of the regular bursts were followed by much fainter secondary bursts after only ≈ 10 min; a third, similar double burst was observed on 1999 Jan 18, by which time the burst interval was somewhat shorter, between 2.1 and 2.5 hr. The steady recurrence times of these double bursts enable a test of whether the fuel burnt in the prompt bursts is leftover from the preceding burst, or is newly accreted. From the burst fluence we estimate the column y at which each burst is ignited (equation 4), assuming that the material is spread evenly over the NS surface. We then calculate the mean mass accretion rate (per unit area) for the interval preceding the burst as $\dot{m} = y/\Delta t$, where Δt is the burst interval (Fig. 19). For perfectly steady bursts and complete consumption of the accreted fuel, we expect this quantity to be constant for each burst. Indeed, the inferred accretion rate from the strong bursts on 1997 April 25–27 was relatively steady at $(3.2 \pm 0.3) \times 10^3 (d/10\mathrm{kpc})^2$ g cm^{-2} s^{-1} in the mean, similar to the inferred rate between the two bursts on 1999 January 18 (bursts #11 & 12).

If only newly accreted fuel is burnt during the prompt bursts (#5, 7 and 11), then we expect to measure an identical accretion rate for those bursts, to that of the regular bursts. Conversely, if some of the fuel burnt during the prompt bursts is leftover from the previous burst,

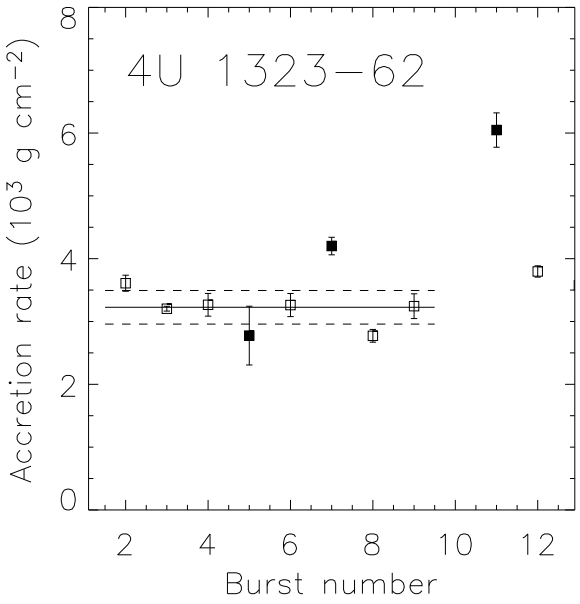

FIG. 19.— Inferred accretion rate $\dot{m}$ in 4U 1323−62 (assuming $d = 10$ kpc) from bursts observed by *RXTE* during 1997 April 25–27 (bursts #2–9) and 1999 January 18 (#11,12). The rate for the three prompt bursts (#5, 7 and 11) is indicated by the filled squares. The horizontal lines show the mean (*solid*) and $\pm 1\sigma$ (*dashed*) limits for $\dot{m}$ excluding the prompt bursts.

the apparent rate will be *in excess* of the mean rate before and after. For the first prompt burst on 1997 April 26 (#5), the inferred $\dot{m}$ was consistent with the mean inferred rate before and after. However, for the prompt bursts on 1997 April 27 and 1999 January 18 (#7, 11) the inferred rate was significantly higher than the mean at the 3.2 and 7.4σ levels, respectively. This strongly suggests that fuel leftover from the previous burst is burning, possibly in addition to any material accreted since (i.e. the truncated model; Fujimoto et al. 1987). We estimate that unburnt fuel makes up 20–50% of the fuel burnt in bursts #7 and 11, respectively. Since the total fluence of the prompt bursts in 4U 1323−62 is only 10 and 15% respectively of the typical fluence for the bright bursts $(0.103 \pm 0.008) \times 10^{-6}$ ergs cm^{-2}, the fraction of fuel unburnt by the preceding burst is thus $\approx 8\%$. This is comparable to the $\sim 10\%$ measured for EXO 0748−676 by Gottwald et al. (1987). Thus, these results suggest that both newly accreted fuel and fuel leftover from the previous burst may give rise to the smaller second burst, although a contribution from leftover fuel does not appear to be strictly required. On the other hand, the highly variable α-values measured for 4U 1702−429 suggest that as much as 50% of the burst fuel may be left unburnt (see §3.10).

4.3. *Burst duration, time scales and fuel composition*

We now turn to the variation of the properties of individual bursts as a function of accretion rate. The characteristic time scale of evolution $\tau = E_b/F_{\rm pk}$ has long served as a quantitative measure of the properties of bursts observed with low-sensitivity instruments, and the marked differences in the burning rates for H and He fuel suggests that τ should also indicate approximately the fuel composition. Using the high signal-to-noise data obtained with *RXTE*, we are now able to test this measure against precisely-determined α values. For the bursts observed by *RXTE* we have also measured decay constant(s) τ_1, τ_2 for the 1(2) exponential fits to the flux evolution. A second exponential decay segment was required for fits of 723 of the 988 lightcurves with sufficient points to fit at all. We note that in general τ and τ_1 were roughly proportional; for the 960 bursts with both τ and $\tau_1 < 50$, $\tau_1 = 0.59 + 0.44\tau$ (rms 2.7 s). Similarly for those bursts with two exponential fits and $\tau < 80$ s, we found $\tau_2 = 4.5 + 1.17\tau$ (rms 7.7 s).

For 276 PRE bursts (including those with marginal evidence for radius expansion; see §2.3) with γ values, the time scale τ was significantly anticorrelated with γ (Spearman's $\rho = -0.35$, significant to 5.9σ; Fig. 20, upper panel), as was also found by van Paradijs et al. (1988a). The *RXTE* data extends the correlation identified by the latter authors up to $\gamma \approx 1$, with extremely short ($\tau \sim 2$ s) bursts from Cyg X-2 (see §3.45) and GX 17+2 (see §3.35). The long bursts from GX 17+2 also at $\gamma \approx 1$ are a notable exception, with τ up to ≈ 400. The energetics of these bursts appear to be significantly different from normal type-I bursts (see e.g. in 't Zand et al. 2004b), and thus we exclude them from this discussion. For the 473 non-PRE bursts from the other sources, we found no correlation between τ and γ. We point out that for the PRE bursts, the τ values are biased since the $F_{\rm pk}$ values are limited. That is, regardless of how large is the fluence for a PRE burst, $F_{\rm pk}$ cannot significantly exceed the Eddington flux for the source, so that the τ value will likely be lower than it would have been, were the peak flux not limited. Thus, the anticorrelation between τ and γ observed for the PRE bursts is partly a consequence of an anticorrelation between the normalised fluence U_b and γ ($\rho = -0.38$, significant to 6.2σ). For the PRE bursts, the decay constants τ_1, τ_2 for the exponential fits to the burst lightcurve following the peak may a less biased measure of the burst time scale, although we still find significant anticorrelations between both τ_1 and γ ($\rho = -0.23$, 3.8σ) and τ_2 and γ ($\rho = -0.36$, 5.9σ) for the PRE bursts. For the non-PRE bursts we observe no significant correlations between τ_1 or τ_2 and γ, as is found for τ. It is worthwhile comparing our results with those of (Cornelisse et al. 2003), who plotted τ as a function of F_p for bursts detected by *BeppoSAX* from 9 sources, separately. While those authors came to similar conclusions regarding the variation with accretion rate, the PRE and non-PRE bursts were combined, masking the different behavior of these two groups. Furthermore, the trends they identify all occur over less than a decade in F_p, which are (arguably) distinct from the much wider-range correlations we have discussed.

With the additional parameters related to the persistent emission available from the *RXTE* data, we may also test for correlations between the burst time scales and position on the color-color diagram, S_Z, for the subset of sources for which the latter parameter can be measured (see §2.1). Here we find the opposite situation as for γ, with a significant anticorrelation between τ and S_Z for the 230 non-PRE bursts ($\rho = -0.56$, 8.4σ) but no relation for the 157 PRE bursts (Fig. 20, lower panel); we find similar results for τ_1, τ_2. An exception to the

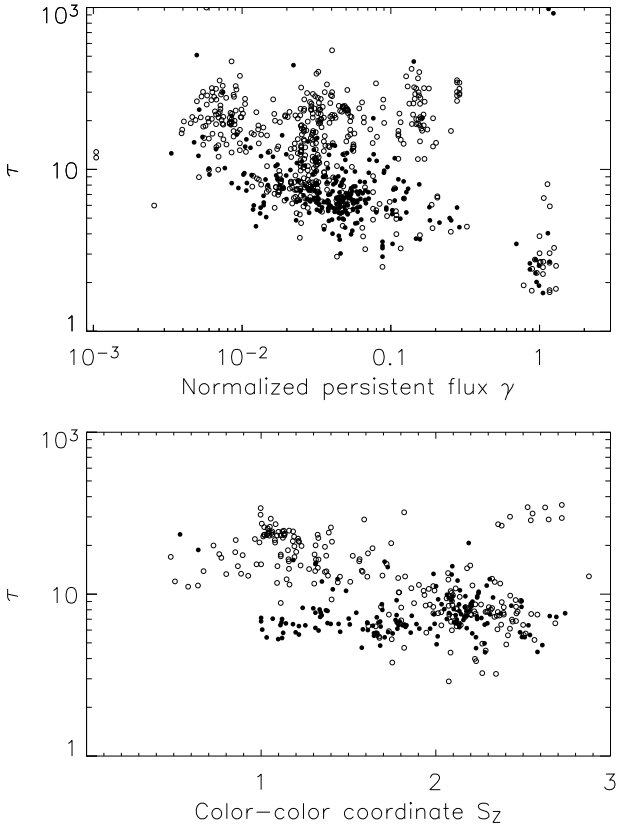

FIG. 20.— Burst time scale $\tau = E_b/F_{\rm pk}$ as a function of normalised persistent flux γ (*top panel*) and the position S_Z on the color-color diagram (*bottom panel*). Open circles indicate non-radius expansion bursts, while closed circles indicate PRE bursts. Note the markedly different distributions for the PRE and non-PRE bursts. The outlying cluster of bursts around $\gamma = 1$ are from Cyg X-2 and GX 17+2; the group at $\tau \approx 20$, $S_Z \approx 2.5$ are from 4U 1728−37.

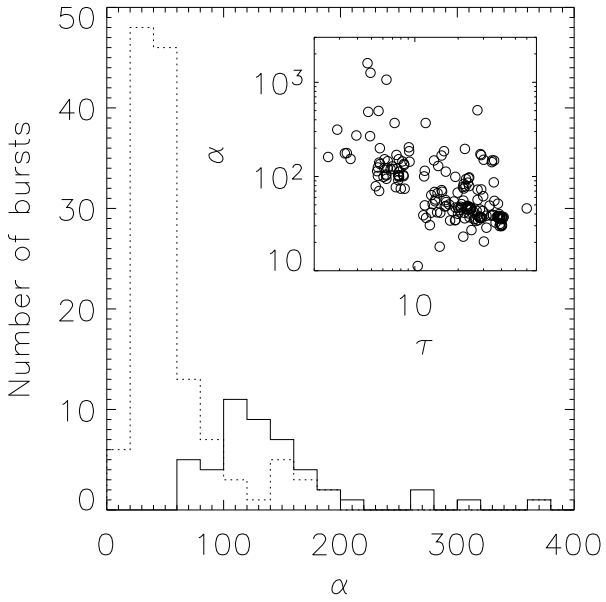

FIG. 21.— Distribution of α for bursts with $\tau < 10$ (*solid histogram*) and $\tau > 10$ (*dotted histogram*). Bursts with low $\alpha < 60$ are all long with $\tau > 10$, while bursts with $\alpha > 60$ are predominantly short with $\tau < 10$. The inset shows α as a function of τ for the individual bursts, clearly showing the correlation between the fuel composition (indicated by α) and the characteristic evolution time-scale for the burst

correlation for the non-PRE bursts is a cluster of long ($\tau > 20$) bursts at $S_Z > 2.2$. These are primarily from 4U 1746−37, detected during 1998 November when the source was in a relatively high state; there are other peculiarities about these bursts (see §3.29). The correlation between τ and S_Z becomes even more significant ($\rho = -0.72$, 10.1σ) if we exclude these bursts. The lack of correlation for the PRE bursts may be attributed to the fact that 71 of the 157 PRE bursts with S_Z values are from 4U 1728−34, for which the burst time scales do not appear to vary substantially in the *RXTE* sample ($\tau = 6.3 \pm 1.3$ s on average; see §3.16). For the remaining sources, the S_Z values for the PRE bursts do not span a sufficient range to measure any correlation.

Finally, with the *RXTE* catalog we are in a position to directly compare the measured τ and α values. From our sample of burst pairs for which we can measure α, we found that τ and α were strongly anticorrelated, with all the bursts with $\tau < 10$ having $\alpha > 70$ (Fig. 21). For those bursts we find a median $\alpha = 130$, although we also measured values as high as 1600 (for Ser X-1). For the bursts with $\tau > 10$, we instead found a median $\alpha = 48$. Perhaps most dramatically, we find no bursts with low α and $\tau < 10$; for those bursts, the minimum value of $\alpha = 70$.

4.4. *Photospheric radius expansion and source distances*

We observed photospheric radius-expansion bursts from 35 of the 45 sources with bursts detected by *RXTE*. We were able to satisfy our criteria for radius-expansion (see §2.3) for bursts peaking at fluxes as low as 5×10^{-9} ergs cm^{-2} s^{-1}; the brightest PRE bursts in our sample reached more than 1.7×10^{-7} ergs cm^{-2} s^{-1} (Table 6).

The $F_{\rm Edd} = \langle F_{\rm pk,PRE} \rangle$ values allowed us to normalize the burst fluxes in order to compare properties of bursts from different sources. The normalized peak fluxes of the radius-expansion bursts were distributed about a mean of 0.98 with standard deviation 0.14 (Fig. 22, upper panel). The overall range was 0.26–1.4. The PRE bursts include those with marginal evidence for radius-expansion; the burst with the smallest normalized peak flux in this class was from 4U 1636−536 (0.26), although (as discussed by Galloway et al. 2006) the spectral variation in this burst may have instead arisen from the same mechanism that gave rise to the double-peaked bursts (see §3.8). The non-PRE bursts were distributed with increasing numbers of bursts towards lower normalized peak flux. The steep decrease in the distribution below 0.2 may be partly instrumental, since it is difficult to distinguish such weak bursts from normal counting noise or flares in the persistent flux. We also plot the distribution of the normalized fluence, $U_b = E_b/F_{\rm Edd}$, in Fig. 22, lower panel. There is much greater overlap between the distributions for the PRE and non-PRE bursts, than for the normalized peak flux. The 17 bursts with the highest normalized fluence ($U_b > 20$, not shown) all exhibited PRE. These include extreme radius expansion bursts from 4U 1724−307 (§3.15) and 4U 2129+12

TABLE 6
Mean peak fluxes and estimated distances from PRE bursts observed by *RXTE*

Source	Number of bursts	$\langle F_{\rm peak}\rangle$ (10^{-9} ergs cm^{-2} s^{-1})	Distance (kpc)[a] $X=0.7$	Distance (kpc)[a] $X=0$	Max. distance (kpc)[b] $X=0.7$	Max. distance (kpc)[b] $X=0$
4U 0513−40[c]	1	17.0	8.9	12	···	···
EXO 0748−676	3	41 ± 5	5.7 ± 0.7	7.4 ± 0.9	< 5.9	< 7.8
1M 0836−425	···	···	< 8.2	< 11	···	···
4U 0919−54	1	81.9	4.0	5.3	···	···
4U 1254−69[c]	4	5.6 ± 0.7	15.5 ± 1.9	20 ± 2	< 17	< 22
4U 1323−62	···	···	< 11	< 15	···	···
4U 1608−52	12	132 ± 14	3.2 ± 0.3	4.1 ± 0.4	< 3.4	< 4.4
4U 1636−536[d]	40	64 ± 5	5.95 ± 0.12	6.0 ± 0.5	< 6.0	< 6.6
MXB 1659−298	12	17 ± 4	9 ± 2	12 ± 3	< 11	< 14
4U 1702−429	4	76 ± 3	4.18 ± 0.17	5.5 ± 0.2	< 4.3	< 5.5
4U 1705−44	3	39.3 ± 1.7	5.8 ± 0.2	7.6 ± 0.3	< 5.9	< 7.8
XTE J1709−267[c]	1	11.0	11	14	···	···
XTE J1710−281	1	9.25	12	16	···	···
XTE J1723−376	···	···	< 10	< 13	···	···
4U 1724−307	2	53 ± 17	5.0 ± 1.6	7 ± 2	< 5.7	< 7.4
4U 1728−34	69	84 ± 9	4.0 ± 0.4	5.2 ± 0.5	< 4.6	< 5.9
Rapid Burster	···	···	< 9.2	< 12	···	···
KS 1731−260	4	43 ± 6	5.6 ± 0.7	7.2 ± 1.0	< 6.0	< 7.8
SLX 1735−269	···	···	< 5.6	< 7.3	···	···
4U 1735−44	6	31 ± 5	6.5 ± 1.0	8.5 ± 1.3	< 7.6	< 10
KS 1741−293	···	···	< 5.7	< 7.5	···	···
GRS 1741.9−2853	6	38 ± 10	6.0 ± 1.6	8 ± 2	< 7.8	< 10
2E 1742.9−2929	2	40.07 ± 0.08	5.770 ± 0.011	7.523 ± 0.015	< 5.8	< 7.5
SAX J1747.0−2853	10	50 ± 8	5.2 ± 0.8	6.7 ± 1.1	< 5.7	< 7.5
SLX 1744−300	···	···	< 8.4	< 11	···	···
GX 3+1	1	53.0	5.0	6.5	···	···
SAX J1748.9−2021	6	34 ± 5	6.2 ± 1.0	8.1 ± 1.3	< 6.9	< 9.0
EXO 1745−248	2	59.6 ± 1.1	4.73 ± 0.09	6.17 ± 0.11	< 4.8	< 6.2
4U 1746−37	3	5.3 ± 0.9	16 ± 3	21 ± 4	< 17	< 22
SAX J1750.8−2900	2	49.2 ± 1.0	5.21 ± 0.11	6.79 ± 0.14	< 5.2	< 6.8
GRS 1747−312	3	16 ± 6	9 ± 3	12 ± 4	< 12	< 15
XTE J1759−220	···	···	< 16	< 21	···	···
SAX J1808.4−3658	4	174 ± 8	2.77 ± 0.11	3.61 ± 0.14	< 2.9	< 3.7
XTE J1814−338[c]	1	21.3	7.9	10	···	···
GX 17+2	2	14.8 ± 1.7	9.8 ± 0.4	12.8 ± 0.6	< 10	< 13
3A 1820−303	4	55.3 ± 1.7	4.91 ± 0.15	6.40 ± 0.20	< 5.0	< 6.5
GS 1826−24	···	···	< 6.7	< 8.8	···	···
XB 1832−330	1	29.7	6.7	8.7	···	···
Ser X-1	2	23 ± 3	7.7 ± 0.9	10.0 ± 1.1	< 8.0	< 10
HETE J1900.1−2455	2	102 ± 13	3.6 ± 0.5	4.7 ± 0.6	< 3.8	< 4.9
Aql X-1	9	89 ± 15	3.9 ± 0.7	5.0 ± 0.9	< 4.6	< 6.0
4U 1916−053	12	29 ± 4	6.8 ± 1.0	8.9 ± 1.3	< 7.5	< 10
XTE J2123−058	···	···	< 14	< 19	···	···
4U 2129+12	1	39.6	5.8	7.6	···	···
Cyg X-2	5	12 ± 3	10 ± 2	14 ± 3	< 13	< 17

Note. — The distances here are derived assuming a canonical neutron star with $M = 1.4 M_\odot$ and $R = 10$ km. The corresponding distances for a $2 M_\odot$ neutron star will be a factor of 9.3% larger.

[a] Where no radius expansion bursts have been observed, the upper limit on the distance is calculated from the peak flux of the brightest burst observed by *RXTE*.

[b] Upper limits on the distance calculated from the peak flux of the faintest burst exhibiting radius expansion

[c] Only marginal cases of radius-expansion were available for this source

[d] For 4U 1636−536, the peak flux distribution is bimodal, with a separation factor of ≈ 1.7. The lower flux radius-expansion bursts are thus identified with the Eddington limit for material with cosmic abundances ($X = 0.7$), while the brigher bursts are assumed to reach the Eddington limit for He-only. The two distances are thus calculated using the appropriate group for each of the two abundance options

(§3.44), amongst others, as well as the very long bursts from GX 17+2 (§3.35).

We identified four distinct types of radius-expansion bursts, which we can distinguish based on their spectral evolution, peak flux, and fluence.

Faint symmetric bursts— Several bursts observed from 4U 1746−37 and GRS 1747−312 appeared to exhibit PRE but reached significantly sub-Eddington fluxes. The three PRE bursts from 4U 1746−37 reached peak fluxes of $(4.5\text{–}6.3) \times 10^{-9}$ ergs cm^{-2} s^{-1}, which for an isotropically emitting source at $d = 11$ kpc (the estimated distance to the host cluster NGC 6441) indicates a peak luminosity of $(7\text{–}9) \times 10^{37}$ ergs s^{-1}. This is well below the expected luminosity even for a burst reaching the Eddington limit for H-rich material, $\approx 1.6 \times 10^{38}$ ergs s^{-1} (equation 5 with $X = 0.7$). Similar results were found for this source by Sztajno et al. (1987), who measured a lower limit for $(d/10\,{\rm kpc})^2/\xi_b > 1.59$ (where ξ_b parametrises the degree of beaming of the burst flux), so that either the burst flux is strongly beamed away

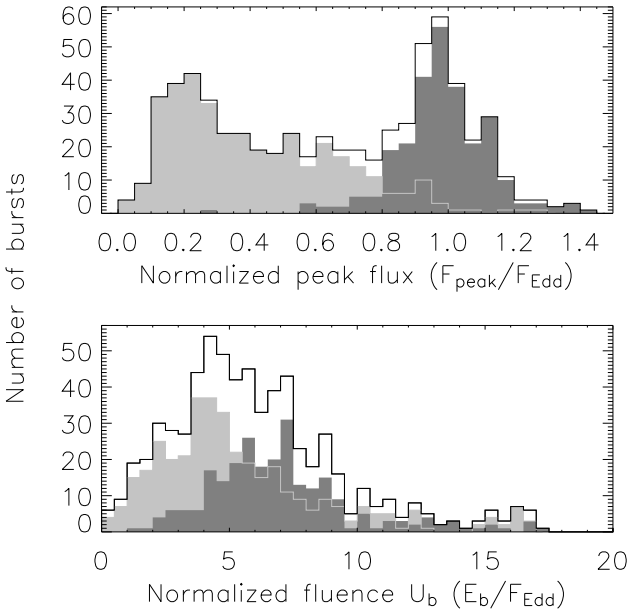

FIG. 22.— *Top panel* Distribution of (normalized) peak burst flux $F_{\rm pk}/F_{\rm Edd}$ for radius-expansion (*dark gray*) and non-radius expansion (*light gray*) bursts. The distribution of peak fluxes of the radius-expansion bursts is broad, with standard deviation 0.14. The radius-expansion burst with the lowest peak flux $\simeq 0.3F_{\rm Edd}$ is from 4U 1636−536 (see also §3.8). The black histogram shows the combined distribution. *Bottom panel* Distribution of normalized fluence $U_b = E_b/F_{\rm Edd}$ for both types of bursts. There is significant overlap between the two distributions, suggesting that the amount of accreted fuel is relatively unimportant in determining whether bright bursts exhibit radius expansion or not. Not shown are 17 extremely bright radius-expansion bursts with $U_b > 20$ s, from 4U 1724−307 (1), 4U 1608−52 (1), GRS 1741.9−2853 (2), GRS 1747−312 (1), 4U 1636−536 (1), GX 17+2 (8), XB 1832−330 (1), HETE J1900.1−2455 (1) and 4U 2129+12 (1).

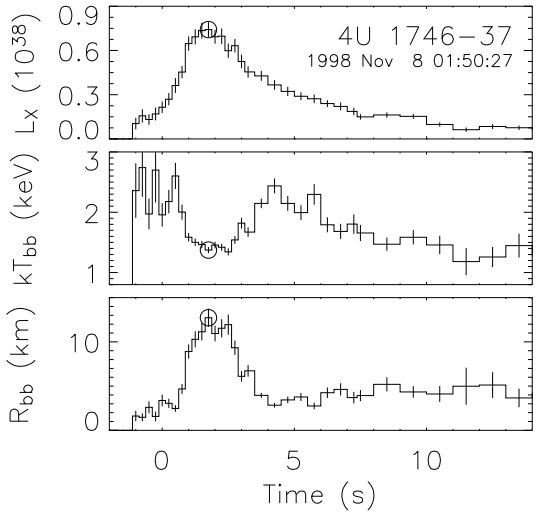

FIG. 23.— A thermonuclear burst from 4U 1746−37 which exhibited photospheric radius-expansion but reached a peak flux significantly below the Eddington limits for He or H-rich material. *Top panel* Burst luminosity (in units of 10^{38} ergs s^{-1}); *middle panel* blackbody (color) temperature $kT_{\rm bb}$; and *bottom panel* blackbody radius $R_{\rm bb}$. L_X and $R_{\rm bb}$ are calculated assuming a distance to the host globular cluster NGC 6441 of 11.0 kpc (Kuulkers et al. 2003). The time at which the flux reaches a maximum is indicated by the open circle. The spectral evolution during this burst (as well as other bursts from this source and GRS 1747−312) is different from the typical behavior (e.g. Fig. 2). Note in particular that the temperature decay begins only when the burst flux has dropped to about half the peak value; for typical PRE bursts, the flux peak occurs at the end of the PRE episode, and the temperature decay begins immediately afterwards.

from the observer ($\xi_b < 1$), or that the distance to the cluster is larger than 11 kpc. We note that several of these bursts interrupted otherwise regular sequences of bursts (see §3.29). One of the three bursts observed from GRS 1747−312 was similarly faint, reaching a peak flux of 1.0×10^{-9} ergs cm^{-2} s^{-1} which (for the estimated distance of Terzan 6 of 9.5 kpc) corresponds to a luminosity of 1.1×10^{38} ergs s^{-1}.

The spectral evolution of these bursts was distinctly different from the PRE bursts from other sources (Fig. 23; see also Galloway et al. 2004a). The burst profiles were more symmetric than usual, and the peak flux was reached coincident with the peak blackbody radius. Cooling of the spectrum commenced only when the burst flux had dropped to (typically) < 0.5 of the maximum, in contrast to typical PRE bursts, in which the cooling commences immediately following the peak flux. We note that Kuulkers et al. (2003) did not identify these bursts as radius-expansion, although they clearly meet our criteria specified in §2.3. Two other PRE bursts were detected from GRS 1747−312, one with profile similar to that shown in Fig. 23 that reached a peak flux of 1.7×10^{-9} ergs cm^{-2} s^{-1}, and a third with extremely large fluence which reached 2.2×10^{-9} ergs cm^{-2} s^{-1}. Assuming that all these bursts actually did originate from GRS 1747−312 (the origin of the faintest PRE burst cannot be constrained; see §3.31), the implied range for the peak fluxes of PRE bursts was a factor of 2.2, by far the largest of all the sources with multiple PRE bursts observed by *RXTE*. The short bursts observed from Cyg X-2 have similar spectral evolution. The characteristic burst profiles exemplified by Fig. 23 define a distinct class of bursts which appear to exhibit radius expansion but which reach peak luminosities significantly below the Eddington limit, and may also exhibit a much greater variation in their peak fluxes (for an individual source) than for typical PRE bursts.

Hydrogen-limited bursts— Variations in atmospheric composition are the principal uncertainty in determining distances from PRE burst fluxes, and may also play a role in the variations of PRE burst peak fluxes from individual sources. We found just two bursts in the entire *RXTE* sample which evidence suggests reached the Eddington limit for H-rich material $L_{\rm Edd,H}$, rather than $L_{\rm Edd,He}$. The majority of the 40 PRE bursts observed by *RXTE* from 4U 1636−536 had peak fluxes distributed about 6.4×10^{-8} ergs cm^{-2} s^{-1} (with a standard deviation of 7.6%), but we also found two PRE bursts with much smaller peak fluxes of (37.6 ± 0.8) and $(36.0 \pm 0.9) \times 10^{-9}$ ergs cm^{-2} s^{-1}, respectively. These two bursts reached maximum fluxes an average of 1.69 ± 0.13 lower than the mean for the remaining PRE bursts, and represent a highly significant deviation from the otherwise normal distribution of peak fluxes for the latter group. This value is just what we expect if the bright PRE bursts from 4U 1636−536 reached the Ed-

dington limit for pure He ($X = 0.0$), $L_{\rm Edd,He}$, while the fainter bursts reached $L_{\rm Edd,H}$ ($X = 0.7$; see also §3.8 and Galloway et al. 2006). The peak flux for the two faint bursts was achieved at the same time as the peak radius, in contrast to typical PRE bursts (see below); otherwise the profiles were relatively typical for bursts from this source, and did not resemble the faint PRE bursts from 4U 1746−37 and GRS 1747−312 (see above). Unlike those sources, 4U 1636−536 is not located in a globular cluster, and so we have no independent estimate of the distance with which to calculate the peak luminosity. Assuming variations in composition do indeed explain the distribution of peak PRE burst fluxes in 4U 1636−536, there arise difficulties as to how to remove or eject the accreted H in the normal (bright) PRE bursts from this source.

Helium-limited bursts— The majority of PRE bursts all had qualitatively similar patterns of spectral variation. The maximum radius was reached in the first few seconds of the burst, while the flux was still increasing. The maximum flux was generally reached at the point where the radius expansion had ceased, and the temperature began to decrease again (e.g. Fig. 2; notable exceptions to this rule were the dipping sources, including EXO 0748−676). The maximum inferred radius was typically $\lesssim 2$ times the subsequent minimum (which we may identify with $R_{\rm NS}$) and following the radius expansion the radius frequently increased throughout the decay. The evidence from 4U 1636−536 leads us to identify these bursts as reaching the limit for H-poor material, although this is by no means certain.

Giant bursts— The intrinsically brightest bursts were from 4U 2129+12 and 4U 1724−307, and exhibited unusually large fluences, long timescales, and expansion to large radii (e.g. Fig. 10). The estimated distance to the host globular clusters of these sources is ≈ 10 kpc, for which the expected maximal Eddington flux (for $X = 0$) is 2.2×10^{-8} ergs cm^{-2} s^{-1}. However, the observed peak flux for the burst from 4U 2129+12 was almost a factor of two larger at 4×10^{-8} ergs cm^{-2} s^{-1}, and for 4U 1724−307 almost a factor of 3 larger at 6.6×10^{-8} ergs cm^{-2} s^{-1}. As with the other PRE bursts, we applied the gravitational redshift correction in equation 5 with $R = R_{\rm NS}$. If the photospheric radius is larger at the flux maximum, the intrinsic luminosity will be overestimated. However, examination of the spectral evolution of these two bursts indicates that the blackbody radius at flux maximum is similar to the asymptotic value in the tail of the burst. Thus, the redshift correction cannot explain the unusually large peak fluxes. On the other hand, to explain the apparently super-Eddington flux as due to the T_e term in equation 5 would require a temperature in the photosphere of up to $\sim 10^9$ K.

The factor by which the peak flux exceeded the Eddington value did not appear to depend upon the normalized fluence in the burst. For example, the bursts from 4U 2129+12 and 4U 1724−307 had $U_b = 30$ and 54, respectively; a much more energetic burst from GRS 1747−312 had $U_b = 157$, although it reached a peak flux of just 2.2×10^{-8} ergs cm^{-2} s^{-1} (consistent with the expected Eddington value for a He-rich burst at 10 kpc). However, for each source the peak flux was proportional to the fluence (this was attributed to reprocessing in PRE bursts from 4U 1728−34; Galloway et al. 2003). Conversely, the two PRE bursts from EXO 1745−248 had modest fluences with $U_b \approx 7$, resembling typical PRE bursts from many other sources. However, the peak flux of $\approx 6 \times 10^{-8}$ ergs cm^{-2} s^{-1} implies for $d = 8.7$ kpc a luminosity of 5.4×10^{38} ergs s^{-1}, also well in excess of the maximal value expected by a factor of ≈ 2. Giant bursts were also observed from sources outside globular clusters. The brightest burst from GRS 1741.9−2853, on 1996 July, reached a peak flux 25% higher than the next brightest PRE burst. The burst was also much more intense than any other, with $U_b = 65$ compared to the next highest value of 23. Simiarly, the first burst observed by *RXTE* from the millisecond accretion-powered pulsar HETE J1900.1−2455 had a peak flux 20% greater than the second, again with a much higher $U_b = 55$ compared to 15.

These different classes of bursts contributed to significant variations in the peak PRE burst flux from many of the 26 sources from which we observed more than one PRE burst. For individual bursts, the estimated (statistical) uncertainty on the measured peak flux was typically $\sim 2\%$, while the fractional variation of peak fluxes from all PRE bursts from a given source was as much as an order of magnitude larger. For 16 of the 26 sources we found highly significant ($> 5\sigma$) variations in the peak flux of the radius expansion bursts. The mean fractional standard deviation over all 26 sources was $(14 \pm 9)\%$, with a maximum of 38% for GRS 1747−312. Interactions of the burst flux with the surrounding material almost certainly contribute to variations in the peak PRE burst flux. For example, the distribution of peak burst fluxes from 4U 1728−34 observed by *RXTE* has already been well studied, as reported in Galloway et al. (2003). The $F_{\rm pk,PRE}$ were normally distributed with a fractional standard deviation of 10%. From regular ASM measurements we found evidence for quasi-periodic variations of the persistent intensity on a time scale of ≈ 40 d. The peak fluxes of PRE bursts also appeared to vary with approximately the same time scale. The residual variation of $F_{\rm pk,PRE}$ for subsets of bursts observed close together in time (once the long-term trend was subtracted) was consistent with the measurement uncertainties, indicating that the intrinsic variation of the peak PRE burst luminosity is $\lesssim 1\%$. We also found a correlation between the fluence and the peak flux, which may arise if a variable fraction of the observed flux is reprocessed by material surrounding the neutron star. One possible site for such reprocessing is the accretion disk. The fraction of reprocessed flux may vary from burst to burst as a result of varying projected area of the disk, through precession of the disk possibly accompanied by radiation-induced warping. That the persistent flux from 4U 1728−34 varies quasi-periodically on a similar time scale to $F_{\rm pk,PRE}$ is qualitatively consistent with such a cause. If interactions with the accretion disk are a significant factor for producing variations in the observed peak flux of PRE bursts, we might expect that the variation would be systematically greater in sources with high inclinations. Indeed, one of the two known high-inclination sources with PRE bursts observed by *RXTE* (MXB 1659−298) has an unusually high fractional standard deviation of 23%, although the other

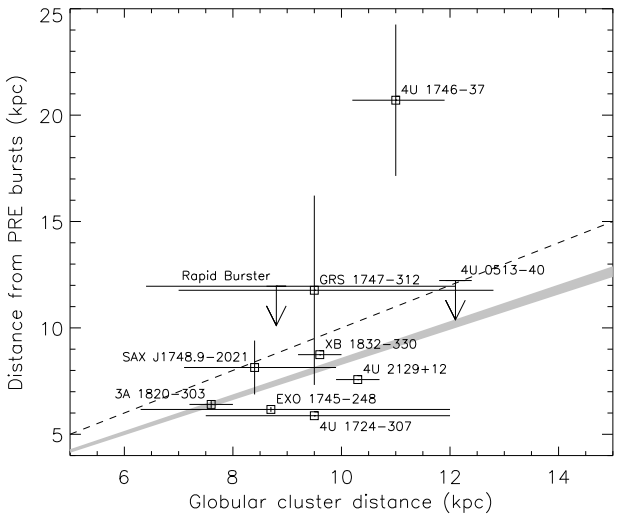

FIG. 24.— Comparison of distances derived from PRE bursts observed by *RXTE* for sources in globular clusters. The distance is calculated from the mean peak flux of the PRE bursts, assuming that the bursts reach $L_{\rm Edd,He}$ ($X = 0$ in equation 5) at the same time the photosphere touches down onto the neutron star. The vertical error bars indicate the standard deviation of the PRE burst peak fluxes. Where only non-PRE bursts were observed, we show upper limits for those sources (Rapid Burster and 4U 0513−40). Error bars indicate the 1σ uncertainties. The dashed line indicates a 1:1 correspondence between the distances, and a deviation below (above) this line indicates that the bursts reach peak fluxes above (below) the expected value for the cluster distance. The grey band shows the equivalent correspondence assuming instead the empirical value for the peak luminosity of the PRE bursts of $(3.79 \pm 0.15) \times 10^{38}$ ergs s^{-1} calculated by Kuulkers et al. (2003).

(4U 1916−053) has a standard deviation consistent with the mean value (see also Kuulkers et al. 2003). It appears that high inclination alone is not sufficient to result in higher-than-average variation of the peak PRE burst fluxes.

We estimated the distances to the sources with PRE bursts by substituting the $F_{\rm Edd}$ values into equation 5. Since the peak flux was typically reached at the end of the PRE episode, when we presume that the photosphere had touched down on the NS surface again (see e.g. Fig. 2), we corrected for gravitational redshift at the surface of a canonical neutron star with $R_{\rm NS} = 10$ km and $M_{\rm NS} = 1.4\ M_\odot$. We also estimated the upper limits to the distance for sources without PRE bursts, from the maximum peak flux of the non-PRE bursts. We made no correction for the apparently super-Eddington luminosity of bursts from 4U 2129+12 and 4U 1724−307, or the apparently sub-Eddington luminosity of bursts from 4U 1746−37 and GRS 1747−312. We did however calculate the distance to 4U 1636−536 in Table 6 in a different manner to the other sources with PRE bursts. The listed $\langle F_{\rm pk} \rangle$ is for the high peak flux ($> 50 \times 10^{-9}$ ergs cm^{-2} s^{-1}) PRE bursts, and we used this value to calculate the distance assuming that those bursts reach $L_{\rm Edd,He}$ (fifth column). For the distance estimates in columns 4 and 6, with $X = 0.7$, we used only the two PRE bursts with much lower peak fluxes. The two distances are consistent. The distances and limits are also shown in Table 6.

The globular cluster sources serve to verify the calibration of the PRE burst distance scale, since the distances can be determined independently of the bursts. Kuulkers et al. (2003) used a somewhat different approach, using the known cluster distances to test the hypothesis that peak PRE burst fluxes measured by several instruments (including *RXTE*) were consistent with the Eddington limit. Those authors concluded that the PRE bursts in the majority of globular cluster sources reached peak fluxes consistent with, or slightly higher than, the expected range of the Eddington limit, and derived a mean empirical Eddington luminosity of $(3.79 \pm 0.15) \times 10^{38}$ ergs s^{-1}. The sample of bursts studied by Kuulkers et al. (2003) includes a subset of the bursts we consider here, including the "giant" bursts from 4U 1724−307, 4U 2129+12, and the super-Eddington bursts from EXO 1745−248. In Fig. 24 we compare the distances calculated assuming that the bursts reached the Eddington limit for pure He fuel, $L_{\rm Edd,He}$, with the distances to the host globular clusters calculated by Kuulkers et al. (2003). The choice of $L_{\rm Edd,He}$ as opposed to the (lower) limit for H-rich material $L_{\rm Edd,H}$ is motivated primarily by the large empirical values measured by various authors, but is also consistent with our assumption that most PRE bursts reach $L_{\rm Edd,He}$. We found substantial deviations both above and below the line of equality, primarily due to the different classes of bursts present in this sample.

4.5. *Millisecond oscillations*

We searched 466 bursts for oscillations, and detected oscillations from 183 in this manner; fewer than 10 should be spurious detections of noise signals according to our selection criteria. Our analyses led to the discovery of 267 Hz burst oscillations in 4U 1916−053 (Galloway et al. 2001), as well as 620 Hz oscillations in 4U 1608−52 (Hartman et al. 2006, in preparation). We omitted 8 bursts from our analysis, generally because they lacked data with sufficiently high time resolution to search for oscillations. We also omitted bursts from EXO 0748−676 from our analysis, since the oscillations in that source have only been detected in summed FFTs from many bursts (Villarreal & Strohmayer 2004). The bursts from the vicinity of the Galactic center exhibiting 589 Hz oscillations were originally thought to originate from MXB 1743−29, although we attribute them instead to GRS 1741.9−2853, a newly-discovered source at the time (§A.5; §3.22). The most recent burst oscillation detection was at 530 Hz in A 1744−361 (Bhattacharyya et al. 2006); the *RXTE* sample contains no public bursts from this source.

We list the numbers of bursts with oscillations by source in Table 4. Among individual sources, between 6 and 100% of bursts exhibited oscillations. Two of the millisecond pulsars with bursts (SAX J1808.4−3658 and XTE J1814−314) exhibited oscillations in every burst detected; excluding these two, the next most frequent burst oscillation source was 4U 1702−429, with 72% of bursts exhibiting oscillations.

We have previously explored the properties of the burst oscillations detected in the *RXTE* sample in detail in a series of papers. The frequencies of the oscillations initially drift by up to 1.2%, but generally reach a stable value on the time scales of seconds (Muno et al. 2002b; see also Strohmayer et al. 1997a). The amount of the

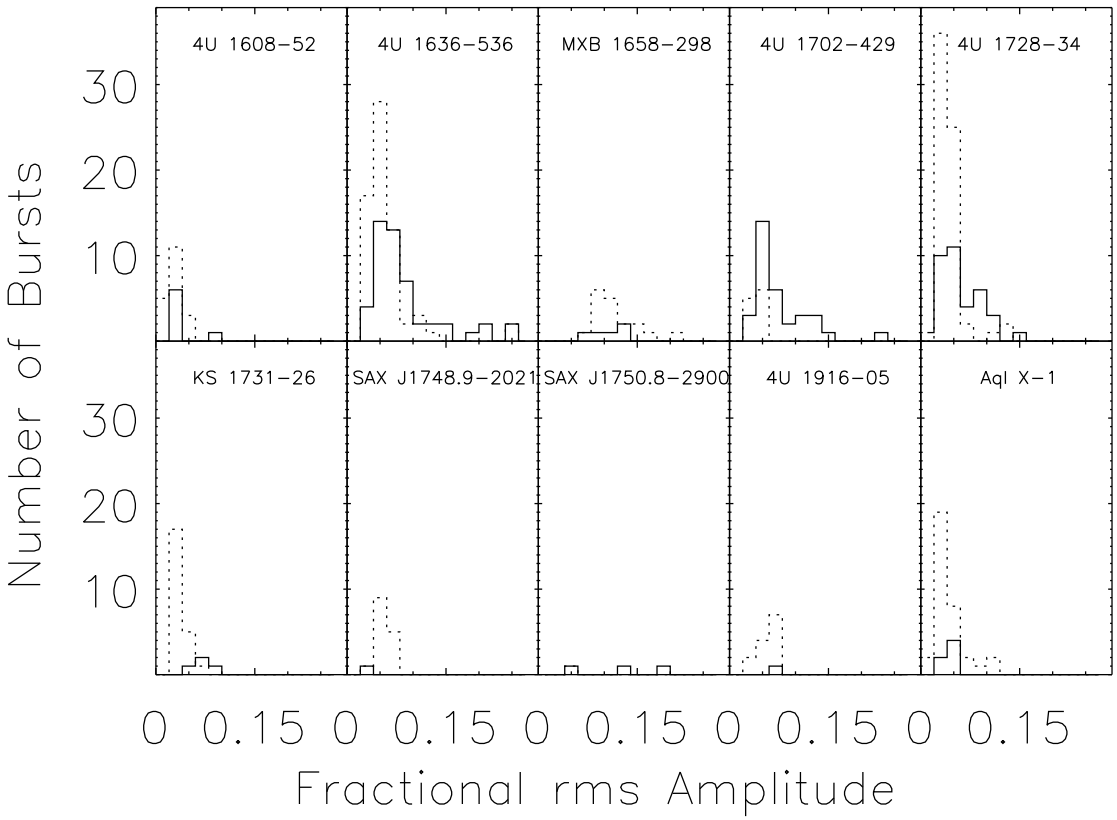

FIG. 25.— Histograms of the largest fractional rms amplitudes of detected oscillations (*solid lines*), and of the upper limits on the rms amplitude in the burst decay when oscillations are not detected (*dotted line*).

frequency drift appears larger when the oscillations are observed earlier in the burst. This suggests that the evolution is triggered by the start of the burst. However, the time scale and magnitude of the frequency evolution does not appear to be correlated with other properties of the burst, such as its decay time scale, peak flux, or fluence. The frequency evolution in about 5% of oscillation trains exhibit anomalous behavior, including decreases in the oscillation frequency at the end of a burst (Strohmayer 1999; Muno et al. 2000), and the appearance of two simultaneous signals separated in frequency by around 1 Hz (Miller 2000; Galloway et al. 2001).

Although the frequency evolution qualitatively appears to saturate according to an exponential function, there is evidence that the mechanism that determines the frequency can be unstable on time scales of both seconds and years. About 30% of the oscillation trains do not exhibit smooth phase and frequency evolution, as both low order polynomials and exponential models are statistically inconsistent with the data (see also Strohmayer 2001). The possible explanations include that (*i*) there are discrete phase jumps that occur on time scales of less than a second; (*ii*) the frequencies of the oscillations shift dramatically on time scales of 0.25 s, or that (*iii*) two signals may be present simultaneously, invalidating our assumption that there is a single signal in our analysis. On longer time scales, the maximum frequencies observed during these oscillation trains exhibit a fractional dispersion of $\Delta\nu_{\rm max}/\langle\nu_{\rm max}\rangle \leq 4\times10^{-3}$. For 5 of the sources studied, this dispersion was consistent with orbital Doppler shifts. However, the dispersion in the maximum frequencies in 4U 1636−536 is uncorrelated with its known orbital period (c.f. Giles et al. 2002). This behavior is quite distinct from the oscillations observed during a superburst in that source, which drifted in frequency precisely as expected for Doppler shifts resulting from the 3.8 hr orbit (Strohmayer & Markwardt 2002).

In contrast to the relatively smooth frequency evolution, the amplitudes of the oscillations do not evolve in systematic manners as the bursts proceed. We found that large intrinsic variations in the fractional amplitudes cause the oscillations to appear and disappear, but the amplitude maxima are not simply related to the underlying flux in the bursts (Muno et al. 2002a). The only consistent trend is that oscillations are not observed during episodes of photospheric radius expansion; when radius expansion occurs, oscillations are usually only seen in the rise and/or the tail of the burst (see also Strohmayer et al. 1997a; Smith et al. 1997). Oscillation trains that appear continuously from the rise to the tail of the burst occur in bursts without radius expansion in 90% of the bursts studied.

The profiles of the burst oscillations are remarkably sinusoidal, with the notable exception of the pulsar XTE J1814-334 (Strohmayer et al. 2003; see also Watts et al. 2005). In all of the bursts examined, no signals are evident in Fourier transforms of 1 s intervals at 0.5, 1.5, or 2 times the main frequency, with upper limits as low as 5% during the brightest portions of bursts. By summing the pulse profiles for a sample of six sources, we placed upper

limits on the amplitudes of harmonic and half-frequency signals of as low as 0.3% (95% confidence). These upper limits are only 6% of the amplitudes of the strongest signals.

We also examined the energy-resolved pulse profiles the oscillation trains in order to search for Doppler effects from the rapid rotation of the neutron star (Muno et al. 2003). We found that on average (*i*) the amplitudes of the oscillations increase as a function of energy and (*ii*) the pulses observed in the higher energy bands arrive later than those in lower energy bands. However, the magnitude of the energy dependence varies significantly from burst to burst. Averaging groups of bursts from individual sources, we found that fractional rms amplitudes of the oscillations increase as a function of energy by 0.25% keV^{-1} to 0.9% keV^{-1} between $3-20$ keV, and are as large as 20% in the $13-20$ keV band. We also show that the average delays between pulses observed in the high and low energy bands are 0.03–0.12 cycles, or time delays that range from 100–200 μs. Applying our theoretical models, we found that the increase in the pulse amplitude with photon energy can be explained if the cooler regions on the neutron star emit in the lower energy bands, reducing the flux variations there. On the other hand, the Doppler shifts caused by the rapid rotation of the neutron star should cause the hard pulses to precede the soft pulses by about 0.05 cycles (100 μs), in contrast to the observations. This suggests that the photons originating from the stellar surface are reprocessed by a hot corona of electrons before they reach the observer.

The presence of detectable oscillations into the burst tail remains a puzzle. During the burst rise, it is expected that the burning will spread to cover the entire surface of the neutron star, so that subsequent anisotropy in the emission will be small. Nevertheless, oscillations are frequently detectable as much as 10 s after the burst peak. In Table 4 we list the number of bursts with oscillations detected in each part of the lightcurve: rise (R), peak (P) and decay (D). In the 4th column of Table 4 we list the number of bursts for which we detected no oscillations in the 1-s FFTs, but did detect oscillations in the 4-s intervals. Using the above definitions, 51% of the oscillations were detected in the rises of bursts, 48% in the peaks, 74% in the tails, and 10% only in the 4-s FFTs for which the location could not be determined (see Table 4). Even if all the oscillations which were only detected in the 4-s FFTs were actually present only during the burst rise or peak, the most frequent part of the burst in which oscillations were detected remains the burst tail.

In Table 5 we list the properties of the oscillations for individual bursts from each source: where the oscillations occurred, the maximum (Leahy-normalized) power, and the mean % rms. Histograms of the amplitudes of the detected oscillations are displayed by source in Figure 25 (*solid lines*). The rms amplitudes range from 2% to 20%, with a median amplitude of about 5%. When oscillations were not detected, we report the upper limit on the rms amplitude from the first 5 s of the decay in Figure 25 (*dotted lines*). The median values of the upper limits are typically lower than the detected oscillations, which indicates that they are not detected because their amplitudes are lower, and not because of a lack of sensitivity in some of the bursts. In fact, oscillations were almost exclusively observed at high accretion rates ($S_Z > 1.5$ on the color-color diagram), and were not detected at lower accretion rates (Muno et al. 2004).

5. SUMMARY

We have assembled a catalog of 1035 thermonuclear (type-I) bursts observed by *RXTE* from 45 LMXBs. Although this is not the largest sample of bursts accumulated by recent satellite missions, the unparalleled PCA sensitivity offers the best signal-to-noise for precise measurements of burst flux, fluence, time-scales, and energetics. Furthermore, the high timing capability has allowed a detailed comparison of the properties of the bursts and the burst oscillations, where detected. Below we summarize the principal results obtained through our study of this sample.

- We identified bursts in the sample corresponding to all three cases of ignition understood theoretically, as described by Fujimoto et al. (1981). Case 3 bursts arising from H-igition in a H/He environment were observed from EXO 0748−676 in a range of accretion rate $\approx$ 0.5–1% $\dot{M}_{\rm Edd}$. At slightly higher accretion rates ($\approx$ 2–5% $\dot{M}_{\rm Edd}$) we found infrequent, short bursts from SAX J1808.4−3658 arising from He-ignition in an almost pure He enviroment (Case 2). Our analysis of the long bursts from GS 1826−24 confirm that these arise from He-ignition in a H/He environment, where the burst interval is insufficient to completely exhaust the accreted H (Case 1). These observations confirm the theoretical prediction that the boundary between Case 3 and 2 occurs around 1% $\dot{M}_{\rm Edd}$.

- We estimated the mean burst rates for samples of bursts combined from different sources, both as a function of normalized persistent flux γ and position on the color-color diagram S_Z. We measured a peak burst rate at around 0.2–0.3 hr^{-1} at between $\gamma \approx 0.02$ and 0.06 (equivalent to $\approx 10^{37}$ ergs s^{-1}) or $S_Z \simeq 1$. The decrease in burst rate (and increase in α) observed above this luminosity may be evidence for the "delayed mixed burst" regime of Narayan & Heyl (2003).

- The recurrence time measured between burst pairs exhibited large deviations compared to the mean derived burst rate. We found evidence for distinctly different burst behavior as a function of γ/S_Z, particularly for the two sources with the largest number of bursts, 4U 1636−536 and 4U 1728−34. It is possible that 4U 1728−34 accretes primarily He from an evolved donor, while 4U 1636−536 accretes mixed H/He like the majority of LMXBs. At low accretion rates we found significant differences between the rates for bursts arising from H- and He-ignition, but also at accretion rates above $\approx$ 10% $\dot{M}_{\rm Edd}$ the rate for certain sources was an order of magnitude larger than that inferred for the combined population. It is clear that combined burst samples from different sources must be viewed with caution.

- The mean α-values reached a minimum of ~ 100 in the γ/S_Z range where the burst rate peaked,

between $\gamma = 0.03$ and 0.06 or $S_Z \simeq 1$. As with the mean burst rates, α measurements for individual bursts deviated significantly from the mean behavior. We again found significantly different behaviour for 4U 1636−536 and 4U 1728−34, further evidence for the different compositions of the accreted material in those two sources.

- We compared the variation of the burst time scale as a function of γ/S_Z separately for the PRE and non-PRE bursts. The strong anticorrelation between τ and γ noted by van Paradijs et al. (1988a) was only found for the PRE bursts observed by *RXTE*, and appears to be primarily the result of a correlation between γ and the normalized burst fluence U_b. Conversely, the τ values for most of the non-PRE bursts were significantly anticorrelated with S_Z, while no relationship was found between the same pair of parameters for the PRE bursts. As expected from time-dependent ignition models, the timescale τ is anticorrelated with the measured α, and in particular all bursts with $\tau < 10$ had $\alpha > 70$ (indicating He-rich fuel), while the majority of bursts with $\tau > 10$ had $\alpha \approx 40$ (H-rich).

- We found evidence for two distinct types of burst pairs with short ($\lesssim$ 30 min) recurrence times; the first, corresponding to the "classical" double burst with a much weaker second burst following the first by $\lesssim$ 15 min, and the second, with bursts having much more even fluences. Short-recurrence time burst pairs immediately following each other — that is, trains of three or four bursts all with $\Delta t \lesssim 30$ min — made up a significant fraction of these groups. The regular double bursts from 4U 1323−62 suggest that the fuel for the smaller, secondary bursts comes primarily from $\approx 8\%$ of the fuel accumulated prior to the larger, initial burst, which is left unburnt.

- We found significant variations in the peak flux of photospheric radius-expansion bursts from most sources with more than one such burst. Most of the variation can be attributed to four apparently distinct classes of PRE bursts; faint symmetric bursts, reaching significantly sub-Eddington luminosities in 4U 1746−37 and GRS 1747−312; hydrogen-limited bursts in 4U 1636−536; helium limited bursts, comprising the largest group of PRE bursts; and "giant" bursts reaching fluxes in excess of the Eddington limit, typically the most energetic bursts from each source. Because the globular cluster sources exhibit both the faintest and brightest PRE bursts, the distances derived from the peak burst flux may either over- or under-estimate the source distance.

- We analysed all the public bursts from the sources with known oscillations and characterised them based on the peak rms and where in the burst the oscillations are present. Oscillations were equally likely ($\approx$ 50% of bursts) in the rise and peak, but found in almost 75% of the burst tails. The rms amplitudes were between 2 and 20%, with a median of around 5%. We identified the likely source of the 589 Hz oscillations originally detected in bursts from the Galactic center region as GRS 1741.9−2853, based on the localization of those bursts within the *RXTE* field of view and comparisons of the burst properties with bursts detected by other satellites.

This research has made use of data obtained through the High Energy Astrophysics Science Archive Research Center Online Service, provided by the NASA/Goddard Space Flight Center. This work was supported in part by the NASA Long Term Space Astrophysics program under grant NAG 5-9184 (PI: Chakrabarty).

APPENDIX

DETERMINING THE ORIGIN OF BURSTS

The mechanical collimators on each of the PCUs aboard *RXTE* admit photons over a relatively large field of view ($\approx 1^\circ$ radius). The collimator response decreases approximately $\propto 1/\Delta\theta$, where $\Delta\theta$ is the angle between the source position and the nominal pointing direction, in degrees. The wide field of view means that correctly attributing bursts to sources in crowded fields (particularly the Galactic center) is problematic.

Where bursts were observed in fields containing multiple sources, we attempted to match the bursts with the known characteristics of individual sources (see Table A7). We also exploited the fact that the 5 PCUs are not perfectly aligned. As a result, the ratio of observed count rates in each PCU depends upon the position of the source within the field of view. From the modeled collimator responses for each PCU we have deduced the most probable origin for each burst. We first determined an interval covering the burst over which the count rate was greater than $\approx 10\%$ of the maximum (neglecting the pre-burst persistent emission), and accumulated all the counts observed in each PCU over this interval. We then stepped over a grid of positions covering the field of view and performed a linear fit to test the hypothesis that the variations in the PCU-to-PCU total count rates arose solely from differences in the collimator responses at each position. Although we used the same set of collimator responses over all gain epochs, we renormalised the responses based on observed count rates for Crab observations close in time to each burst. We then identified the source at which position we found the minimum goodness of fit statistic (χ^2) as the most probable origin of the burst.

Naturally, this calculation can most easily distinguish between sources which are widely separated in the field of view. For more crowded fields, we may only be able to narrow down the possible origin as one of a few nearby sources. While this method works best for very bright bursts, where we observe only faint bursts (whether intrinsically faint or originating from sources that are far off-axis), we can combine counts from multiple bursts, so long as the pointing and spacecraft orientation is consistent, to improve the localization.

TABLE A7
Type-I X-ray bursters towards the Galactic center

Source	Alt. name	RA	Dec	Peak burst flux (10^{-9} ergs cm^{-2} s^{-1})	Energy range	PRE	Ref.
KS 1741−293	AX J1744.8-2921	17 44 49.20	-29 21 6	14 ± 3	2–30 keV	single peak	[1]
GRS 1741.9−2853	AX J1745.0−2855	17 45 0.56	-28 54 6.5	17 ± 2 31 ± 2	3–28 keV	N Y	[2]
1A 1742−289	AX J1745.6−2901	17 45 37.0	-29 1 6	9.2 ± 0.8	bolometric	N	[3]
2E 1742.9−2929	GC X-1/1A 1742−293/4	17 46 6.2	-29 31 5	13 ± 5[b] 38 ± 3	3–20 keV	N? Y?	[4]
SAX J1747.0−2853	GX +0.2,−0.2	17 47 2.60	-28 52 58.9[a]	22^{+6}_{-8} 31.8 ± 2.7	bolometric bolometric	N Y	[5] [6]
SLX 1744−299	AX J1747.4−3000	17 47 25.9	-29 59 58	25	3–20 keV		[7]
SLX 1744−300	AX J1747.4−3003	17 47 25.9	-30 2 30	35 ± 5	2–30 keV		[8]
SAX J1750.8−2900	AX J1750.5−2900	17 50 24.0	-29 2 18	39 ± 11[c]	2–26 keV	single peaks	[9]
SAX J1752.3−3138		17 52 24	-31 37 42	23 ± 10	2–19 keV	Y	[10]

Note. — References. 1. in 't Zand et al. (1991); 2. Cocchi et al. (1999); 3. Maeda et al. (1996); 4. Lutovinov et al. (2001); 5. Sidoli et al. (1998); 6. Natalucci et al. (2000); 7. Pavlinsky et al. (1994); 8. Patterson et al. (1989); 9. Natalucci et al. (1999); 10. (Cocchi et al. 2001b)

[a]Revised position from *Chandra* observation of Wijnands et al. (2002a)
[b]Weighted mean and standard deviation of peak flux from 19 fainter bursts (mean 2–60 keV flux $\lesssim 5.8 \times 10^{-9}$ ergs cm^{-2} s^{-1})
[c]Mean and standard deviation of peak flux from 7 bursts which were not affected by atmospheric attenuation

Once the burst origin was identified with confidence, for bursts observed $\gtrsim 0.^\circ 1$ off-axis we scaled the measured burst flux and fluence by the ratio of the collimator response (averaged over those PCUs that were operating) at the aimpoint, to the response at the source location.

Below we describe close pairs of bursting sources, and the attribution of bursts in each case. Where a burst from an observation centered on one source is later attributed to another, we flag that burst as uncertain in origin in Table 2.

4U 1728−34 and the Rapid burster ($\Delta\theta = 0.^\circ 56$)

4U 1728−34 is one of the most prolific bursters (see §4.4), and also produces a large proportion of PRE bursts (Galloway et al. 2003). The Rapid Burster, on the other hand, tends to produce preferentially non-PRE thermonuclear bursts (Fox et al. 2001), in addition to the much more frequent type-II bursts (e.g. Lewin et al. 1993). The peak fluxes of the majority of bursts observed in the 4U 1728−34 field were bimodally distributed, with non-PRE bursts peaking at around 4×10^{-8} ergs cm^{-2} s^{-1} on average, and PRE bursts peaking at 9×10^{-8} ergs cm^{-2} s^{-1}. We also observed six bursts with peak fluxes around 5×10^{-9} ergs cm^{-2} s^{-1} and no evidence of PRE, each close to the time of one of the semi-regular transient Rapid Burster outbursts. Four of these bursts (on 1996 May 3 13:56:30, 13:57:49, 13:59:15 and 14:00:16 UT; obsid #10410-01-01-00) had no evidence of decreasing blackbody temperature with time, and also exhibited recurrence times much shorter than expected for thermonuclear bursts (~ 100 s). Thus, we identified these as type-II bursts from the Rapid Burster. The other two bursts (on 2001 May 27 09:15:59 and May 29 09:05:57 UT) did, however, show weak evidence of cooling. The first of these bursts was consistent with an origin at either 4U 1728−34 or the Rapid Burster, but the second was consistent with an origin only at the latter source (4U 1728−34 was excluded at the $> 5\sigma$ level). Based on this evidence, and the similar long $\tau \approx 11$ s for these bursts, we identified them as type-I bursts from the Rapid Burster.

The majority of the bursts observed in the field centered on the Rapid Burster, on the other hand, peaked at $\approx 1 \times 10^{-8}$ ergs cm^{-2} s^{-1} with relatively long rise times ($\gtrsim 2$ s) and time scales ($\gtrsim 10$). At least 13 bursts were notable exceptions, with profiles much more similar to bursts from 4U 1728−34. The Rapid Burster was excluded as an origin for these bursts at (typically) the 3–5σ level. Thus, we attribute these bursts to 4U 1728−34, instead. We note that the corrected peak fluxes were similar to the other bursts observed from 4U 1728−34.

SAX J1750.8−2900 and SAX J1747.0−2853 ($\Delta\theta = 0.^\circ 750$)

Four bursts were observed in the field of SAX J1750.8−2900 (see §3.30) and SAX J1747.0−2853 (see §3.24) by *RXTE*, all during the rise to the second peak of the SAX J1750.8−2900 outburst. Three of the bursts reached apparent peak fluxes of $\approx 5.5 \times 10^{-8}$ ergs cm^{-2} s^{-1}, and two of those exhibited PRE, while the fourth reached just 9×10^{-9} ergs cm^{-2} s^{-1}. The three bright bursts exhibited count rate variations between the PCUs inconsistent to a high level of confidence with an origin at SAX J1747.0−2853; furthermore, their corrected peak fluxes (assuming they arose instead from that source) would also be inconsistent with the distance to the Galactic center. While the origin of the faint burst cannot be constrained within the 1° field of view, if it originated from SAX J1747.0−2853 the corrected peak flux would be a factor of two larger than that of bursts observed previously from the source (Table A7). Thus, we attribute all these bursts to SAX J1750.8−2900 (see also Kaaret et al. 2002).

Aql X-1 and 1A 1905+00 ($\Delta\theta = 0.^\circ 82$)

Bursts from 1A 1905+00 were discovered by *SAS-3* (Lewin et al. 1976e), and were attributed to a previously known persistent source (Seward et al. 1976). The apparent burst recurrence time was 8.9 hr; one long radius-expansion

burst was observed in a 17 hr observation by *EXOSAT* (Chevalier & Ilovaisky 1990), with a peak flux of $(2.4 \pm 0.2) \times 10^{-8}$ ergs cm^{-2} s^{-1}. We found three bursts from observations towards 1A 1905+00 (on 1996 July 24 08:56:40, July 24 09:07:18 and 2002 February 15 22:56:28 UT), with peak fluxes 0.8–1.0 $\times 10^{-8}$ ergs cm^{-2} s^{-1}. All three bursts were observed during periods of transient activity by Aql X-1. The corrected peak fluxes for these three bursts (assuming they originated from Aql X-1) were consistent with those of other bursts from that source. Furthermore, the most probable origin for two of the three bursts (given the variations in count rate between the PCUs) were within $< 0.^\circ1$ of Aql X-1, although we can formally exclude an origin at 1A 1905+00 at only the 2.5–3.1σ confidence level. For the third burst, the most probable origin is within $0.^\circ25$ of Aql X-1, and we can exclude 1A 1905+00 at only the 1.8σ level. Given the lack of evidence of bursting behaviour from the latter source during the *RXTE* observations, we attribute all three to Aql X-1.

Galactic center fields

Observations towards the Galactic center were categorized based on the pointing direction into 10 (generally overlapping) fields, with pointing directions separated by $> 0.^\circ1$. Below we describe the fields for which bursts were observed, and which sources we attribute them to.

Galactic center field 1

This field, centered on $\alpha = 17^{\rm h}44^{\rm m}02.6$, $\delta = -29^\circ43'26''$ (J2000.0), includes the known burst sources KS 1741−293 ($\Delta\theta = 0.^\circ41$ from the center of the field), 2E 1742.9−2929 ($\Delta\theta = 0.^\circ49$), 1A 1742−289 ($\Delta\theta = 0.^\circ78$), SLX 1744−299/300 ($\Delta\theta = 0.^\circ80$), and GRS 1741.9−2853 ($\Delta\theta = 0.^\circ85$), as well as the Bursting Pulsar GRO J1744−28 at the edge of the field ($\Delta\theta = 0.^\circ99$). We observed 13 bursts with most of the peak fluxes below 1×10^{-8} ergs cm^{-2} s^{-1}. Six of the faint bursts observed in 1997, on Feb 26 01:12:24, Feb 27 01:21:04 and 21:25:59, Mar 21 20:13:01, Mar 23 12:15:07 and Mar 25 17:32:13, had roughly symmetric profiles and no evidence of a temperature decrease in the burst tail (although the first three were affected by data gaps following the peak). The ratio of the integrated count rate in different PCUs indicates that the best candidate for the burst origin was GRO J1744−28; we note also that the bursts were coincident with the second outburst observed by *RXTE* from this source, beginning around December 1996. The burst profiles were similar to other type-II bursts observed previously from that source (Giles et al. 1996). Thus, we attributed all six to GRO J1744−28. Of the two brighter bursts, one (on 1997 March 21 20:07:28 UT) exhibited two distinct peaks at 1×10^{-8} ergs cm^{-2} s^{-1}, separated by ≈ 3 s, while the other (on 1997 Mar 20 17:07:16 UT) featured strong PRE and peaked at 2.3×10^{-8} ergs cm^{-2} s^{-1}. Both of these bursts were consistent with an origin at 2E 1742.9−2929 ($\approx 0.6\sigma$), with the next best candidates inconsistent at the 2–3σ level. Two more bursts (on 1997 Apr 19 23:52:43 and 1997 Apr 21 00:13:27 UT) were also consistent with an origin at this source, although we cannot rule out other sources (KS 1741−293, 1A 1742−289) at quite as high confidence due to the lower flux of these bursts.

The remaining three bursts were all consistent with an origin at SLX 1744−299/300 (see §3.25), which was close to the edge of the field, and we can rule out the alternatives at between 2.5–5.4σ confidence. SLX 1744−299 has previously exhibited at least one very bright, long burst, with exponential decay time 43.3 s (Table A7), while the three bursts detected by *RXTE* were all much shorter, with decay times of 3–5 s. Thus, we attribute the bursts to SLX 1744−300, although it is possible they actually originated from SLX 1744−299.

Galactic center field 3

Centered approximately on the position of SAX J1747.0−2853 ($\Delta\theta = 0.^\circ02$), GC field 3 also includes the bursters 1A 1742−289 ($\Delta\theta = 0.^\circ36$), GRS 1741.9−2853 ($\Delta\theta = 0.^\circ47$), 2E 1742.9−2929 ($\Delta\theta = 0.^\circ68$), KS 1741−293 ($\Delta\theta = 0.^\circ69$), and SAX J1750.8−2900 ($\Delta\theta = 0.^\circ73$), as well as the Bursting Pulsar GRO J1744−28 ($\Delta\theta = 0.^\circ59$). We found four faint ($F_{\rm pk} < 5 \times 10^{-9}$ ergs cm^{-2} s^{-1}) bursts in observations of this field, on 2000 Mar 12 06:22:25 and 2001 Oct 8 13:06:03, 17:32:56 and 17:51:14 UT. While these bursts exhibited variations between the count rates for each PCU consistent with an origin in a number of sources, their low peak fluxes and long time scales suggest the most likely origin was 2E 1742.9−2929. Thus, we attribute them to that source.

Galactic center field 10

This field, centered on $\alpha = 17^{\rm h}45^{\rm m}12.0$, $\delta = -28^\circ48'18''$ (J2000.0), includes the burst sources GRS 1741.9−2853 ($\Delta\theta = 0.^\circ11$), 1A 1742−289 ($\Delta\theta = 0.^\circ23$), SAX J1747.0−2853 ($\Delta\theta = 0.^\circ41$), KS 1741−293 ($\Delta\theta = 0.^\circ55$), and 2E 1742.9−2929 ($\Delta\theta = 0.^\circ74$), as well as the Bursting Pulsar GRO J1744−28 ($\Delta\theta = 0.^\circ16$). This field was observed intensely for 355 ks between 2001 September 26 and 2001 October 6.

We found 80 bursts from these observations, with three-quarters of the bursts reaching apparent peak fluxes $< 10^{-8}$ ergs cm^{-2} s^{-1}. For these faint bursts the mean $\tau = 25 \pm 11$ s, and the median delay time was 2.6 hr. These properties, once the off-axis angle is taken into account, suggest that the bursts arose from 2E 1742.9−294 (aka 1A 1742−294; Lutovinov et al. 2001). While the ratio of count rates from different PCUs were not particularly constraining in determining the bursts location, due to their faintness, only 6 bursts were inconsistent with an origin in 2E 1742.9−294, and then only at the 3–5σ level.

Several of the brighter bursts exhibited PRE, often with a pronounced double-peaked structure in the bolometric flux. Variations in the count rates in different PCUs could not distinguish between a number of closely-spaced sources as origins for these bursts. However, all the bursts were observed over a short time interval, between 2001 September 26–29 and October 3–6. The only source in the field of view which was active around this time was SAX J1747.0−2853

(Wijnands et al. 2002a), from which bursts were also observed during 2001 September by *BeppoSAX* (Werner et al. 2004). Thus, we attribute the bright bursts from this field to that source.

GRO J1744−28

We found 19 type-I (thermonuclear) bursts in observations of the field of the "Bursting Pulsar", GRO J1744−28, which also includes the sources KS 1741−293 ($\Delta\theta = 0.^\circ62$), 1A 1742−289 ($\Delta\theta = 0.^\circ36$), 2E 1742.9−2929 ($\Delta\theta = 0.^\circ85$), SAX J1747.0−2853 ($\Delta\theta = 0.^\circ56$), XTE J1739−285 ($\Delta\theta = 1.^\circ05$) and GRS 1741.9−2853 ($\Delta\theta = 0.^\circ19$). These bursts were comparatively easily distinguished from the much more frequent type-II bursts from GRO J1744−28 by the fast rise and exponential decay profile, as well as the detection of falling blackbody temperature in the burst tail. GRO J1744−28 is not known to exhibit thermonuclear bursts, and all the type-I bursts we observe from the field we attribute to nearby sources.

Eleven of the bursts had low measured peak fluxes of $\lesssim 5 \times 10^{-9}$ ergs cm^{-2} s^{-1}, and long time scales. Each of these bursts were consistent with an origin at 2E 1742.9−2929, although only for the brighter bursts could we exclude other sources in the field. We attributed all the faint bursts to that source.

Millisecond oscillations at 589 Hz were previously detected in three of the eight brighter bursts from the field, on 1996 May 15 19:32:23, Jun 4 14:41:12 and Jun 19 09:55:44 UT (Strohmayer et al. 1997a). These bursts were attributed by the latter authors to MXB 1743−29, which is in turn thought to be identified with either KS 1741−293 or 1A 1742−289. Another candidate source which was not considered at the time is GRS 1741.9−2853 (see §3.22). We could only conclusively exclude KS 1741−293 or 1A 1742−289 as the origin for one of the 8 bursts, on 1996 Jul 8 01:57:47 UT. Since the *BeppoSAX* observations indicate bursting activity shortly after the bursts observed by *RXTE*, and the scaled peak fluxes for the bursts assuming an origin in GRS 1741.9−2853 are consistent with those observed by *BeppoSAX* (Cocchi et al. 1999), we assume that source as the origin.

REFERENCES

Agrawal, V. K., Sreekumar, P., Seetha, S., & Agrawal, P. C. 2001, Bulletin of the Astronomical Society of India, 29, 361

Anders, E. & Ebihara, M. 1982, Geochim. Cosmochim. Acta, 46, 2363

Anderson, S. F., Margon, B., Deutsch, E. W., Downes, R. A., & Allen, R. G. 1997, ApJ, 482, L69

Aoki, T., Dotani, T., Ebisawa, K., Itoh, M., Makino, F., Nagase, F., Takeshima, T., Mihara, T., & Kitamoto, S. 1992, PASJ, 44, 641

Auriere, M., Le Fevre, O., & Terzan, A. 1984, A&A, 138, 415

Ayasli, S. & Joss, P. C. 1982, ApJ, 256, 637

Bałucińska-Church, M., Church, M. J., Oosterbroek, T., Segreto, A., Morley, R., & Parmar, A. N. 1999, A&A, 349, 495

Bałucińska-Church, M., Church, M. J., & Smale, A. P. 2004, MNRAS, 347, 334

Bandyopadhyay, R. M., Charles, P. A., Shahbaz, T., & Wagner, R. M. 2002, ApJ, 570, 793

Barnard, R., Balucińska-Church, M., Smale, A. P., & Church, M. J. 2001, A&A, 380, 494

Barret, D., Motch, C., & Pietsch, W. 1995, A&A, 303, 526

Basinska, E. M., Lewin, W. H. G., Sztajno, M., Cominsky, L. R., & Marshall, F. J. 1984, ApJ, 281, 337

Bazzano, A., Cocchi, M., Ubertini, P., Heise, J., in 't Zand, J., & Muller, J. M. 1997, IAU Circ., 6668

Becker, R. H., Pravdo, S. H., Serlemitsos, P. J., Swank, J. H., & Hoffman, J. 1976, IAU Circ., 2953

Becker, R. H., W., S. B., H., S. J., Boldt, E. A., Holt, S. S., Pravdo, S. H., & Serlemitsos, P. J. 1977, ApJ, 216, L101

Belian, R. D., Conner, J. P., & Evans, W. D. 1972, ApJ, 171, L87

—. 1976, ApJ, 206, L135

Belloni, T., Hasinger, G., Pietsch, W., Mereghetti, S., Bignami, G. F., & Caraveo, P. 1993, A&A, 271, 487

Bhattacharyya, S. & Strohmayer, T. E. 2006, ApJ, 636, L121

Bhattacharyya, S., Strohmayer, T. E., Markwardt, C. B., & Swank, J. H. 2006, ApJ, in press, 639

Bildsten, L. 1998, in The Many Faces of Neutron Stars, ed. R. Buccheri, J. van Paradijs, & A. Alpar (Dordrecht: Kluwer), 419

Bildsten, L. 2000, in Cosmic Explosions, the 10th Annual October Astrophysics Conference, Maryland, October 11–13 1999, AIP Conf. 522, ed. S. Holt & W. Zhang (Woodbury NY: AIP), 359–369

Bloser, P. F., Grindlay, J. E., Kaaret, P., Zhang, W., Smale, A. P., & Barret, D. 2000, ApJ, 542, 1000

Bonnet-Bidaud, J. M., Haberl, F., Ferrando, P., Bennie, P. J., & Kendziorra, E. 2001, A&A, 365, L282

Bowyer, S., Byram, E. T., Chubb, T. A., & Friedman, H. 1965, Science, 147, 394

Bradt, H., Naranan, S., Rappaport, S., & Spada, G. 1968, ApJ, 152, 1005

Brandt, S., Castro-Tirado, A. J., Lund, N., Dremin, V., Lapshov, I., & Syunyaev, R. 1992, A&A, 262, L15

Callanan, P. J., Curran, P., Filippenko, A. V., Garcia, M. R., Margon, B., Deutsch, E., Anderson, S., Homer, L., & Fender, R. P. 2002, ApJ, 574, L143

Chakrabarty, D. & Morgan, E. H. 1998, Nature, 394, 346

Chakrabarty, D., Morgan, E. H., Muno, M. P., Galloway, D. K., Wijnands, R., van der Klis, M., & Markwardt, C. B. 2003, Nature, 424, 42

Charles, P. A., Clarkson, W. I., & van Zyl, L. 2002, New Astronomy, 7, 21

Charles, P. A., Jones, D. C., & Naylor, T. 1986, Nature, 323, 417

Chelovekov, I. V., Lutovinov, A. A., Grebenev, S. A., & Sunyaev, R. A. 2005, Astronomy Letters, 31, 681

Chevalier, C. & Ilovaisky, S. A. 1987, A&A, 172, 167

—. 1990, A&A, 228, 115

—. 1991, A&A, 251, L11

Chou, Y. & Grindlay, J. E. 2001, ApJ, 563, 934

Christian, D. J. & Swank, J. H. 1997, ApJS, 109, 177

Clark, G. & Li, F. 1977, IAU Circ., 3092

Clark, G. W., Jernigan, J. G., Bradt, H., Canizares, C., Lewin, W. H. G., Li, F. K., Mayer, W., McClintock, J., & Schnopper, H. 1976, ApJ, 207, L105

Clark, G. W., Li, F. K., Canizares, C., Hayakawa, S., Jernigan, G., & Lewin, W. H. G. 1977, MNRAS, 179, 651

Clark, G. W., Markert, T. H., & Li, F. K. 1975, ApJ, 199, L93

Cocchi, M., Bazzano, A., Natalucci, L., Ubertini, P., Heise, J., & in 't Zand, J. J. M. 2001a, Memorie della Societa Astronomica Italiana, 72, 757

Cocchi, M., Bazzano, A., Natalucci, L., Ubertini, P., Heise, J., Kuulkers, E., Cornelisse, R., & in 't Zand, J. J. M. 2001b, A&A, 378, L37

Cocchi, M., Bazzano, A., Natalucci, L., Ubertini, P., Heise, J., Muller, J. M., & in 't Zand, J. J. M. 1999, A&A, 346, L45

Cocchi, M., Bazzano, A., Natalucci, L., Ubertini, P., Heise, J., Muller, J. M., Smith, M. J. S., & in 't Zand, J. J. M. 1998, ApJ, 508, L163

Cominsky, L., Jones, C., Forman, W., & Tananbaum, H. 1978, ApJ, 224, 46

Cominsky, L. R. & Wood, K. S. 1984, ApJ, 283, 765

Corbet, R. H. D., Thorstensen, J. R., Charles, P. A., Menzies, J. W., Naylor, T., & Smale, A. P. 1986, MNRAS, 222, 15

Cornelisse, R., Heise, J., Kuulkers, E., Verbunt, F., & in 't Zand, J. J. M. 2000, A&A, 357, L21

Cornelisse, R., in 't Zand, J. J. M., Verbunt, F., Kuulkers, E., Heise, J., den Hartog, P. R., Cocchi, M., Natalucci, L., Bazzano, A., & Ubertini, P. 2003, A&A, 405, 1033
Cornelisse, R., Kuulkers, E., in 't Zand, J. J. M., Verbunt, F., & Heise, J. 2002a, A&A, 382, 174
Cornelisse, R., Verbunt, F., in 't Zand, J. J. M., Kuulkers, E., Heise, J., Remillard, R. A., Cocchi, M., Natalucci, L., Bazzano, A., & Ubertini, P. 2002b, A&A, 392, 885
Cottam, J., Kahn, S. M., Brinkman, A. C., den Herder, J. W., & Erd, C. 2001, A&A, 365, L277
Cottam, J., Paerels, F., & Mendez, M. 2002, Nature, 420, 51
Courvoisier, T. J. ., Parmar, A. N., Peacock, A., & Pakull, M. 1986, ApJ, 309, 265
Cowley, A. P., Crampton, D., & Hutchings, J. B. 1979, ApJ, 231, 539
Crampton, D., Stauffer, J., Hutchings, J. B., Cowley, A. P., & Ianna, P. 1986, ApJ, 306, 599
Cumming, A. 2003, ApJ, 595, 1077
Cumming, A. 2004, in Proceedings of the 2nd BeppoSAX Conference: "The Restless High-Energy Universe", Amsterdam, 5–9 May 2003, ed. E. P. J. van den Heuvel, R. A. M. J. Wijers, & J. J. M. in 't Zand, Vol. 132, 435–445
Cumming, A. & Bildsten, L. 2000, ApJ, 544, 453
Cumming, A., Macbeth, J., in 't Zand, J. J. M., & Page, D. 2005, ApJ, submitted (astro-ph/0508432)
Cumming, A., Morsink, S. M., Bildsten, L., Friedman, J. L., & Holz, D. E. 2002, ApJ, 564, 343
Damen, E., Magnier, E., Lewin, W. H. G., Tan, J., Penninx, W., & van Paradijs, J. 1990, A&A, 237, 103
Davidsen, A. 1975, IAU Circ., 2824
den Hartog, P. R., in 't Zand, J. J. M., Kuulkers, E., Cornelisse, R., Heise, J., Bazzano, A., Cocchi, M., Natalucci, L., & Ubertini, P. 2003, A&A, 400, 633
Deutsch, E. W., Margon, B., & Anderson, S. F. 2000, ApJ, 530, L21
Deutsch, E. W., Margon, B., Anderson, S. F., Wachter, S., & Goss, W. M. 1999, ApJ, 524, 406
Dieters, S. W. & van der Klis, M. 2000, MNRAS, 311, 201
Dotani, T., Inoue, H., Murakami, T., Nagase, F., & Tanaka, Y. 1990, Nature, 347, 534
Doxsey, R. 1975, IAU Circ., 2820
Doxsey, R., Bradt, H., Johnston, M., Griffiths, R., Leach, R., Schwartz, D., Schwarz, J., & Grindlay, J. 1979, ApJ, 228, L67
Ebisuzaki, T. 1987, PASJ, 39, 287
Emelyanov, A. N., Aref'ev, V. A., Churazov, E. M., Gilfanov, M. R., & Sunyaev, R. A. 2001, Astronomy Letters, 27, 781
Fabbiano, G., Gursky, H., Schwartz, D. A., Schwarz, J., Bradt, H. V., & Doxsey, R. E. 1978, ApJ, 221, L49
Ford, E. C., van der Klis, M., & Kaaret, P. 1998, ApJ, 498, L41
Forman, W. & Jones, C. 1976, ApJ, 207, L177
Forman, W., Jones, C., Cominsky, L., Julien, P., Murray, S., Peters, G., Tananbaum, H., & Giacconi, R. 1978, ApJS, 38, 357
Forman, W., Jones, C., & Tananbaum, H. 1976a, ApJ, 207, L25
Forman, W., Tananbaum, H., & Jones, C. 1976b, ApJ, 206, L29
Fox, D. B. 2005, The Astronomer's Telegram, 526
Fox, D. W., Lewin, W. H. G., Rutledge, R. E., Morgan, E. H., Guerriero, R., Bildsten, L., van der Klis, M., van Paradijs, J., Moore, C. B., Dotani, T., & Asai, K. 2001, MNRAS, 321, 776
Franco, L. M. 2001, ApJ, 554, 340
Friedman, H., Byram, E. T., & Chubb, T. A. 1967, Science, 156, 374
Fujimoto, M. Y. & Gottwald, M. 1989, MNRAS, 236, 545
Fujimoto, M. Y., Hanawa, T., & Miyaji, S. 1981, ApJ, 247, 267
Fujimoto, M. Y., Sztajno, M., Lewin, W. H. G., & van Paradijs, J. 1987, ApJ, 319, 902
Fushiki, I. & Lamb, D. Q. 1987, ApJ, 323, L55
Galloway, D. K., Chakrabarty, D., Cumming, A., Kuulkers, E., Bildsten, L., & Rothschild, R. 2004a, in X-ray Timing 2003: Rossi and Beyond, ed. P. Kaaret, F. K. Lamb, & J. H. Swank (Melville, NY: AIP)
Galloway, D. K., Chakrabarty, D., Muno, M. P., & Savov, P. 2001, ApJ, 549, L85
Galloway, D. K. & Cumming, A. 2006, ApJ, accepted (astro-ph/0607213)
Galloway, D. K., Cumming, A., Kuulkers, E., Bildsten, L., Chakrabarty, D., & Rothschild, R. E. 2004b, ApJ, 601, 466
Galloway, D. K., Morgan, E. H., Kaaret, P., Chakrabarty, D., & Suzuki, M. 2005, The Astronomer's Telegram, 657
Galloway, D. K., Psaltis, D., Chakrabarty, D., & Muno, M. P. 2003, ApJ, 590, 999
Galloway, D. K., Psaltis, D., Muno, M. P., & Chakrabarty, D. 2006, ApJ, 639, 1033
Giacconi, R., Gorenstein, P., Gursky, H., Usher, P. D., Waters, J. R., Sandage, A., Osmer, P., & Peach, J. V. 1967, ApJ, 148, L129
Giacconi, R., Gursky, H., Paolini, F., & Rossi, B. 1962, Phys. Rev. Lett., 9, 439
Giacconi, R., Murray, S., Gursky, H., Kellogg, E., Schreier, E., Matilsky, T., Koch, D., & Tananbaum, H. 1974, ApJS, 27, 37
Giacconi, R., Murray, S., Gursky, H., Kellogg, E., Schreier, E., & Tananbaum, H. 1972, ApJ, 178, 281
Gierliński, M. & Done, C. 2002, MNRAS, 331, L47
Giles, A. B., Hill, K. M., & Greenhill, J. G. 1999, MNRAS, 304, 47
Giles, A. B., Hill, K. M., Strohmayer, T. E., & Cummings, N. 2002, ApJ, 568, 279
Giles, A. B., Swank, J. H., Jahoda, K., Zhang, W., Strohmayer, T., Stark, M. J., & Morgan, E. H. 1996, ApJ, 469, L25+
Gotthelf, E. V. & Kulkarni, S. R. 1997, ApJ, 490, L161
Gottwald, M., Haberl, F., Langmeier, A., Hasinger, G., Lewin, W. H. G., & van Paradijs, J. 1989, ApJ, 339, 1044
Gottwald, M., Haberl, F., Parmar, A. N., & White, N. E. 1986, ApJ, 308, 213
—. 1987, ApJ, 323, 575
Grindlay, J., Gursky, H., Schnopper, H., Parsignault, D. R., Heise, J., Brinkman, A. C., & Schrijver, J. 1976, ApJ, 205, L127
Grindlay, J. E. 1978, ApJ, 224, L107
Grindlay, J. E., Bailyn, C. D., Cohn, H., Lugger, P. M., Thorstensen, J. R., & Wegner, G. 1988, ApJ, 334, L25
Grindlay, J. E. & Liller, W. 1978, ApJ, 220, L127
Grindlay, J. E., Marshall, H. L., Hertz, P., Weisskopf, M. C., Elsner, R. F., Ghosh, P., Darbro, W., Sutherland, P. G., & Soltan, A. 1980, ApJ, 240, L121
Grindlay, J. E., McClintock, J. E., Canizares, C. R., Cominsky, L., Li, F. K., Lewin, W. H. G., & van Paradijs, J. 1978, Nature, 274, 567
Gruber, D. E., Blanco, P. R., Heindl, W. A., Pelling, M. R., Rothschild, R. E., & Hink, P. L. 1996, A&AS, 120, C641
Guerriero, R., Fox, D. W., Kommers, J., Lewin, W. H. G., Rutledge, R., Moore, C. B., Morgan, E., van Paradijs, J., van der Klis, M., Bildsten, L., & Dotani, T. 1999, MNRAS, 307, 179
Haberl, F., Stella, L., White, N. E., Gottwald, M., & Priedhorsky, W. C. 1987, ApJ, 314, 266
Haberl, F. & Titarchuk, L. 1995, A&A, 299, 414
Hanawa, T. & Fujimoto, M. Y. 1982, PASJ, 34, 495
Hasinger, G. & van der Klis, M. 1989, A&A, 225, 79
Heinke, C. O., Edmonds, P. D., & Grindlay, J. E. 2001, ApJ, 562, 363
Heinke, C. O., Grindlay, J. E., Lugger, P. M., Cohn, H. N., Edmonds, P. D., Lloyd, D. A., & Cool, A. M. 2003, ApJ, 598, 501
Heyl, J. S. 2004, ApJ, 600, 939
Hjellming, R. M. 1978, ApJ, 221, 225
Hoffman, J. A., Cominsky, L., & Lewin, W. H. G. 1980, ApJ, 240, L27
Hoffman, J. A., Lewin, W. H. G., Doty, J., Hearn, D. R., Clark, G. W., Jernigan, G., & Li, F. K. 1976, ApJ, 210, L13
Hoffman, J. A., Wheaton, W. A., Primini, F. A., Campbell, P., Matteson, J. L., Gruber, D. E., Peterson, L. E., Swank, J. H., Boldt, E. A., & Holt, S. S. 1978, Nature, 276, 587
Homan, J., Méndez, M., Wijnands, R., van der Klis, M., & van Paradijs, J. 1999, ApJ, 513, L119
Homer, L., Anderson, S. F., Margon, B., Deutsch, E. W., & Downes, R. A. 2001a, ApJ, 550, L155
Homer, L., Anderson, S. F., Margon, B., Downes, R. A., & Deutsch, E. W. 2002, AJ, 123, 3255
Homer, L., Charles, P. A., & O'Donoghue, D. 1998, MNRAS, 298, 497
Homer, L., Deutsch, E. W., Anderson, S. F., & Margon, B. 2001b, AJ, 122, 2627
Hunt, J. & Battrick, B., eds. 1989, Proc. 23rd ESLAB Symposium on Two Topics in X-ray Astronomy, Bologna, Italy, 13-20 September No. SP-296 (ESTEC, Noordwijk, The Netherlands: ESA)
Ilovaisky, S. A., Auriere, M., Koch-Miramond, L., Chevalier, C., Cordoni, J.-P., & Crowe, R. A. 1993, A&A, 270, 139

in 't Zand, J., Bazzano, A., Cocchi, M., Ubertini, P., Muller, J. M., & Torroni, V. 1998a, IAU Circ., 6846
in 't Zand, J., Cornelisse, R., Kuulkers, E., Verbunt, F., & Heise, J. 2004a, in X-ray Timing 2003: Rossi and Beyond, ed. P. Kaaret, F. K. Lamb, & J. H. Swank, Vol. 714 (Melville, NY: AIP), 253–256
in 't Zand, J. J. M., Cornelisse, R., & Cumming, A. 2004b, A&A, 426, 257
in 't Zand, J. J. M., Cornelisse, R., Kuulkers, E., Heise, J., Kuiper, L., Bazzano, A., Cocchi, M., Muller, J. M., Natalucci, L., Smith, M. J. S., & Ubertini, P. 2001a, A&A, 372, 916
in 't Zand, J. J. M., Heise, J., Brinkman, A. C., Jager, R., Skinner, G. K., Patterson, T. G., Pan, H.-C., Nottingham, M. R., Willmore, A. P., & Al-Emam, O. 1991, Advances in Space Research, 11, 187
in 't Zand, J. J. M., Heise, J., Kuulkers, E., Bazzano, A., Cocchi, M., & Ubertini, P. 1999a, A&A, 347, 891
in 't Zand, J. J. M., Heise, J., Muller, J. M., Bazzano, A., Cocchi, M., Natalucci, L., & Ubertini, P. 1998b, A&A, 331, L25
in 't Zand, J. J. M., Hulleman, F., Markwardt, C. B., Méndez, M., Kuulkers, E., Cornelisse, R., Heise, J., Strohmayer, T. E., & Verbunt, F. 2003a, A&A, 406, 233
in 't Zand, J. J. M., Kuulkers, E., Verbunt, F., Heise, J., & Cornelisse, R. 2003b, A&A, 411, L487
in 't Zand, J. J. M., Strohmayer, T. E., Markwardt, C. B., & Swank, J. 2003c, A&A, 409, 659
in 't Zand, J. J. M., van Kerkwijk, M. H., Pooley, D., Verbunt, F., Wijnands, R., & Lewin, W. H. G. 2001b, ApJ, 563, L41
in 't Zand, J. J. M., Verbunt, F., Heise, J., Bazzano, A., Cocchi, M., Cornelisse, R., Kuulkers, E., Natalucci, L., & Ubertini, P. 2004c, in Proceedings of the 2nd BeppoSAX Conference: "The Restless High-Energy Universe", Amsterdam, 5–9 May 2003, ed. E. P. J. van den Heuvel, R. A. M. J. Wijers, & J. J. M. in 't Zand, Vol. 132, 486–495
in 't Zand, J. J. M., Verbunt, F., Heise, J., Muller, J. M., Bazzano, A., Cocchi, M., Natalucci, L., & Ubertini, P. 1998c, A&A, 329, L37
in 't Zand, J. J. M., Verbunt, F., Strohmayer, T. E., Bazzano, A., Cocchi, M., Heise, J., van Kerkwijk, M. H., Muller, J. M., Natalucci, L., Smith, M. J. S., & Ubertini, P. 1999b, A&A, 345, 100
Inoue, H., Koyama, K., Makino, F., Makishima, K., Matsuoka, M., Murakami, T., Oda, M., Ogawara, Y., Ohashi, T., Shibazaki, N., Tanaka, Y., Hayakawa, S., Kunieda, H., Masai, K., Nagase, F., Tawara, Y., Miyamoto, S., Tsunemi, H., Yamashita, K., & Kondo, I. 1984, PASJ, 36, 855
Jahoda, K., Markwardt, C. B., Radeva, Y., Rots, A., Stark, M. J., Swank, J. H., Strohmayer, T. E., & Zhang, W. 2006, ApJS, accepted (astro-ph/0511531)
Jahoda, K., Swank, J. H., Giles, A. B., Stark, M. J., Strohmayer, T., Zhang, W., & Morgan, E. H. 1996, Proc. SPIE, 2808, 59
Jernigan, J. G., Bradt, H. V., Doxsey, R. E., McClintock, J. E., & Apparao, K. M. V. 1977, Nature, 270, 321
Jonker, P. G., Galloway, D. K., McClintock, J. E., Buxton, M., Garcia, M., & Murray, S. 2004, MNRAS, 354, 666
Jonker, P. G., van der Klis, M., Homan, J., Méndez, M., van Paradijs, J., Belloni, T., Kouveliotou, C., Lewin, W., & Ford, E. C. 2001, ApJ, 553, 335
Jonker, P. G., van der Klis, M., Homan, J., Wijnands, R., van Paradijs, J., Méndez, M., Kuulkers, E., & Ford, E. C. 2000, ApJ, 531, 453
Juett, A. M. & Chakrabarty, D. 2003, ApJ, 599, 498
Juett, A. M., Psaltis, D., & Chakrabarty, D. 2001, ApJ, 560, L59
Kaaret, P., in 't Zand, J. J. M., Heise, J., & Tomsick, J. A. 2002, ApJ, 575, 1018
Kaaret, P., Lamb, F. K., & Swank, J. H., eds. 2004, X-ray Timing 2003: Rossi and Beyond, Vol. 714 (Melville, NY: AIP)
Kaaret, P., Morgan, E., & Vanderspek, R. 2005, The Astronomer's Telegram, 538
Kaaret, P., Zand, J. J. M. i., Heise, J., & Tomsick, J. A. 2003, ApJ, 598, 481
Kahn, S. M. & Grindlay, J. E. 1984, ApJ, 281, 826
Kaluzienski, L. J., Holt, S. S., Boldt, E. A., & Serlemitsos, P. J. 1977, Nature, 265, 606
Kaminker, A. D., Pavlov, G. G., Shibanov, Y. A., Kurt, V. G., Smirnov, A. S., Shamolin, V. M., Kopaeva, I. F., & Sheffer, E. K. 1989, A&A, 220, 117
Kawai, N., Suzuki, M., & for the HETE Team. 2005, The Astronomer's Telegram, 534
King, A. R. & Watson, M. G. 1986, Nature, 323, 105
King, I. R., Stanford, S. A., Albrecht, R., Barbieri, C., Blades, J. C., Boksenberg, A., Crane, P., Disney, M. J., Deharveng, J. M., Jakobsen, P., Kamperman, T. M., Macchetto, F., Mackay, C. D., Paresce, F., Weigelt, G., Baxter, D., Greenfield, P., Jedrzejewski, R., Nota, A., Sparks, W. B., & Sosin, C. 1993, ApJ, 413, L117
Kitamoto, S., Tsunemi, H., Miyamoto, S., & Roussel-Dupre, D. 1993, ApJ, 403, 315
Kong, A. K. H., Homer, L., Kuulkers, E., Charles, P. A., & Smale, A. P. 2000, MNRAS, 311, 405
Koyama, K., Inoue, H., Makishima, K., Matsuoka, M., Murakami, T., Oda, M., Osgawara, Y., Ohashi, T., Shibazaki, N., Tanaka, Y., Marshall, F. J., Kondo, I. S., Hayakawa, S., Kunieda, H., Makino, F., Masai, K., Nagase, F., Tawara, Y., Miyamoto, S., Tsunemi, H., & Yamashita, K. 1981, ApJ, 247, L27
Kuulkers, E. 2002, A&A, 383, L5
Kuulkers, E., den Hartog, P. R., in 't Zand, J. J. M., Verbunt, F. W. M., Harris, W. E., & Cocchi, M. 2003, A&A, 399, 663
Kuulkers, E., Homan, J., van der Klis, M., Lewin, W. H. G., & Méndez, M. 2002, A&A, 382, 947
Kuulkers, E., in 't Zand, J., Homan, J., van Straaten, S., Altamirano, D., & van der Klis, M. 2004, in X-ray Timing 2003: Rossi and Beyond, ed. P. Kaaret, F. K. Lamb, & J. H. Swank, Vol. 714 (Melville, NY: AIP), 257–260
Kuulkers, E. & van der Klis, M. 2000, A&A, 356, L45
Langmeier, A., Sztajno, M., Hasinger, G., Truemper, J., & Gottwald, M. 1987, ApJ, 323, 288
Lattimer, J. M. & Prakash, M. 2001, ApJ, 550, 426
Levine, A., Swank, J., & Smith, E. 1998, IAU Circ., 6955
Levine, A. M., Bradt, H., Cui, W., Jernigan, J. G., Morgan, E. H., Remillard, R., Shirey, R. E., & Smith, D. A. 1996, ApJ, 469, L33
Lewin, W., Marshall, H., Primini, F., Wheaton, W., Cominsky, L., Jernigan, G., & Ossman, W. 1978, IAU Circ., 3190
Lewin, W. H. G., Clark, G., & Doty, J. 1976a, IAU Circ., 2922
Lewin, W. H. G., Doty, J., Clark, G. W., Rappaport, S. A., Bradt, H. V. D., Doxsey, R., Hearn, D. R., Hoffman, J. A., Jernigan, J. G., Li, F. K., Mayer, W., McClintock, J., Primini, F., & Richardson, J. 1976b, ApJ, 207, L95
Lewin, W. H. G., Hoffman, J. A., & Doty, J. 1976c, IAU Circ., 2994
Lewin, W. H. G., Hoffman, J. A., Doty, J., Hearn, D. R., Clark, G. W., Jernigan, J. G., Li, F. K., McClintock, J. E., & Richardson, J. 1976d, MNRAS, 177, 83P
Lewin, W. H. G., Hoffman, J. A., Doty, J., Li, F. K., & McClintock, J. E. 1977, IAU Circ., 3075
Lewin, W. H. G., Li, F. K., Hoffman, J. A., Doty, J., Buff, J., Clark, G. W., & Rappaport, S. 1976e, MNRAS, 177, 93P
Lewin, W. H. G., Penninx, W., van Paradijs, J., Damen, E., Sztajno, M., Truemper, J., & van der Klis, M. 1987, ApJ, 319, 893
Lewin, W. H. G., van Paradijs, J., Cominsky, L., & Holzner, S. 1980, MNRAS, 193, 15
Lewin, W. H. G., van Paradijs, J., & Taam, R. E. 1993, Space Sci. Rev., 62, 223
Li, F. & Clark, G. 1977, IAU Circ., 3095
Li, F. K., Lewin, W. H. G., Clark, G. W., Doty, J., Hoffman, J. A., & Rappaport, S. A. 1977, MNRAS, 179, 21
Liller, W. 1977, ApJ, 213, L21
Lochner, J. C. & Roussel-Dupre, D. 1994, ApJ, 435, 840
London, R. A., Taam, R. E., & Howard, W. M. 1986, ApJ, 306, 170
Lutovinov, A., Revnivtsev, M., Molkov, S., & Sunyaev, R. 2005, A&A, 430, 997
Lutovinov, A., Walter, R., Belanger, G., Lund, N., Grebenev, S., & Winkler, C. 2003, The Astronomer's Telegram, 155
Lutovinov, A. A., Grebenev, S. A., Pavlinsky, M. N., & Sunyaev, R. A. 2001, Astronomy Letters, 27, 501
Méndez, M., van der Klis, M., & Ford, E. C. 2001, ApJ, 561, 1016
Maeda, Y., Koyama, K., Sakano, M., Takeshima, T., & Yamauchi, S. 1996, PASJ, 48, 417
Makishima, K., Inoue, H., Koyama, K., Matsuoka, M., Murakami, T., Oda, M., Ogawara, Y., Ohashi, T., Shibazaki, N., Tanaka, Y., Hayakawa, S., Kunieda, H., Makino, F., Masai, K., Nagase, F., Tawara, Y., Miyamoto, S., Tsunemi, H., Yamashita, K., & Kondo, I. 1982, ApJ, 255, L49
—. 1981a, ApJ, 244, L79

Makishima, K., Mitsuda, K., Inoue, H., Koyama, K., Matsuoka, M., Murakami, T., Oda, M., Ogawara, Y., Ohashi, T., Shibazaki, N., Tanaka, Y., Marshall, F. J., Hayakawa, S., Kunieda, H., Makino, F., Nagase, F., Tawara, Y., Miyamoto, S., Tsunemi, H., Tsuno, K., Yamashita, K., & Kondo, I. 1983, ApJ, 267, 310
Makishima, K., Ohashi, T., Inoue, H., Koyama, K., Matsuoka, M., Murakami, T., Oda, M., Ogawara, Y., Shibazaki, N., Tanaka, Y., Kondo, I., Hayakawa, S., Kunieda, H., Makino, F., Masai, K., Nagase, F., Tawara, Y., Miyamoto, S., Tsunemi, H., & da Yamashita, K. 1981b, ApJ, 247, L23
Markert, T. H., Backman, D. E., Canizares, C. R., Clark, G. W., & Levine, A. M. 1975, Nature, 257, 32
Markert, T. H., Canizares, C. R., Clark, G. W., Hearn, D. R., Li, F. K., Sprott, G. F., & Winkler, P. F. 1977, ApJ, 218, 801
Markwardt, C. B., Marshall, F. E., Swank, J., & Takeshima, T. 1998, IAU Circ., 6998
Markwardt, C. B., Marshall, F. E., Swank, J. H., & Wei, C. 1999a, IAU Circ., 7300
Markwardt, C. B., Strohmayer, T. E., & Swank, J. H. 1999b, ApJ, 512, L125
Markwardt, C. B., Strohmayer, T. E., Swank, J. H., & Zhang, W. 2000, IAU Circ., 7482
Markwardt, C. B., Swank, J., Wijnands, R., & Zand, J. I. 2005, The Astronomer's Telegram, 505
Markwardt, C. B. & Swank, J. H. 2000, IAU Circ., 7454
Markwardt, C. B. & Swank, J. H. 2002, in BAPS, Vol. 47 (2), Proceedings of the American Physical Society April Meeting, held jointly with the High Energy Astrophysics Division (HEAD) of the American Astronomical Society, 219
—. 2003a, The Astronomer's Telegram, 156
—. 2003b, IAU Circ., 8144
—. 2005, The Astronomer's Telegram, 495
Markwardt, C. B., Swank, J. H., & Marshall, F. E. 1999c, IAU Circ., 7120
Marshall, F. E. & Markwardt, C. B. 1999, IAU Circ., 7103
Marshall, F. E., Swank, J. H., Thomas, B., Angelini, L., Valinia, A., & Ebisawa, K. 1997, IAU Circ., 6543
Marshall, F. E., Ueda, Y., & Markwardt, C. B. 1999, IAU Circ., 7133
Martí, J., Mirabel, I. F., Rodriguez, L. F., & Chaty, S. 1998, A&A, 332, L45
Masetti, N. 2002, A&A, 381, L45
Matsuba, E., Dotani, T., Mitsuda, K., Asai, K., Lewin, W. H. G., van Paradijs, J., & van der Klis, M. 1995, PASJ, 47, 575
Matsuoka, M., Inoue, H., Koyama, K., Makishima, K., Murakami, T., Oda, M., Ogawara, Y., Ohashi, T., Shibazaki, N., Tanaka, Y., Kondo, I., Hayakawa, S., Kunieda, H., Makino, F., Masai, K., Nagase, F., Tawara, Y., Miyamoto, S., Tsunemi, H., & Yamashita, K. 1980, ApJ, 240, L137
McClintock, J. E., Bradt, H. V., Doxsey, R. E., Jernigan, J. G., Canizares, C. R., & Hiltner, W. A. 1977, Nature, 270, 320
McClintock, J. E., Canizares, C. R., & Backman, D. E. 1978, ApJ, 223, L75
McClintock, J. E. & Petro, L. D. 1981, IAU Circ., 3615
Migliari, S., Di Salvo, T., Belloni, T., van der Klis, M., Fender, R. P., Campana, S., Kouveliotou, C., Méndez, M., & Lewin, W. H. G. 2003, MNRAS, 342, 909
Mignani, R. P., Chaty, S., Mirabel, I. F., & Mereghetti, S. 2002, A&A, 389, L11
Miller, M. C. 1999, ApJ, 515, L77
—. 2000, ApJ, 531, 458
Molkov, S., Revnivtsev, M., Lutovinov, A., & Sunyaev, R. 2004, A&A, submitted (astro-ph/0408258)
Molkov, S. V., Grebenev, S. A., & Lutovinov, A. A. 2000, A&A, 357, L41
Moore, C. B., Rutledge, R. E., Fox, D. W., Guerriero, R. A., Lewin, W. H. G., Fender, R., & van Paradijs, J. 2000, ApJ, 532, 1181
Morgan, E., Kaaret, P., & Vanderspek, R. 2005, The Astronomer's Telegram, 523
Morrison, R. & McCammon, D. 1983, ApJ, 270, 119
Motch, C., Barret, D., Pietsch, W., Hasinger, G., & Giraud, E. 1994, IAU Circ., 6101
Motch, C., Pedersen, H., Courvoisier, T. J.-L., Beuermann, K., & Pakull, M. W. 1987, ApJ, 313, 792
Mukai, K. & Smale, A. P. 2000, ApJ, 533, 352
Muller, J. M., Smith, M. J. S., D'Andreta, G., Bazzano, A., Ubertini, P., in 't Zand, J., & Heise, J. 1998, IAU Circ., 6867
Muno, M. P., Özel, F., & Chakrabarty, D. 2002a, ApJ, 581, 550
—. 2003, ApJ, 595, 1066
Muno, M. P., Chakrabarty, D., Galloway, D. K., & Psaltis, D. 2002b, ApJ, 580, 1048
Muno, M. P., Chakrabarty, D., Galloway, D. K., & Savov, P. 2001, ApJ, 553, L157
Muno, M. P., Fox, D. W., Morgan, E. H., & Bildsten, L. 2000, ApJ, 542, 1016
Muno, M. P., Galloway, D. K., & Chakrabarty, D. 2004, ApJ, 608, 930
Muno, M. P., Remillard, R. A., & Chakrabarty, D. 2002c, ApJ, 568, L35
Murakami, T., Inoue, H., Koyama, K., Makishima, K., Matsuoka, M., Oda, M., Ogawara, Y., Ohashi, T., Makino, F., Shibazaki, N., Tanaka, Y., Hayakawa, S., Kunieda, H., Nagase, F., Masai, K., Tawara, Y., Miyamoto, S., Tsunemi, H., Yamashita, K., & Kondo, I. 1983, PASJ, 35, 531
Murakami, T., Inoue, H., Koyama, K., Makishima, K., Matsuoka, M., Oda, M., Ogawara, Y., Ohashi, T., Shibazaki, N., Tanaka, Y., Hayakawa, S., Kunieda, H., Makino, F., Masai, K., Nagase, F., Tawara, Y., Miyamoto, S., Tsunemi, H., Yamashita, K., & Kondo, I. 1980a, PASJ, 32, 543
Murakami, T., Inoue, H., Koyama, K., Makishima, K., Matsuoka, M., Oda, M., Ogawara, Y., Ohashi, T., Shibazaki, N., Tanaka, Y., Tawara, Y., Hayakawa, S., Kunieda, H., Makino, F., Masai, K., Nagase, F., Miyamoto, S., Tsunemi, H., Yamashita, K., & Kondo, I. 1980b, ApJ, 240, L143
Narayan, R. & Heyl, J. S. 2003, ApJ, 599, 419
Natalucci, L., Bazzano, A., Cocchi, M., Ubertini, P., Cornelisse, R., Heise, J., & Zand, J. J. M. i. 2004, A&A, 416, 699
Natalucci, L., Bazzano, A., Cocchi, M., Ubertini, P., Heise, J., Kuulkers, E., & in 't Zand, J. J. M. 2000, ApJ, 543, L73
Natalucci, L., Cornelisse, R., Bazzano, A., Cocchi, M., Ubertini, P., Heise, J., in 't Zand, J. J. M., & Kuulkers, E. 1999, ApJ, 523, L45
Naylor, T., Charles, P. A., & Longmore, A. J. 1991, MNRAS, 252, 203
Oda, M., Kahn, S., Grindlay, J., Halpern, J., & Ladd, E. 1981, IAU Circ., 3624
Olive, J. F., Barret, D., Boirin, L., Grindlay, J. E., Swank, J. H., & Smale, A. P. 1998, A&A, 333, 942
Ortolani, S., Bica, E., & Barbuy, B. 1997, A&A, 326, 614
Parmar, A. N., Gottwald, M., van der Klis, M., & van Paradijs, J. 1989, ApJ, 338, 1024
Parmar, A. N., Oosterbroek, T., Sidoli, L., Stella, L., & Frontera, F. 2001, A&A, 380, 490
Parmar, A. N., White, N. E., Giommi, P., & Gottwald, M. 1986, ApJ, 308, 199
Patterson, T. G., Skinner, G. K., Willmore, A. P., Emam, O., Brinkman, A. C., Heise, J., in 't Zand, J. J. M., Jager, R., Sunyaev, R., Churazov, E., Gilfanov, M. R., & Yamburenko, N. 1989, in Proc. 23rd ESLAB Symposium on Two Topics in X-ray Astronomy, Bologna, Italy, 13-20 September, ed. J. Hunt & B. Battrick No. SP-296 (ESTEC, Noordwijk, The Netherlands: ESA), 567–572
Pavlinsky, M. N., Grebenev, S. A., & Sunyaev, R. A. 1994, ApJ, 425, 110
Piro, L., Heise, J., Jager, R., Feroci, M., D'Andreta, G., Spoliti, G., Coletta, A., Muller, H., & Ricci, D. 1997, IAU Circ., 6538
Pooley, D., Lewin, W. H. G., Anderson, S. F., Baumgardt, H., Filippenko, A. V., Gaensler, B. M., Homer, L., Hut, P., Kaspi, V. M., Makino, J., Margon, B., McMillan, S., Portegies Zwart, S., van der Klis, M., & Verbunt, F. 2003, ApJ, 591, L131
Pooley, D., Lewin, W. H. G., Verbunt, F., Homer, L., Margon, B., Gaensler, B. M., Kaspi, V. M., Miller, J. M., Fox, D. W., & van der Klis, M. 2002, ApJ, 573, 184
Predehl, P., Hasinger, G., & Verbunt, F. 1991, A&A, 246, L21
Press, W. H., Teukolsky, S. A., Vetterling, W. T., & Flannery, B. P. 1996, Numerical Recipes in Fortran 77: The Art of Scientific Computing, 2nd edn. (Cambridge, New York, Melbourne: Cambridge University Press), 1447
Priedhorsky, W. 1986, Ap&SS, 126, 89
Priedhorsky, W. & Terrell, J. 1984a, ApJ, 284, L17
Priedhorsky, W. C. & Terrell, J. 1984b, ApJ, 280, 661
Proctor, R. J., Skinner, G. K., & Willmore, A. P. 1978, MNRAS, 185, 745
Revnivtsev, M. G. & Sunyaev, R. A. 2002, Astronomy Letters, 28, 19

Sansom, A. E., Dotani, T., Asai, K., & Lehto, H. J. 1993, MNRAS, 262, 429
Seward, F. D., Page, C. G., Turner, M. J. L., & Pounds, K. A. 1976, MNRAS, 175, 39P
Shahbaz, T., Thorstensen, J. R., Charles, P. A., & Sherman, N. D. 1998, MNRAS, 296, 1004
Shaposhnikov, N., Titarchuk, L., & Haberl, F. 2003, ApJ, 593, L35
Sidoli, L., Mereghetti, S., Israel, G. L., Cusumano, G., Chiappetti, L., & Treves, A. 1998, A&A, 336, L81
Skinner, G. K., Foster, A. J., Willmore, A. P., & Eyles, C. J. 1990, MNRAS, 243, 72
Skinner, G. K., Willmore, A. P., Eyles, C. J., Bertram, D., & Church, M. J. 1987, Nature, 330, 544
Smale, A. P. 1995, AJ, 110, 1292
—. 1998, ApJ, 498, L141
—. 2001, ApJ, 562, 957
Smale, A. P., Mason, K. O., White, N. E., & Gottwald, M. 1988, MNRAS, 232, 647
Smith, D. A., Morgan, E. H., & Bradt, H. 1997, ApJ, 479, L137
Soria, R., Wu, K., & Galloway, D. K. 1999, MNRAS, 309, 528
Spitkovsky, A., Levin, Y., & Ushomirsky, G. 2002, ApJ, 566, 1018
Stella, L., White, N. E., & Priedhorsky, W. 1987, ApJ, 312, L17
Strohmayer, T. & Bildsten, L. 2006, in Compact Stellar X-Ray Sources, ed. W. H. G. Lewin & M. van der Klis (Cambridge University Press), (astro–ph/0301544)
Strohmayer, T. E. 1999, ApJ, 523, L51
—. 2001, Advances in Space Research, 28, 511
Strohmayer, T. E. & Brown, E. F. 2002, ApJ, 566, 1045
Strohmayer, T. E., Jahoda, K., Giles, A. B., & Lee, U. 1997a, ApJ, 486, 355
Strohmayer, T. E. & Markwardt, C. B. 2002, ApJ, 577, 337
Strohmayer, T. E., Markwardt, C. B., Swank, J. H., & in 't Zand, J. 2003, ApJ, 596, L67
Strohmayer, T. E., Zhang, W., & Swank, J. H. 1997b, ApJ, 487, L77
Strohmayer, T. E., Zhang, W., Swank, J. H., & Lapidus, I. 1998a, ApJ, 503, L147
Strohmayer, T. E., Zhang, W., Swank, J. H., Smale, A., Titarchuk, L., Day, C., & Lee, U. 1996, ApJ, 469, L9
Strohmayer, T. E., Zhang, W., Swank, J. H., White, N. E., & Lapidus, I. 1998b, ApJ, 498, L135
Sugimoto, D., Ebisuzaki, T., & Hanawa, T. 1984, PASJ, 36, 839
Sunyaev, R., Gilfanov, M., Churazov, E., Loznikov, V., Yamburenko, N., Skinner, G. K., Patterson, T. G., Willmore, A. P., Emam, O., Brinkman, A. C., Heise, J., in 't Zand, J. J. M., & Jager, R. 1990, Pis ma Astronomicheskii Zhurnal, 16, 136
Swank, J. H., Becker, R. H., Boldt, E. A., Holt, S. S., Pravdo, S. H., & Serlemitsos, P. J. 1977, ApJ, 212, L73
Swank, J. H., Becker, R. H., Pravdo, S. H., Saba, J. R., & Serlemitsos, P. J. 1976a, IAU Circ., 3000
—. 1976b, IAU Circ., 3010
Swank, J. H., Becker, R. H., Pravdo, S. H., & Serlemitsos, P. J. 1976c, IAU Circ., 2963
Swank, J. H., Boldt, E. A., Holt, S. S., Serlemitsos, P. J., & Becker, R. H. 1978, MNRAS, 182, 349
Sztajno, M., Basinska, E. M., Cominsky, L. R., Marshall, F. J., & Lewin, W. H. G. 1983, ApJ, 267, 713
Sztajno, M., Fujimoto, M. Y., van Paradijs, J., Vacca, W. D., Lewin, W. H. G., Penninx, W., & Trumper, J. 1987, MNRAS, 226, 39
Sztajno, M., van Paradijs, J., Lewin, W. H. G., Langmeier, A., Trumper, J., & Pietsch, W. 1986, MNRAS, 222, 499
Tanaka, Y. 1989, in Proc. 23rd ESLAB Symposium on Two Topics in X-ray Astronomy, Bologna, Italy, 13-20 September, ed. J. Hunt & B. Battrick No. SP-296 (ESTEC, Noordwijk, The Netherlands: ESA), 3–13
Tananbaum, H., Chaisson, L. J., Forman, W., Jones, C., & Matilsky, T. A. 1976, ApJ, 209, L125
Tawara, Y., Hirano, T., Kii, T., Matsuoka, M., & Murakami, T. 1984, PASJ, 36, 861
Tennant, A. F., Fabian, A. C., & Shafer, R. A. 1986, MNRAS, 219, 871
Thorsett, S. E. & Chakrabarty, D. 1999, ApJ, 512, 288
Thorstensen, J., Charles, P., & Bowyer, S. 1978, ApJ, 220, L131
Thorstensen, J. R., Bowyer, S., & Charles, P. A. 1980, ApJ, 238, 964
Titarchuk, L. 1994a, ApJ, 434, 570
—. 1994b, ApJ, 429, 340
Titarchuk, L. & Shaposhnikov, N. 2002, ApJ, 570, L25
Tomsick, J. A., Halpern, J. P., Kemp, J., & Kaaret, P. 1999, ApJ, 521, 341
Tomsick, J. A., Heindl, W. A., Chakrabarty, D., Halpern, J. P., & Kaaret, P. 2001, ApJ, 559, L123
Tomsick, J. A., Heindl, W. A., Chakrabarty, D., & Kaaret, P. 2002, ApJ, 581, 570
Ubertini, P., Bazzano, A., Cocchi, M., Natalucci, L., Heise, J., Jager, R., in 't Zand, J., Muller, J. M., Smith, M., Celidonio, G., Coletta, A., Ricci, R., Giommi, P., Ricci, D., Capalbi, M., Menna, M. T., & Rebecchi, S. 1997, IAU Circ., 6611
Ubertini, P., Bazzano, A., Cocchi, M., Natalucci, L., Heise, J., Muller, J. M., & in 't Zand, J. J. M. 1999, ApJ, 514, L27
Ulmer, M. P., Lewin, W. H. G., Hoffman, J. A., Doty, J., & Marshall, H. 1977, ApJ, 214, L11
Vacca, W. D., Lewin, W. H. G., & van Paradijs, J. 1986, MNRAS, 220, 339
van den Heuvel, E. P. J., Wijers, R. A. M. J., & in 't Zand, J. J. M., eds. 2004, Proceedings of the 2nd BeppoSAX Conference: "The Restless High-Energy Universe", Amsterdam, 5–9 May 2003, Vol. 132
van der Klis, M., van Paradijs, J., Jansen, F. A., & Lewin, W. H. G. 1984, IAU Circ., 3961
van Paradijs, J. 1978, Nature, 274, 650
van Paradijs, J., Dotani, T., Tanaka, Y., & Tsuru, T. 1990a, PASJ, 42, 633
van Paradijs, J. & Lewin, W. H. G. 1986, A&A, 157, L10
van Paradijs, J., Penninx, W., & Lewin, W. H. G. 1988a, MNRAS, 233, 437
van Paradijs, J., Penninx, W., Lewin, W. H. G., Sztajno, M., & Truemper, J. 1988b, A&A, 192, 147
van Paradijs, J., van der Klis, M., van Amerongen, S., Pedersen, H., Smale, A. P., Mukai, K., Schoembs, R., Haefner, R., Pfeiffer, M., & Lewin, W. H. G. 1990b, A&A, 234, 181
van Straaten, S., van der Klis, M., Kuulkers, E., & Méndez, M. 2001, ApJ, 551, 907
Vanderspek, R., Morgan, E., Crew, G., Graziani, C., & Suzuki, M. 2005, The Astronomer's Telegram, 516
Verbunt, F., van Kerkwijk, M. H., in 't Zand, J. J. M., & Heise, J. 2000, A&A, 359, 960
Villarreal, A. R. & Strohmayer, T. E. 2004, ApJ, 614, L121
Vrtilek, S. D., Raymond, J. C., Garcia, M. R., Verbunt, F., Hasinger, G., & Kurster, M. 1990, A&A, 235, 162
Wachter, S., Wellhouse, J. W., Patel, S. K., Smale, A. P., Alves, J., & Bouchet, P. 2004, ApJ, accepted (astro-ph/0411360)
Walter, F. M., Mason, K. O., Clarke, J. T., Halpern, J., Grindlay, J. E., Bowyer, S., & Henry, J. P. 1982, ApJ, 253, L67
Watts, A. L., Strohmayer, T. E., & Markwardt, C. B. 2005, ApJ, 634, 547
Werner, N., in 't Zand, J. J. M., Natalucci, L., Markwardt, C. B., Cornelisse, R., Bazzano, A., Cocchi, M., Heise, J., & Ubertini, P. 2004, A&A, 416, 311
White, N. E. & Angelini, L. 2001, ApJ, 561, L101
White, N. E. & Swank, J. H. 1982, ApJ, 253, L61
Wijnands, R. 2001, ApJ, 554, L59
Wijnands, R. 2004, in Proceedings of the 2nd BeppoSAX Conference: "The Restless High-Energy Universe", Amsterdam, 5–9 May 2003, ed. E. P. J. van den Heuvel, R. A. M. J. Wijers, & J. J. M. in 't Zand, Vol. 132, 496–505
Wijnands, R., Groot, P. J., Miller, J. J., Markwardt, C., Lewin, W. H. G., & van der Klis, M. 2001a, The Astronomer's Telegram, 72
Wijnands, R., Homan, J., Miller, J. M., & Lewin, W. H. G. 2004, ApJ, 606, L61
Wijnands, R., Miller, J. M., Markwardt, C., Lewin, W. H. G., & van der Klis, M. 2001b, ApJ, 560, L159
Wijnands, R., Miller, J. M., & Wang, Q. D. 2002a, ApJ, 579, 422
Wijnands, R., Muno, M. P., Miller, J. M., Franco, L. ., Strohmayer, T., Galloway, D., & Chakrabarty, D. 2002b, ApJ, 566, 1060
Wijnands, R., Strohmayer, T., & Franco, L. M. 2001c, ApJ, 549, L71
Wijnands, R. & van der Klis, M. 1998, Nature, 394, 344
—. 1999, A&A, 345, L35
Wilson, C. A., Patel, S. K., Kouveliotou, C., Jonker, P. G., van der Klis, M., Lewin, W. H. G., Belloni, T., & Méndez, M. 2003, ApJ, 596, 1220
Wolff, M. T., Becker, P. A., Ray, P. S., & Wood, K. S. 2005, ApJ, 632, 1099

Woosley, S. E., Heger, A., Cumming, A., Hoffman, R. D., Pruet, J., Rauscher, T., Fisker, J. L., Schatz, H., Brown, B. A., & Wiescher, M. 2004, ApJS, 151, 75
Woosley, S. E. & Weaver, T. A. 1984, in High Energy Transients in Astrophysics, 273
Zhang, W., Jahoda, K., Kelley, R. L., Strohmayer, T. E., Swank, J. H., & Zhang, S. N. 1998, ApJ, 495, L9